Charles University

Second Faculty of Medicine

Study field: Cell biology and pathology

MUDr. Mohamed Ashraf Khalil Abdel-Rahman

Epigenetic and Cytotoxic Effects of Histone Deacetylase Inhibitors in Combination with Cytostatics on Neuroblastoma

Epigenetické a cytotoxické účinky inhibitorů histondeacetyláz v kombinaci s cytostatiky na buňky neuroblastomu

Ph.D. thesis

Supervisor: Prof.MUDr. Tomáš Eckschlager,CSc

Prague, 2018

Declaration:

I hereby declare that I have prepared the Ph.D. thesis personally and that I have properly stated and cited all utilized sources and literature. I further declare that this thesis was not used for the purposes of gaining the same or another degree.

I agree with the permanent deposition of the electronic version of my work in the database of the inter-university system project Theses.cz for the purposes of systematic control of Ph.D. theses.

In Prague, 15.2.2018

MOHAMED ASHRAF KHALIL ABDEL-RAHMAN

Signature:

Acknowledgements

I would like to express my appreciation and gratitude to all those who have helped me along the path towards the completion of this thesis. A very special gratitude goes to:

My supervisor, **Prof. MUDr. Tomáš Eckschlager**, for his continuous support and guidance throughout my postgraduate study as well his valuable suggestions during revising my Ph.D. thesis.

My consultant and mentor, **MVDr. Jan Hraběta, PhD,** for his tolerance, continuous scientific discussion and great concern.

My genius colleague, Mgr. Pavel Procházka, PhD., for performing "*Methylation-sensitive high resolution melting analysis"* which enriched the topic and provided essential data to explain our results in details.

My dear colleagues and lovely friends, Mgr. Tomáš Groh. Ph.D, Ing. Helena Doktorová and MUDr. Olga Zimmermannová for their priceless encouragement and sharing of scientific discussions.

Pavel Semerák and Daniel Thurner in the laboratory of Childhood Leukaemia Investigation Prague "CLIP", for their assistance concerning cytometric settings beside their joyful and friendly atmosphere.

The government of the Czech republic represented by the Ministry of Education, Youth and Sports for rewarding the scholarship that opened the path to gain experience about Czech culture and to accomplish my postgraduate study in Charles University in Prague.

At last and not the least, I deeply appreciate my sweet mom, my gorgeous sisters; Dr. Salma Ashraf and PharmD. Maha Ashraf, for their warm affection and continuous encouragement. I am fully indebted to my father; my role model in life that always pushes me forward to achieve my dreams.

Identification record:

ABDEL-RAHMAN, Mohamed Ashraf Khalil. *Epigenetic and Cytotoxic Effects of Histone Deacetylase Inhibitors in Combination with Cytostatics on Neuroblastoma.* Prague, 2018. 115 pages. Ph.D. thesis. Charles University in Prague, Second Faculty of Medicine, Department of Pediatric Hematology and Oncology. Thesis supervisor: Prof. Eckschlager, Tomáš

Keywords: histone deacetylase inhibitors (HDACi), valproic acid (VPA), neuroblastoma, cancer stem cell (CSC), CD133.

Abstract

The enhanced expression of histone deacetylases (HDACs) in a variety of malignancies drew attention to investigate a new category of anti-cancer drugs that are based on the inhibition of those enzymes. Valproic acid (VPA) is a well-known antiepileptic drug that exhibits antitumor activities through inhibition of HDACs class I and IIa. Cancer stem cells (CSCs) have been recognized to drive the tumor growth and progression hence; attention has been given to target this small subpopulation of CSCs rather than the whole bulk tumor cells. CD133 is considered to be a CSC marker in several tumors and its transcription is strongly influenced by epigenetic changes that will be altered upon administration of histone deacetylase inhibitors (HDACi) in cancer treatment. Therefore, we evaluated the epigenetic and cytotoxic effects of treatment with 1 mM VPA in combination with other chemotherapeutics and its influence on the expression of CD133 in human neuroblastoma (NB) cell lines.

Our results revealed that addition of VPA to DNA-damaging chemotherapeutics induced a synergistic anti-tumor effect that was associated with caspase-3 dependent induction of apoptosis in UKF-NB-4 cells. This synergism was related to the increase of the acetylation status of histones H3 and H4 and was only produced either by simultaneous treatment with both drugs or when the cells were pretreated with DNA-damaging chemotherapeutics before their exposure to VPA. On the other hand, our results showed that VPA induced CD133 expression that was dependent on increased acetylation of histones H3 and H4. On treatment with VPA and cytostatics, CD133+ cells were mainly detected in the proliferative phases of the cell cycle and they showed less activated caspase-3 compared to CD133− cells. UKF-NB-3 cells which express CD133 displayed higher colony and neurosphere formation capacities when treated with VPA, unlike IMR-32 cells which lack the CD133 protein. Induction of CD133 in UKF-NB-3 was associated with increased expression of phosphorylated Akt and pluripotency transcription factors (Oct4, Sox2 and Nanog). VPA did not induce CD133 expression in cell lines with methylated P1 and and P3 promoters, unless they were pretreated with demethylating agent 5-aza-2'-deoxycytidine. In conclusion, VPA potentiates the cytotoxicity of DNA-damaging chemotherapeutics in NB that is conditioned by the sequence of drugs administrated. CD133 expression in NB can be regulated by histone acetylation and/or methylation of its CpG promoters hence influenced by VPA therapy. VPA can induce CD133+ cells which display high proliferation potential and low sensitivity to cytostatics in NB. Even though these results confirm the potentiating cytotoxic effect of VPA in cancer therapy; they give new insight into a possible limitation to use VPA in some types of cancer which require caution before its use in clinical application.

Souhrn

Zvýšená exprese histondeacetyláz (HDAC) u řady nádorů obrátila pozornost k možnosti využít jejich inhibici k protinádorové léčbě. Kyselina valproová (VPA) je nejen užívané antiepileptikum, ale vykazuje i protinádorové účinky podmíněné inhibicí HDAC třídy I a IIa. Předpokládá se, že nádorové kmenové buňky (CSC) jsou odpovědné za růst a progresi nádorů a proto je snaha zacílit léčbu na malou subpopulaci CSC spíše než na celý nádor. CD133 byl rozpoznán jako marker CSC u řady nádorů. Jeho exprese je významně ovlivněna epigenetickými změnami, mezi něž patří podání inhibitorů HDAC užívaných v léčbě nádorů. Proto jsme se zabývali epigenetickými a cytotoxickými účinky VPA v kombinaci s některými chemoterapeutiky a jejím vlivem na expresi antigenu CD133 u lidských neuroblastomových (NB) buněčných linií.

Naše výsledky ukázaly, že kombinace VPA s DNA poškozujícími cytostatiky má u buněk UKF-NB-4 synergistický účinek podmíněný indukcí apoptózy závislé na aktivaci caspázy-3. Tento synergizmus byl ve vztahu ke zvýšení acetylace histonů H3 a H4 a byl přítomen pouze při současné inkubaci s oběmi látkami nebo při inkubaci s DNA poškozujícím cytostatikem následované inkubací s VPA. Výsledky další studie ukazují, že VPA indukuje expresi CD133, která je závislá na zvýšení acetylace histonů H3 a H4. Při inkubaci s VPA a cytostatikem bylo více CD133+ buněk v proliferační fázi a tyto buňky vykazovaly nižší aktivaci caspázy-3 než buňky CD133-. UKF-NB-3 buňky exprimující CD133 vykazovaly vyšší tvorbu kolonií a neurosfér po ovlivnění VPA na rozdíl od buněk IMR-32, které CD133 neexprimovaly. Indukce CD133 u UKF-NB-3 byla provázena fosforylací Akt a expresí transkripčních faktorů typických pro kmenové buňky (Oct4, Sox2 a Nanog). VPA neindukoval expresi CD133 u buněčných linií s metylovanými promotory CD133 P1 a P3, pokud nebyly preinkubovány s demetylačním činidlem 5-aza-2'-deoxycytidinem.

Lze tedy shrnout, že VPA potencuje cytotoxické účinky DNA poškozujících cytostatik u NB, tato potenciace závisí na sekvenci těchto léků. Exprese CD133 u NB je regulována acetylací histonů a/nebo metylací jeho CpG promotorů, tedy může být ovlivněna terapií VPA. VPA u NB může indukovat CD133+ buňky, které mají velký proliferační potenciál a mají nízkou citlivost k cytostatikům. Přestože naše výsledky potvrzují potenciaci cytotoxického účinku některých cytostatik VPA, ukazují i nový pohled na možná omezení jeho použití u některých nádorů.

Table of contents

List of abbreviations

Akt	Protein kinase B
ALDH1	Aldehyde dehydrogenase1
ALK	Anaplastic lymphoma kinase gene
ATM	Ataxia-telangiectasia mutated
ATR	Ataxia telangiectasia and Rad3-related protein
ATRA	All trans retinoic acid
AZA	5-aza-2'-deoxycytidine
B2M	β-2-microglobulin
Bcl-2	B-cell lymphoma 2
bFGF	Basic fibroblast growth factor
BMPs	Bone morphogenetic proteins
BRCA1	Breast cancer 1
CDDP	Cisplatin
CDK	Cyclin-dependent kinase
CHK2	Checkpoint kinase 2
CI	Cell Index
CoI	Combination index
CSC	Cancer stem cell
C_T	Cycle threshold
DAPI	4',6-Diamidino-2-Phenylindole
DMSO	Dimethyl sulfoxide
DNMTs	DNA methyltransferases
DTT	Dithiothreitol
EGF	Epidermal growth factor
EMT	Epithelial mesenchymal transition
EpCAM	Epithelial cell adhesion molecule
FACS	Fluorescence-activated cell sorting
FBS	Fetal bovine serum
FDA	Food and drug administration
GABA	gamma-Aminobutyric acid
GD2	Disialoganglioside 2
HAND2	Heart and neural crest derivatives expressed 2
HATs	Histone acetyl transferases
HDAC	Histone deacetylase
HDACi	Histone deacetylase inhibitor
HR	Homologous recombination
Hrs	Hours

HVA	Homovanillic acid
IC_{50}	Half maximal inhibitory concentration
IMDM	Iscove's modified Dulbecco's medium
INSS	International neuroblastoma staging system
iPSCs	induced pluripotent stem cells
Klf-4	Kruppel-like factor 4
MASH1	Murine achaete-scute homolog 1
MIBG	Metaiodobenzylguanidine
MS-275	Entinostat
MS-HRM	Methylation-sensitive high resolution melting
MTT	3-(4,5-dimethylthiazol-2-yl)-2,5-diphenyltetrazolium bromide
MYCN	v-myc avian myelocytomatosis viral related oncogene neuroblastoma derived homolog
NB	Neuroblastoma
NC	Neural crest
NF-M	Neurofilament medium polypeptide.
NHEJ	Nonhomologous end joining
Oct4	Octamer-binding transcription factor 4
PBS	Phosphate-buffered solution
PE	Phycoerythrin
PHOX2B	Paired-like homeobox-2
PI	Propidium iodide
PI3K	Phosphatidylinositol-3-kinase
Rb	Retinoblastoma
RIPA	Radio immuno precipitation assay
SAHA	Suberoylanilide hydroxamic acid
SDS	Sodium dodecyl sulfate
SFM	Serum free medium
Sox2	Sex determining region Y-box 2
TCA	Trichloroacetic acid
TEMED	Tetramethylethylenediamine
TRAIL	Tumor necrosis factor -related apoptosis -inducing ligand
TrkA	Tropomyosin receptor kinase A
TSA	Trichostatin A
VCR	Vincristin
VMA	Vanillylmandelic acid
VPA	Valproic acid
VPM	Valpromide
Wnt	Wingless-type MMTV integration site family member

Chapter 1

Introduction

Cancer refers to abnormal cell growth that tends to invade or spread to surrounding tissues or distant parts of the body. Treatment of cancers still belongs among the most serious challenges in modern medicine despite improvements in survival that have been achieved for cancer patients in last decades. The constant development of diagnostic and therapeutic methods led to improvement of survival rate; however many cancers remain difficult to cure.

Tumor represents a complex tissue composed of multiple distinct cell types that react with the surrounding environment and with one another. Cancer cells display hallmarks capabilities that enable them to survive and maintain their growth within the body. Those hallmarks include continuous proliferative signaling, evasion of programmed cell death, escaping growth suppressors, unlimited number of cell divisions, promoting the angiogenesis and the capacity of invasion. Recently, two more emerging characters have been added to those hallmarks including reprogramming of energy metabolism and evading immune destruction (Hanahan and Weinberg, 2011).

Children cancers are different from adult ones and merely constitutes less than one percent of all cancers but even though the tumors are the second leading cause of death in children.

1.1 Neuroblastoma

Neuroblastoma (NB) is the most commonly diagnosed tumor in infants, the most common extracranial solid tumor of childhood and ranked as 3rd most common malignancy in children (Howlader et al., 2016; London et al., 2005; Ward et al., 2014). NB is an embryonic tumor of the autonomic nervous system that arises from neural crest cells (NC). During embryogenesis, cells that arise from the NC are characterized by a remarkable capacity for motility, invasiveness, proliferation, and pluripotency that help them to reach their final destination and to develop multiple cell types (Maguire et al., 2015). The migrating NC cells give rise to the paravertebral sympathetic ganglia in the trunk, the catecholamine secreting chromaffin cells of the adrenal medulla and the paraganglia and this explains the most common sites for the growing NB (Huber, 2006). Therefore, NB most probably originates from a precursor cell that committed to the sympatho-adrenal lineage, but not yet specified as a neuronal or chromaffin cell (Maguire et al., 2015). Development of NB from NC cells is briefly summarized in figure 1.

Both NC cells and metastatic tumor cells must shed their epithelial phenotype and acquire migratory characteristics in a process called epithelial mesenchymal transition (EMT) but the processes are not identical. While NC cells undergo a controlled developmental pathway leading to organogenesis, tumor from NC cells demonstrate dysregulated growth and proliferation resulting in tumorigenesis at the metastatic sites (Maguire et al., 2015). Unlike NB tumors, progressive limitation of pluripotency occurs for the developed NC cells that end to differentiate into appropriate cell types, including Schwann cells, chromaffin cells and melanocytes (Huber, 2006). On contrary, NB cells can retain multipotency and highly express stem cell related genes such as Oct4 (Pezzolo et al., 2011). Even though neuroblasts and stromal cells represent divergent populations in human NB tumors, they were shown to have same genetic abnormalities which suggest that they derived from single origin (Mora et al., 2001). Thus, the role of cancer stem cells (CSCs) in NB growth and progression is being widely accepted (Kamijo, 2012).

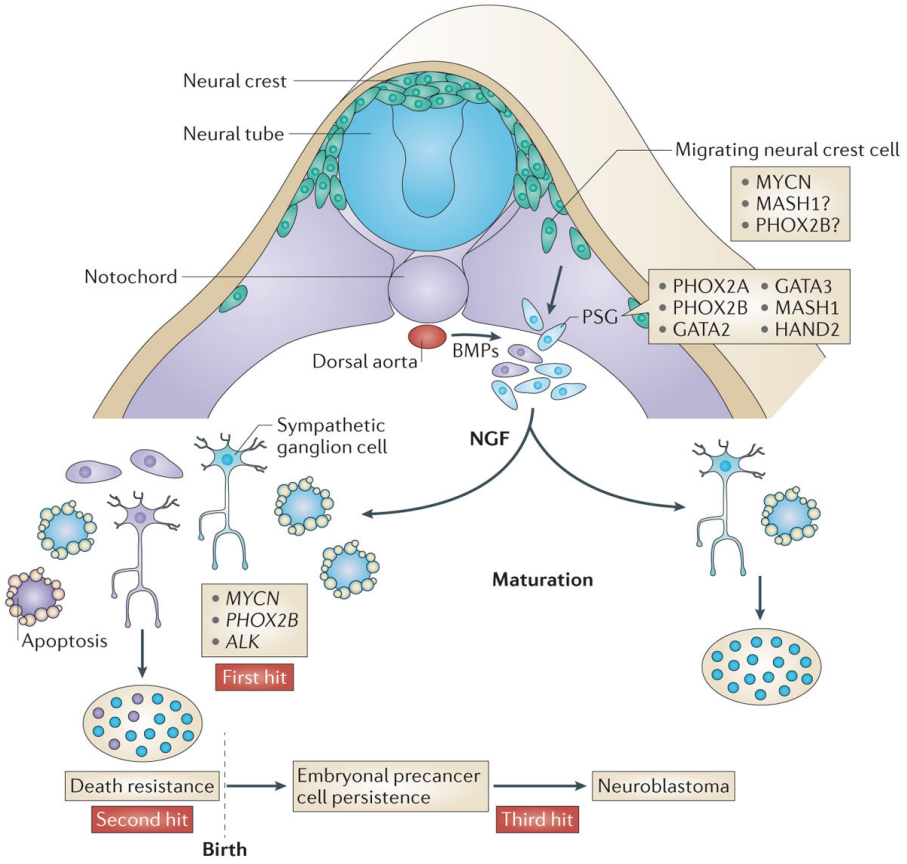

Figure 1: Development of neuroblastoma from NC cells. Migration of neuroblast progenitors from the neural crest occurs under the influence of transcriptional factors including MYCN and bone morphogenetic proteins (BMPs). MYCN mutations and /or alterations in anaplastic lymphoma kinase (*ALK*) and paired-like homeobox 2 (*PHOX2B*) are inherited human susceptibility genes represent a first hit in tumor development. Migrated cells transform into primary sympathetic ganglia (psg) and then divert into neural cells of the mature sympathetic ganglia (sg) or chromaffin cells of the adrenal medulla in a process that requires nerve growth factor (NGF) for maturation otherwise it undergoes apoptotic cell death. Amplification of MYCN reduces the differentiation of susceptible malignant cells and renders it resistant to apoptosis after NGF withdrawal that resulted in postnatal survival of neuroblast rest disease. MASH1, murine achaete-scute homolog 1; HAND2, heart and neural crest derivatives expressed-2; NF-M, neurofilament medium polypeptide. Adapted from (Marshall et al., 2014)

A positive family history of NB is only seen in about 2% of patients (familial neuroblastoma) in which several germ line mutations can be found such as mutation in anaplastic lymphoma kinase gene (*ALK*) (Mossé et al., 2008). ALK is a tyrosine kinase receptor that plays an oncogenic role when mutated in anaplastic large-cell lymphoma as well as in NB. Paired-like homeobox-2 (*PHOX2B*) is

another frequently mutated gene that usually presented by NB in association with congenital central hypoventilation syndrome or Hirschsprung disease reinforcing the connection between NB and defective NC development (Raabe et al., 2008).

1.1.1 Histological types

In fact, the origin of the NB explains why the cellular heterogeneity is a hallmark of these tumors and its cell lines (Walton et al., 2004). Within a single tumor, different cellular phenotypes and maturation stages can be present, particularly neuroblasts, non-neuronal cells (Schwann, perineurial, or satellite) and even melanocytes (Huber, 2006). The volume of Schwannian stroma and maturation of neuroblastic cells in NB tumors are important factors for the prediction of prognosis. Morphologic features of NB can vary from variable aggressive tumor of neuroblasts such as NB (Schwannian stroma-poor) to well differentiated benign tumors of mature ganglia as in ganglioneuroma (Schwannian stroma-dominant) (Du et al., 2008).

According to the cell lines derived from NB, three distinct cellular phenotypic variants can be identified. The first is neuroblast-like cells “N-type” in which cells are rounded with short neuritic processes. This type grows as weakly substrate adherent aggregates and usually shows high plating efficiencies in soft agar. The second is epithelial-like cells “S-type” in which cells are larger, flattened and lacking for neuritic processes. This type adheres strongly to the cultural substrate and usually shows contact inhibition of cell growth. UKF-NB-3 and UKF-NB-4 cell lines which we examined during our studies are shown in figure 2 as examples of human NB cells N-type and S-type respectively. The third cell type is termed I-type because its morphology is intermediate to those of N and S-types. This cell type appears to represent more primitive cells that are capable to turn into both N and S-type cells. It also has been reported to have the highest malignant potential of the three NB cell variants (Walton et al., 2004).

Diagnosis of NB should be fully assessed to evaluate the tumor according to the universally used staging system “international neuroblastoma staging system” (INSS) (Brodeur et al., 1993) and then appropriate therapy can be introduced.

Typical pathological diagnosis is established by biopsy from tumor tissue or without a primary tumor biopsy if the patient has neuroblast in bone marrow with elevated VMA and HVA in urine.

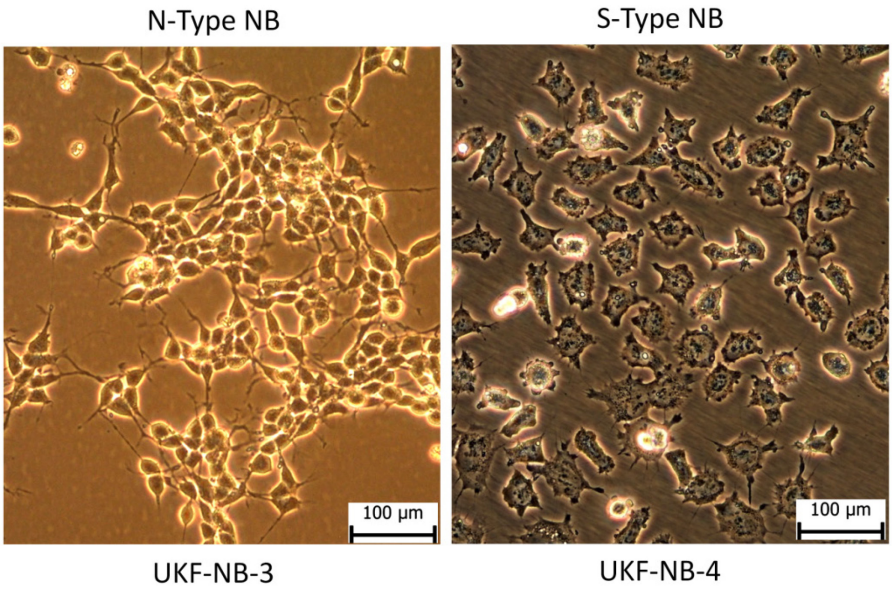

Figure 2: Difference in morphology between S and N-type human NB cells in culture

1.1.2 Prognostic factors

A number of factors have shown to be good predictors for the response and success of treatment together with the staging system. Good prognostic criteria include young age (under 12-18 months), tumor with a favorable histology (low mitotic index, dominant Schwannian stroma**,** few pleomorphism, differentiated), hyperdiploidy of DNA (high DNA index) of NB cells in infants and high expression of nerve growth factor receptor TrkA (Brodeur et al., 2009; Evans et al., 1987; Pinto et al., 2015). Prognostic indicators that are clinically relevant to poor prognosis include chromosomal abnormalities (1p or 11q deletions and 2p24 or 17q gain) (Mueller and Matthay, 2009), poor stromal component, high serum ferritin, neuron-specific enolase and lactate dehydrogenase all impacting the outcome (Evans et al., 1987).

MYCN amplification, an oncogene encodes a Myc family transcription factor, is the most significant factor that is associated with a worse prognosis in NB independent on age or stage. *MYCN* gene is expressed in the post-migratory neural crest, but subsequently downregulated in differentiating sympathetic neurons (Marshall et al., 2014). Tumor cells that amplify *MYCN* fail to express TrkA receptors, which normally allow the binding of nerve growth factor that promotes differentiation, maturation and tumor regression (Hansford et al., 2004). This may explain why NB with amplified *MYCN* is less likely to mature.

1.1.3 Current treatment

Treatment of NB depends on the prognostic group and stage of the tumor. In most of cases, the low-risk form has very good prognosis and high curative rate to extent that stage 4s may regress or mature spontaneously without medical intervention. Basically, surgery is the standard management for stage 1 and 2 while chemotherapy and supportive care is only needed for stage 4s. Chemotherapy such as cyclophosphamide can be introduced in massive liver involvement or in spinal cord compression.

On contrary, prognosis of high-risk NB tumors is still poor because drug resistance arises in the majority of patients and can be rapidly fatal. To date, there are no salvage treatment regimens known to be curative and 50 to 60% of patients with high-risk NB develop a relapse. Treatment of high-risk NB is intensive, starts by very intensive induction chemotherapy, consolidation of remission and finally a maintenance phase to eradicate the minimal residual disease. High doses of chemotherapy that usually lead to toxic effect and different combination must be used. Moreover, surgery for persistent primary tumor and radiation therapy are also frequently used (Maris, 2010).

Newly therapeutic options have been introduced for management of high risk NB such as drugs targeting ALK pathway, retinoids, megachemotherapy with subsequent autologous hematopoietic stem cell transplantation and finally the monoclonal antibody that targets GD2 on NB cells (expression of GD2 is highly restricted on normal tissues) which is recently used routinely for children with high-

risk NB (Fish and Grupp, 2008; Forlenza et al., 2016; Reynolds et al., 2003; Wang et al., 2016). Because the majority of NBs express norepinephrine transporter, the radiolabeling of the norepinephrine analogue (^{131}I-labeled MIBG) has been used as an investigating tool for their detection. Trials to deliver high levels of radiation through this molecule have shown the highest objective response rate of any drug studied in patients with relapse (Matthay et al., 2007).

2.1 Cancer stem cells

Tumor progression has been generally explained by two theories. The stochastic model suggests that cells forming the tumor have the same tumorigenic capacity and can go throw unlimited proliferation cycles. According to this model, the only way to cure the cancer is to eliminate all the cancer cells (Holohan et al., 2013). The second model assumes that tumor is not a homogenous population but contains subpopulation of tumor initiating cells so called cancer stem cells (CSCs). Those CSCs rather than the majority of tumor cells are responsible for driving the tumor growth and progression. This model presumes that CSCs are the main cause for recurrence and metastasis due to their unique characters such as resistance to chemo- and radio-therapy. Thereby targeting CSC can facilitate the mission of chemotherapy to eliminate the tumor as well as decrease the possibility for recurrence (Reya et al., 2001).

The CSCs model gained wide acceptance over the last years, based on continuous observations. In general, the classical chemotherapy and radiotherapy are effective in induction of apoptosis and usually exhibit successful initial effect presented by tumor shrinkage or even clearance of the tumorigenic focal lesions in many cancer types (as detected by imaging methods). Nowadays, combined chemotherapies have shown further improvement in controlling the tumor growth compared to classical chemotherapy or radiotherapy alone. However, the main problem still persists that in later rounds of therapy, the cancer often tends to develop resistance to previous therapies and/or can relapse and metastasize (Lu et al., 2011). CSC model simply explains this problem that the effect of the

chemotherapy is incomplete because it could not target the small subpopulation of CSCs with their unique resistant mechanisms which result in their production of more aggressive clones (Han et al., 2013). For this reason, many thoughts come into belief that complete resection of the tumor with clean margins and not chemotherapy is the only curative treatment for the majority of localized tumors (Marshall et al., 2014). Figure 3 illustrates the effective cancer therapy in the viewpoint of cancer stem cell theory model.

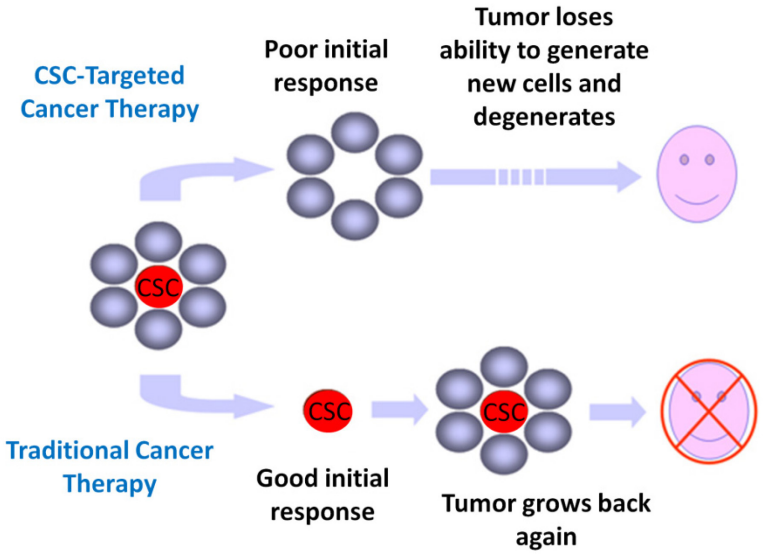

Figure 3: Conventional chemotherapy therapy versus stem cell targeted therapy.

CSCs and normal stem cells share many similarities but the hallmark features of CSCs are self- renewal capacity, the generation of the heterogeneous lineages of cancer cells that comprise the tumor and potent tumorigenicity when injected into immunocompromised mice (Han et al., 2013). CSCs can divide into two identical daughter CSCs (symmetrical self-renewing capacity) or into one daughter CSC and one differentiated progenitor cell (asymmetrical self-renewing cell division) and thus can keep their own clone and expand the tumor on the same time (Clarke et al., 2006).

Identification of CSCs is not a straight forward process because the surface markers of CSCs in one tissue are not necessary shared with the markers of CSCs in other tissues; thereby detection of CSCs based on surface markers

should be associated with other functional assays. Generally, CSCs can be identified by the presence of a single or combination of specific markers such as (CD34+/CD38-) in leukemia, (CD133+, EpCAM^{high}/CD44+, ALDH1+) in colorectal carcinoma and CD133+ in some brain tumors and NB (Kamijo, 2012). Additionally, several assays were shown to be helpful to identify CSCs such as sphere forming assays, Hoechst dye exclusion (side population), detection of enzymatic activity (e.g., ALDH1), transcription factors expression (e.g., Oct4 and Sox2), serial colony forming assays (replating assays) and migration assays (Han et al., 2013).

Targeting CSCs should be focused on the molecules and characters contribute to their therapeutic resistance. For instance, targeting the CSCs´ molecular signaling pathways (e.g. Hedgehog, Notch, Wnt/b-catenin, Bcl2), targeting CSCs´ markers (e.g. anti CD133 antibody drug conjugates), targeting drug detoxifying enzymes (e.g. blocking ALDH activity), targeting drug efflux pumps (e.g. inhibition of ABC drug transporters), targeting CSC niche and cells in the quiescent state (e.g. combination of interferon-α, granulocyte colony stimulating factor and arsenic trioxide with chemotherapeutic agents) and induction of CSC differentiation (e.g. retinoic acid and HDACi). Combined chemotherapy with previously mentioned agents can be of great value to eradicate the cancer but more selective agents should be designed to target only CSCs rather than healthy cells (Dragu et al.,, 2015). Different treatment strategies that target CSCs are listed in figure 4.

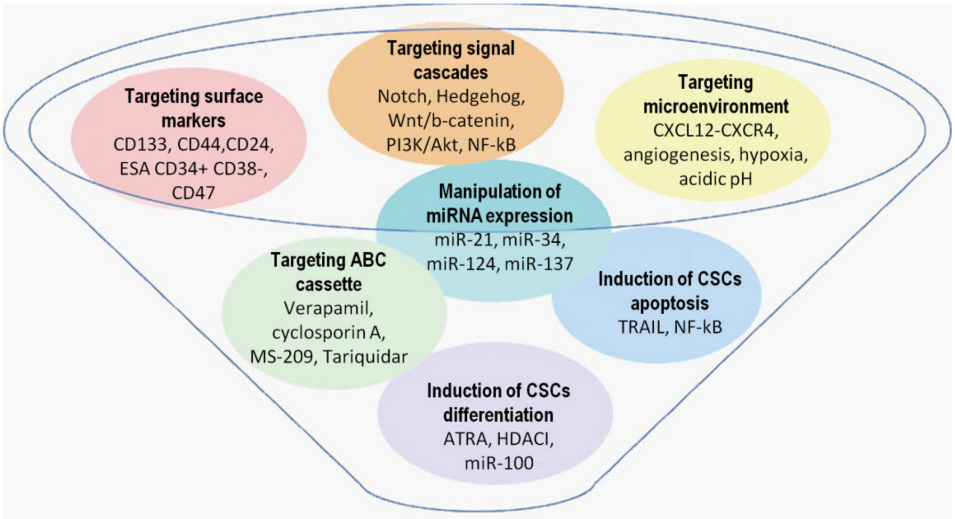

Figure 4: Therapies targeting cancer stem cells. Adapted from (Dragu et al., 2015)

1.2.1 Prominin-1

Prominin-1, also known as CD133, is a pentaspan transmembrane glycoprotein that is expressed on neural precursor cells of postnatal cerebellum (Lee et al., 2005) and several brain tumor cells (Singh et al., 2004). CD133+ cells display CSCs features such as self-renewal capacity (Lathia et al., 2011), high clonogenicity (Yin et al., 2007), high proliferation potential *in vitro* (Tirino et al., 2008) and formation of neurospheres in serum free medium (Brescia et al., 2013). Several groups have also shown that sorted CD133+ cells displayed greater tumorigenicity and resistance to chemotherapeutic agents compared to CD133− cells (Koyama-Nasu et al., 2013; O'Brien et al., 2007; Todaro et al., 2007; Vangipuram et al., 2010; Wu et al., 2013). In addition, high expression of CD133 has been linked to a poor prognosis in several tumors including NB (Horst et al., 2009; Liu et al., 2006; Sartelet et al., 2012; Shin et al., 2013; Tong et al., 2008). Furthermore, Wei *et al*., have recently clarified the functional association of CD133 molecule in the activation of PI3K/Akt pathway that promotes the tumorigenic capacity in glioma stem cells (Wei et al., 2013). PI3K/Akt pathway is considered to be one of the most potent pro-survival signaling pathways that is activated in many types of cancer and associated with poor outcome in NB (Opel et al., 2007). Activation of Akt pathway through membranous CD133 is illustrated in figure 5.

It has been reported that CD133 transcription is controlled by epigenetic modifications such as histone acetylation and promoter methylation (Baba et al., 2009; Irollo and Pirozzi, 2013; Yi et al., 2008). Thus, it is supposed that this correlation between CD133 expression and acetylation status of histones enables the HDAC inhibitors to act as potent regulators of CD133 transcription. In addition, CD133 promoters P1, P2 and P3 have high CpG content therefore they may undergo DNA methylation with consequent repression of gene transcription (Shmelkov et al., 2005). DNA methyltransferases (DNMTs) methylate the DNA in areas rich in CpG dinucleotides that are often found in clusters within gene promoters. Methylation of CpG clusters in gene promoters is associated with transcriptional silencing (Bird, 2002). Treatment with cytidine analog 5-azacytidine

depletes DNMTs from the cell and reduces DNA methylation by forming irreversible adducts with DNMTs during cell division (Jones and Taylor, 1980)

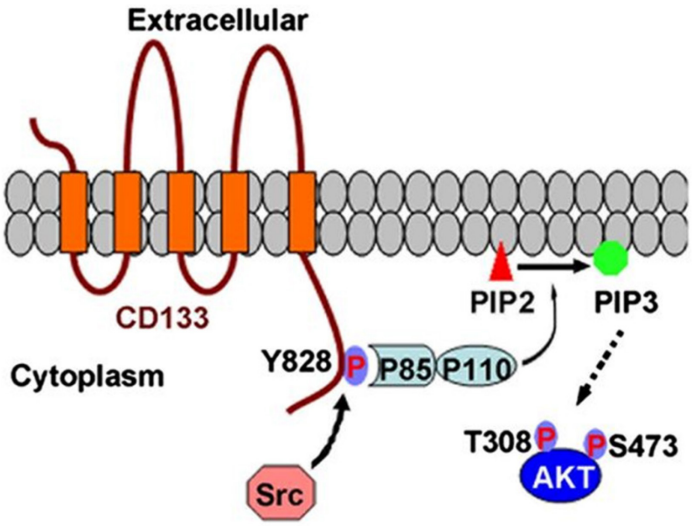

Figure 5: CD133/PI3k/Akt signaling axis. CD133 is an upstream activator of PI3K; phosphorylated Y828 residue in CD133 cytoplasmic tail binds to PI3K regulatory subunit p85, resulting in the activation of PI3K/Akt pathway**.** Adapted from (Wei et al., 2013)

1.3 Histone deacetylase inhibitors

The term “Epigenetics” refers to changes in the genome that affect gene expression but do not involve a change in the nucleotide sequence. The epigenetic alterations are stable and heritable but differ from genetic mutations that they are generally reversible (Ceccacci and Minucci, 2016). Epigenetic changes such as DNA methylation and posttranslational modifications of histones including acetylation, methylation and phosphorylation can greatly alter the transcription regulation of the gene expression either by activation or repression. Thus, it is not surprising that epigenetic changes are associated with cancer development (Li and Seto, 2016).

Nuclear DNA is found in association with histones and non-histone proteins. The basic packaging unit of chromatin is the nucleosome which is formed of two

copies of each histone H2A, H2B, H3 and H4 forming octamer. Histones are rich in lysine and arginine which confer positive charges to bind with the negatively charged DNA. Acetylation of histone tail lessens their overall positive charges that disrupt the interaction with the negatively charged DNA, leading to decompression of chromatin structure (Dokmanovic et al., 2007). Histone acetylation is tightly controlled by a balance between the opposing action of histone acetyl transferases (HATs) and histone deacetylases (HDACs). HATs add acetyl groups to the histone tails in the nucleosomal structure which turn chromatin less compact and relaxed, allowing access for transcription factors with consequent activation of many genomic regions. HDACs work on opposite direction; turn the chromatin dense, compact and generally silenced (Shahbazian and Grunstein, 2007) (see figure 6).

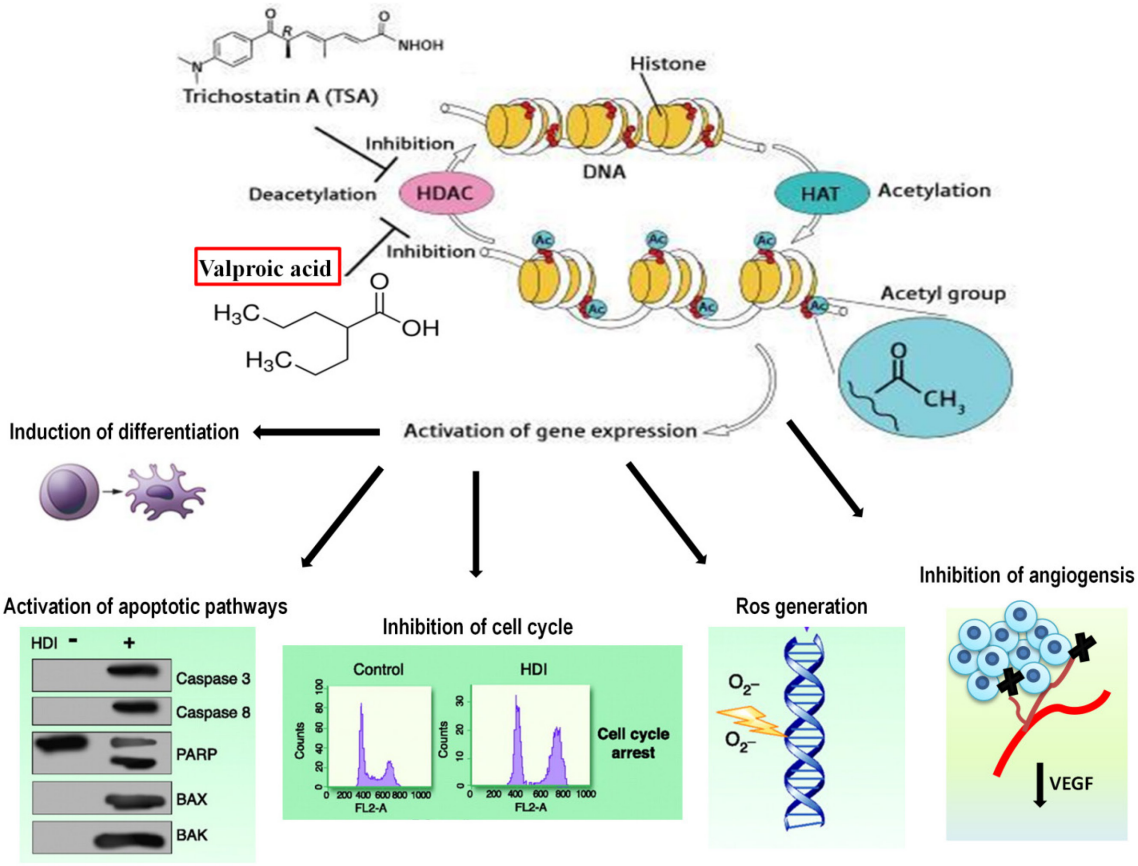

Figure 6: mechanisms of cytotoxicity mediated by HDACi in cancer cells. Adapted and modified from (Schrump, 2009)

In fact, enhanced expression of HDACs is linked to a variety of hematological and solid malignancies as well as their poor outcome. For example, overexpression of HDAC8 and HDAC10 was associated with advanced stage disease and poor survival in NB (Oehme et al., 2013; Rettig et al., 2015). Knockdown of those HDACs in NB cancer cells resulted in cell cycle inhibition, induction of apoptosis and differentiation with significant increase of sensitization to cytotoxic drug treatment; hence the rational for targeting HDACs in cancer therapy. High expression of different HDACs was also reported in a wide range of malignancies such as HDACs 2,5 and 9 in medulloblastoma (Ecker et al., 2015; Milde et al., 2010), HDAC2 in lung cancer (Jung et al., 2012), HDAC4 in gastric cancer (Colarossi et al., 2014) and HDAC11 in rhabdomyosarcoma (Bolden et al., 2006). In breast (Müller et al., 2013), colorectal (Weichert et al., 2008a) and prostate cancers (Weichert et al., 2008b); HDACs 1,2 and 3 were over expressed. Moreover, HDACs also deacetylate a large number of non-histone substrates. For example, acetylation of the oncosuppressor p53 is regulated by HDAC1 and HDAC2 and their over-expression can inhibit its function (Insinga et al., 2004). HDAC inhibitors (HDACi) are promising anticancer drugs because they can reestablish the cellular acetylation homeostasis which is often disturbed in cancer, and thus may enhance the recovery of the repressed tumor-suppressive pathways including cell cycle regulators and DNA repair pathways (Ceccacci and Minucci, 2016). Dynamic formation of chromatin does not only lead to transcriptional activation of different genes but also makes DNA more accessible for DNA-targeted chemotherapeutics (Groh et al., 2015). In contrast to normal cells, HDACs seem to be essential in tumor cells for survival and maintenance of a set of pathways that support their uncontrolled growth which provide additional therapeutic potential of HDACi (Dawson and Kouzarides, 2012).

HDACs are classified according to their homology to yeast enzymes into four classes: Class I is comprised of (HDAC 1, 2, 3, and 8), Class IIa (HDAC 4, 5, 7, and 9), class IIb (HDAC 6 and 10). Class III (NAD-dependent protein deacetylases, consist of seven sirtuins) and Class IV contains only HDAC11. The broad spectrum HDACi inhibitors target only the zinc-dependent deacetylases

(classes I, II, IV) by interfering with HDACs Zn^{+} binding site; thereby inhibiting their enzymatic activity (Li and Seto, 2016). HDACi are classified according to their chemical structure into 4 main groups; hydroxamic acid [ex. vorinostat (SAHA), belinostat, panobinostat and trichostatin A (TSA)], cyclic tetrapeptide [ex. romidepsin], benzamide derivatives [ex. entinostat (MS-275)], short chain fatty acids [ex. valproic acid (VPA) and butyrate]. A number of HDACi including VPA are currently under evaluation in clinical trials while vorinostat, romidepsin, belinostat and panobinostat have already been registered for treatment of some types of T-cell lymphomas and multiple myeloma (Lee et al., 2015; Mottamal et al., 2015). Overview of HDAC inhibitors are shown in table 1.

Despite of the fabulous effects of the HDACi in the preclinical studies that showed potent anticancer effects presented by induction of apoptosis, differentiation, cell cycle arrest, inhibition of angiogenesis, deactivate DNA repairing in cancer cells and reduction of the metastatic potential; however, their clinical outcomes in solid tumors are disappointing when used as monotherapy (Li and Seto, 2016). It is not entirely clear this diversity in the response to HDACi but the lack of selectivity and the poor pharmacokinetic properties along with the side effects and toxicity limit the use of HDACi in patients (Li and Seto, 2016). Although, the broad spectrum inhibitors of HDACs may reactivate some tumor suppressors, they can also affect numerous other genes, for instance; induction of pluripotency in the cancer cells (Kong et al., 2012).

HDACi are continuously explored for being used in combination with other antitumor agents to optimize their efficacy and toxicity. Combining HDACi with primary chemotherapeutic agents that induce DNA damage has shown very promising results in preclinical research studies (Groh et al., 2015). HDAC inhibition might resensitize tumor cells to the primary agents and overcome therapy resistance**.** Therefore, combinations chemotherapy and/or radiotherapy with HDAC inhibitors have been used in clinical trials (Ma et al., 2009).

Table 1: Overview of selected histone deacetylase inhibitors. Adapted from (Ceccacci and Minucci, 2016).

Class	HDAC Inhibitor	Target HDAC Class	Clinical Status
hydroxamic acids	Trichostatin A	pan	preclinical
	SAHA	pan	approved for cutaneous T-cell lymphoma
	Belinostat	pan	approved for peripheral T-cell lymphoma
	Panabiostat	pan	approved for multiple myeloma
	Givinostat	pan	phase II clinical trials—relapsed leukemia and multiple myeloma
	Resminostat	pan	phase I and II clinical trials—hepatocellular carcinoma
	Abexinostat	pan	phase II clinical trial—B-cell lymphoma
	Quisinostat	pan	phase I clinical trial—multiple myeloma
	Rocilinostat	II	phase I clinical trial—multiple myeloma
	Practinostat	I, II and IV	phase II clinical trial—prostate cancer
	CHR-3996	I	phase I clinical trial—advanced/metastatic solid tumors refractory to standard therapy
short chain fatty acids	Valproic acid	I, IIa	approved for epilepsia, bipolar disorders and migraine, phase II clinical trials—several studies
	Butyric acid	I, II	phase II clinical trials—several studies
	Phenylbutyric acid	I, II	phase I clinical trials—several studies
benzamides	Entinostat	I	phase II clinical trials—breast cancer, Hodgkin´s lymphoma, non-small cell lung cancer, phase III clinical trial—hormone receptor positive breast cancer
	Tacedinaline	I	phase III clinical trial—non-small cell lung cancer and pancreatic cancer
	4SC202	I	phase I clinical trial—advanced hematological malignancies
	Mocetinostat	I, IV	phase II clinical trials—Hodgkin´s lymphoma
cyclic tetrapeptides	Romidepsin	I	approved for cutaneous T-cell lymphoma
sirtuins inhibitors	Nicotinamide	all class III	phase III clinical trial—laryngeal cancer
	Sirtinol	SIRT 1 and 2	preclinical
	Cambinol	SIRT 1 and 2	preclinical
	EX-527	SIRT 1 and 2	cancer preclinical, phase I and II clinical trials—Huntington disease, glaucoma

The role of HDACs in DNA-damage repair responses has been shown by numerous studies which explained by the critical role of HDACs in the remodeling of chromatin and maintaining dynamic acetylation equilibrium of DNA-damage-related proteins (Li and Zhu, 2014). For instance, HDAC1 and HDAC2 are recruited to DNA-damage sites to deacetylate histones H3K56 and H4K16, and

facilitate nonhomologous end-joining (NHEJ) suggesting their direct role during DNA replication and double-strand break repair. HDAC3 is also associated with DNA-damage control, although it is not localized to double-strand break DNA-damage sites (Miller et al., 2010). Moreover, class I HDACs regulates other proteins involved in the DNA-damage response, including ATR, ATM and BRCA1 (Thurn et al., 2013). p53 is a tumor suppressor gene that can activate DNA repair proteins to induce cell cycle arrest or transactivate genes involved in the apoptotic machinery. It has been shown to be regulated by HDACs and thus greatly influenced by HDACi. HDAC1–3 directly interact with p53 protein and reduce its activity (Juan et al., 2000). HDAC2 decreases the presence of p53 at the promoter of its target, c-Myc, in breast cancer cells (Harms and Chen, 2007). HDAC4 colocalizes with tumor suppressor p53-binding protein-1 (53BP1) after double strand DNA (dsDNA) break and its depletion reduces 53BP1 expression and abrogates the DNA-damage-induced G2 checkpoint (Kao et al., 2003).

dsDNA breaks are basically repaired by two mechanisms, homologous recombination (HR) and nonhomologous end joining (NHEJ). HR requires the activation and recruitment of ATM to sites of damage which in turn activates various proteins including BRCA1 and CHK2 (Gatei et al., 2000). To initiate DNA damage response by NHEJ mechanism, Ku70–Ku80 heterodimer of the DNA-dependent protein kinase (DNA-PK) catalytic subunit must be recruited to the site of damage. Both repairing mechanisms will result in phosphorylation of DNA damage response protein p53. In relation to these data, HDACi have shown reduction of dsDNA-break repair in many studies. In melanoma cell lines, sodium butyrate decreased the expression of NHEJ components Ku70 while in prostate cancer cells, vorinostat and TSA caused a significant increase in the acetylation of Ku70 that interfere with its DNA binding capability and reduced the ability for dsDNA repair (Chen et al., 2007). HR is also downregulated in prostate cancer cells by HDAC inhibition which resulted in decreased expression of DNA damage repair genes *Rad51*, *CHK1* and *BRCA1* (Kachhap et al., 2010). Downregulation of BRCA1 (involved in HR repair mechanism) was also noticed in squamous carcinoma cells after treatment with TSA and in head and neck cancer cell lines by

phenyl butyrate that sensitized the cancer cells to cisplatin (Burkitt and Ljungman, 2008; Zhang et al., 2007). Deactivation of DNA repairing in cancer cells by HDACi has showed to enhance the efficacy of the combined ionizing radiation in various cancer cell lines including prostate (Camphausen et al., 2004), brain (Camphausen et al., 2005), colon (Folkvord et al., 2009), melanoma and lung (Kim et al., 2010; Munshi et al., 2005). HDACi-mediated radiosensitization was most effective when cells were pretreated with HDACi followed by ionizing radiation (Nome et al., 2005).

1.3.1 Valproic acid

Valproic acid (VPA) is a branched short-chain fatty acid that was synthesized in 1882 by Burton (Burton, 1882). It has been successfully used for the treatment of different types of epilepsy and other neurological disorders such depression and migraine. The main mechanism of VPA in controlling the convulsion is to increase the inhibitory effect of the neurotransmitter gamma amino butyrate (GABA) either by inhibition of GABA degradation or increases its synthesis in the brain cells (Mesdjian et al., 1982). It also decreases the excitatory signals via blocking of Na^+ channels, Ca^{2+} channels, and voltage-gated K^+ channels in the brain (VanDongen et al., 1986). During the last few years, VPA has been under the spot light as a drug can be used in cancer therapy. This interest in VPA was based on its anti-cancer effect due to inhibition of HDACs class I (HDAC 1, 2, 3, and 8) and Class IIa (HDAC 4, 5, 7, and 9) with bearing in mind that it is already a registered drug and has been used safely for long term treatment of epilepsy (Boudadi et al., 2013). In addition, it can cross the blood brain barrier and apply its action on brain tumors due to its lipid nature (Lucke et al., 1994).

VPA as well as other HDACi have anti-proliferative effect and can suppress tumor growth via up-regulation of cyclin-dependent kinase (CDK) inhibitors or down-regulation of cyclins (cyclin D1) and CDKs (CDK4/6). For example, inhibition of HDAC 1, 2 and 5 leads to increase the expression of *p21* and *p27* genes which represent the basic players in cell cycle inhibition. Other mechanism includes reactivation of *Rb* function with subsequent inhibition of transcription factor E2F

leading to cell cycle inhibition. In fact, VPA can induce both G_1 as well as G_2/M phase arrest of cancer cells which implicate its pleiotropic action (Li and Seto, 2016).

VPA has shown to induce apoptosis in cancer cells. A number of different mechanisms are involved such as upregulation of proapoptotic proteins as well as increase the molecules of the extrinsic apoptotic pathway. VPA not only induce apoptosis and cell cycle arrest but it also has anti-angiogenic effects and can induce tumor differentiation (Hrebackova et al., 2010). However, the exact anticancer mechanism of VPA is still unclear and it exhibits different effects in various tumors. For instance, VPA has shown to inhibit the invasiveness in bladder cancer but not in prostate cancer cells (Chen et al., 2006) and it did not induce cell cycle inhibition in some NB cell lines such as SH-SY5Y and SK-N-BE (Stockhausen et al., 2005). Moreover, the expression of the pluripotency factor *Fgf4* decreased in F9 embryonal carcinoma cell line after treatment with VPA while elevated in P19 cells (Shi et al., 2011). Collectively, these remarks lead to suggest that the anticancer effect of VPA may be cancer type specific and dose dependent (Kretsovali et al., 2012). On the other hand, the growing assumption about the role of HDAC inhibitors as potential candidates for inducing the pluripotent stem cells has been confirmed in some studies (Higuchi et al., 2015). For example, the significant effect of VPA on amplification and maintenance of human hematopoietic stem cells (Burba et al., 2011; De Felice et al., 2005), enhancement of the EMT of colorectal cancer cells (Feng et al., 2015) and induction of CD133 in human glioma (Tabu et al., 2008) have been reported in different studies. These previous results raise a question whether treatment with VPA may amplify cancer cells with stem cell features such as CD133+ cells.

1.4 Pluripotency and histone deacetylase inhibitors

Recently, the generation of functioning stem cells from differentiated adult cells could be achieved in Shinya Yamanaka’s lab in Japan and he awarded Nobel Prize for this pioneer invention in 2012. Shinya Yamanaka found that generation of

the induced pluripotent stem cells (iPSCs) was successfully achieved by the transduction of four basic transcription genes *Oct4*, *Sox2*, *c-Myc*, and *Klf-4* into mouse fibroblast (Takahashi and Yamanaka, 2006) and human fibroblast (Takahashi et al., 2007). Later on, different set of genes (*Oct4, Sox2, Nanog*, and *Lin28*) were also successfully used (Yu et al., 2007). Currently, mouse iPSCs can be generated by reprogramming a single gene such as *Oct4* (Li et al., 2011). The generated iPSCs showed unlimited self-renewal capacity and were pluripotent despite that the molecular makeup of these cells were not identical to an embryonic stem cells (Hochedlinger and Plath, 2009). However, the technology used for reprogramming the human cells to iPSC by virus mediated delivery of transcriptional factors was of very low efficiency and time consumable. Moreover, permanent integration of oncogenes such as *c-Myc* is a serious concern in therapeutic applications. Therefore, other reprogramming technologies have been developed to replace the use of viral integration for iPSC production (Higuchi et al., 2015).

In fact, epigenetic changes including histone modification has been shown to play a valuable role in regulating both stem cell self-renewal and pluripotency. Therefore, several epigenetic modifying enzymes molecules have been used to promote the somatic cells reprogramming into iPSCs such as DNA methyltransferases inhibitors, HDACs inhibitors, histone methyltransferases inhibitors, and histone demethylases inhibitors (Kretsovali et al., 2012). Surprisingly, among HDAC inhibitors and all other epigenetic modifiers, VPA exhibited the most potent effect on induction of iPSCs and enhanced the reprogramming efficiency more than 100-fold (Huangfu et al., 2008) that wasn't well understood why it has the most potent influence compared to other HDACi. In agreement with these data, the combination of *Oct4, Sox2*, and VPA was sufficient to reprogram somatic cells into pluripotent stem cells with a similar efficiency to the initial factors used (*Oct4, Sox2, c-Myc* and *Klf4*) (Huangfu et al., 2008).

Differentiation is a process of gradual loss of potency that ends up to the point where specific cell fate is acquired. Effect of HDACi on the differentiation of normal and cancer cells is showing controversy. The differentiating effect of the HDAC

inhibitors was suggested to rely on the dose of HDACi and the differentiation status of the cells. In other words, HDACi may exert an anti-differentiation effect when low doses are applied, whereas higher doses applied on undifferentiated cells provoke differentiations (Karantzali et al., 2008; McCool et al., 2007).

The generation of iPSC cannot be performed with the absence of the transcription factor Oct4 which has often been used as a marker of stemness and is highly expressed in side population cells of NB (Hämmerle et al., 2013). Additionally, the differentiated cells show reduced or absence expression of this marker. It is the core regulatory gene maintaining a multipotent state (self-renewal) of neural stem cells. It has been reported that over expression of *Oct4* is associated with poor prognoses in NB and promotes aggressiveness of *MYCN*-amplified NB cells (Kaneko et al., 2015). Furthermore, Oct4-positive NB cells are resistant to conventional chemotherapy (Kaneko et al., 2015). On contrary, it is downregulated on differentiation of NB cells.

HDACi seem to be a promising group of anti-cancer drugs, particularly in combination with other anti-cancer drugs and/or radiotherapy. Their use in the combination with other drugs and the schedule of such drug combinations need to be investigated in both preclinical and clinical studies. Indeed, recently, we have found that sequence of HDAC inhibitor and DNA-damaging drug is important to increase their cytotoxicity (Groh et al., 2015). The other most important question is whether the pan-HDAC inhibitors or the selective inhibitors will be more efficient in different types of cancers. Furthermore, assumptions about the role of some HDAC inhibitors particularly VPA as cancer stem cells inducers (Khalil et al., 2016; Rudà et al., 2016) or about the phenomenon that HDAC inhibition may enhance the EMT of cancer cells (Feng et al., 2015; Wu et al., 2016) need to be further explored. However, the great potential for epigenetic therapies that is caused by the fact that epigenetic changes are reversible might be considered.

1.5 Aim of the study

The main aim of the presented thesis is to explore the synergistic effect as well the possible limitations of treatment high risk NB cells with HDACi along with commonly used cytostatics. In this work, we could significantly explore and discuss the following issues:

- Cytotoxic effect of low dose of VPA on NB cell lines.
- Cytotoxic effect of low dose of VPA in combination with different cytostatics on NB cell lines.
- Effect of epigenetic alterations on expression of CD133
- Effect of VPA on the expression of CD133
- Effect of CD133 induction on activation of Akt pathway.
- Effect of induction of VPA on the pluripotent transcription factors
- Distribution of the CD133 in the cell.

Chapter 2

Materials and methods

2.1 Chemicals

The following chemicals were purchased from *Sigma Chemical Co., (St. Louis, MO, USA)* unless written otherwise:

- Potassium chloride (KCl), sodium chloride (NaCl) and magnesium chloride ($MgCl_2$).
- Trizma® base.
- Glycin.
- Triton™X-100.
- Igepal CA-630.
- Paraformaldehyde.
- Dithiothreitol (DTT).
- Trichloroacetic acid (TCA).
- 3-(4,5-dimethylthiazol-2-yl)-2,5 diphenyltetrazolium bromid (MTT).
- 1,2-bis(dimethylamino) ethan (TEMED).
- Sodium dodecyl sulfate (SDS); *Thermo Fisher Scientific (Waltham, MA, USA)*
- Sulphuric acid*; Merck Millipore (Darmstadt, Germany).*
- Acetic acid, Giemsa stain and Methanol; *Penta (Prague, Czech Republic).*

2.1.1 Solvents and buffers

- Dimethyl sulfoxid (DMSO); *Amresco (Solon, Ohio).*
- *N,N*-Dimethylformamide.
- Phosphate buffered saline (PBS); *Thermo Fisher Scientific (Waltham, MA, USA).*
- Tris buffered saline (TBS); *Thermo Fisher Scientific (Waltham, MA, USA).*
- Hypotonic lysis buffer (10 mM Tris-HCl pH 8.0, 1 mM KCl, 1.5 mM $MgCl_2$).
- RIPA buffer [25 mM Tris pufr; pH=7,6 containing 150 mM NaCl, 1% detergent Igepal CA-630, 1% Sodium deoxycholate and 0,1% Sodium dodecyl sulfate (SDS)].
- Blocking buffer (PBS containing 0.5% BSA and 0.2% Triton X-100).
- Bovine serum albumin (BSA); *Biorad (Herkules, CA, USA).*
- Blotting grade blocker “Non-fat dry milk”; *Biorad (Herkules, CA, USA).*
- Stripping buffer (0.5 M NaCl and 0.5 M acetic acid).
- TWEEN® 20.
- TBST (TBS + TWEEN).

2.1.2 Culture media and nutritional factors

All the used media components were purchased from *Gibco Life Technologies (Carlsbad, CA, USA)* unless mentioned otherwise.

- Iscove’s modified Dulbecco’s medium (IMDM).
- Ham´s F12 Nutrient Mixture,
- Advanced DMEM
- Fetal bovine serum (FBS)
- EGF, bFGF; *Invitrogen (Carlsbad, CA, USA)*
- B27 supplement.
- Penicillin / streptomycin.
- Trypsin, Accutase® and heparin; *Sigma Chemical Co., (St. Louis, MO, USA).*
- All cultural plates and dishes were purchased from *TPP® tissue culture dishes (Sigma.)*

2.1.3 Histone deacetylase inhibitors

Sodium salt of valproic acid (VPA), trichostatin-A (TSA), vorinostate (SAHA), entinostat (MS-275) and valpromide (VPM) were purchased from *Sigma Chemical Co. (St. Louis, MO, USA)*. Figure 7 shows the difference in chemical structure between VPA and its analogue valpromide.

VPA was dissolved in IMDM as 200 mM stock solution and stored for maximum 1 week at 4°C. Other HDAC inhibitors (TSA, SAHA and MS-275) as well as VPM "VPA analogue" were dissolved in DMSO which was applied with the drugs in final concentration ranged from 0.02% to 0.3%.

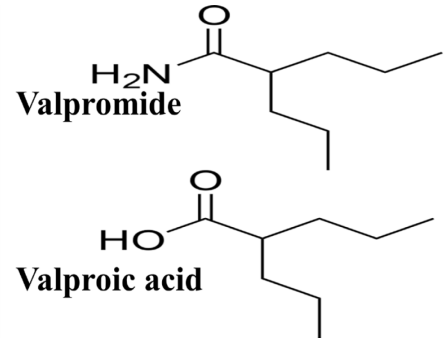

Figure 7: Chemical structures of VPA and valpromide.

2.1.4 Cytostatics

Vincristine sulfate (VCR) 2mg/2ml and cisplatin (CDDP) 50mg/100ml were obtained from *Teva Pharmaceuticals (Prague, Czech Republic)* and *PLIVA-Lachema (Brno, Czech Republic)* respectively. Water solution of cisplatin was prepared according to the manufacturer's instructions. Etoposide was purchased from Sigma (dissolved in DMSO; final volume of DMSO did not exceed 0.5%).

2.2 Cell lines

Human NB cell lines UKF-NB-3 and UKF-NB-4 (Cinatl et al., 1990), established from bone marrow metastases of high-risk NB, were kindly provided by *Prof. J.*

Cinatl, Jr. (J.W. Goethe University, Frankfurt, Germany). IMR-32 and SH-SY5Y were purchased from *ECACC, Salisbury, UK*. Cells were cultivated in IMDM supplemented with 10% FBS and 1% penicillin/streptomycin. Cultured cells were grown in a humidified incubator at 37°C and 5% CO_2. The examined NB cell lines were growing adherent to culture plates and harvested cells did not exceed 90% confluence at time of performing experiments. Cells were kept in exponential growth by passaging the cells every 3-4 days. Daily culture observation was performed using inverted microscope *Olympus IX51 (Olympus, Tokyo, Japan*).

2.3 MTT assay

The principle of MTT assay is that NAD(P)H-dependent cellular oxidoreductase enzymes in living cells can reduce the yellow MTT dye to insoluble purple colored formazan. Therefore, the density of the formed color reflects the number of viable cells.

Cells in exponential phase of growth were seeded at 1×10^4 cells per well in a 96-well microplate. Hundred micro liters of medium were added to each well in the first column of the plate. Through the 2nd to 12th column was added 50µl of medium per well. Then, 50µl of the highest concentration of tested drug were added to wells of the 3rd column, mixed gently and serial dilution was made in the successive wells. This procedure allows the drug to be diluted to half concentration in each following well. Finally, 50µl of cells were added through 2nd to 12th columns and plate was incubated for 72 hrs at 37 °C and 5% CO_2 saturated atmosphere. After 72 hrs, 50µl of the MTT solution (2 mg/ml PBS) was added to all wells. The microplate was incubated for 3 hrs and cells lysed by adding 100µl of 50% *N*, *N*-dimethylformamide containing 20% of SDS (pH 4.5). The absorbance at 570 nm was measured for each well by multiwell ELISA reader *VERSA max (Molecular devices, CA, USA).* The mean absorbance of medium control was subtracted as a background. The viability of control cells was taken as 100% and the values of treated cells were calculated as a percentage of control. The IC_{50}

values represented the concentration of the tested drug that induces 50% less living cells than in control.

In our experiments, the IC_{50} values of VPA, CDDP and VCR regards NB cell lines after 72 hrs of treatment was assessed. The average value was calculated from at least 3 independent experiments using the linear regression of the dose-log response curves by SOFTmaxPro software. For the dose response curve, a serial dilutions of the mentioned drugs (0.1–50 mM VPA), (0.08–40 μM CDDP) and (0.04–20 nM VCR) were used.

2.4 Real-time monitoring of cell viability by xCELLigence system

The xCELLigence RTCA DP Instrument *(ACEA Bioscience Inc., San Diego, CA, USA)* placed in a humidified incubator at 37˚C and 5% CO_2 was used for real-time label-free monitoring of cell viability (Ke et al., 2011). The presence of adherent cells at the electrode-solution interface impedes electrons flow across gold microelectrodes fused to the bottom surface of a micro-plate well. The magnitude of this impedance is dependent on the number of cells, the size and shape of the cells, and the cell-substrate attachment quality. Importantly, neither the gold microelectrode surfaces nor the applied electric potential (22 mV) have an effect on cell health or behavior. Cells in a density of 2×10^4 were seeded into 16-well plates for impedance-based detection. Each condition (ex. control, 1 mM VPA, 4 μM cisplatin and combination of 1 mM VPA with 4 μM cisplatin) was tested in duplicate. Cell index (CI) was monitored every 30 min along the desired period and data recorded by the supplied RTCA software.

2.5 Assessment of apoptosis

In normal live cells, phosphatidylserine (PS) is a component of the inner leaflet of the cell membrane. However, one of the early signs of apoptosis is translocation of PS to the outer leaflet of the plasma membrane. Annexin V is a Ca^{2+} dependent phospholipid-binding protein that shows high affinity for PS in an environment with

high calcium concentration. Annexin V labeled with a fluorophore can strongly bind to the cell membrane of apoptotic cells. On the other hand, PI can bind tightly to the nucleic acids in dead cells while it is impermeant to live or early apoptotic cells. Thereby, double staining with Annexin V and PI can easily distinguish live, early apoptotic and late apoptotic or necrotic cells. Other method to detect the apoptosis is to demonstrate the cleavage of the effector caspases such as caspase-3. Both methods we used in our experiments as follow

2.5.1 Annexin V / propidium iodide (PI) labeling

Annexin V-fluorescein isothiokyanate (FITC) Apoptosis Detection Kit *(Biovision, Milpitas, CA, USA)* was used for detection of apoptosis according to the manufacturer's instructions.

Culture medium containing dead cells was collected in a tube followed by addition of the adherent cells remaining in the culture dish after being dissociated by gentle trypsinization. Tube was centrifuged at 300 g for 2 min. After washing step with cold PBS and spinning, cells were re-suspended in 100 µl of Annexin binding buffer (HEPES buffer with high Ca^{2+} concentration) containing 5 µl of Annexin V- FITC and 5 µl of PI. Cells were gently vortexed and incubated for 20 min in dark at room temperature. Binding buffer (400 µl) was added to each tube then centrifuged at 300 *g* for 2 min. Formed cell pellet was suspended in Annexin binding buffer then immediately measured using LSR II flow cytometer *(BD, Franklin Lakes, CA, USA).* The sum values of early apoptotic cells (Annexin V+/PI-) and late apoptotic cells (Annexin V+/PI+) represented the total apoptosis.

2.5.2 Detection of active caspase-3.

UKF-NB-4 cells at density of 0.8 x 10^6 cells were plated in 60-mm dishes and treated with individual drugs or their combinations for 48 hrs. Percentage of active caspase-3 positive cells was detected using the CaspGLOW™ Flourescein Active Caspase-3 Staining kit *(eBioscience, San Diego, CA, USA)*. The procedure used was as described in the manufacturer's instructions. Briefly, control or treated cells were washed with cold PBS, trypsinized and collected by centrifugation. Cell

pellets were washed with cold PBS, centrifuged and re-suspended in 300 µl of a complete medium containing 1 µl of FITC labeled DEVD-FMK (synthetic peptide that binds to catalytic site of activated caspase-3). Then the cells were incubated for 30 min at 37˚C and 5% CO_2. Cells were centrifuged and pellet was re-suspended in washing buffer. Finally, cells were measured using the LSR II flow cytometer *(BD, USA)* and analyzed by FlowLogic software *(Inivai Technologies, Balcombe, Australia).*

2.5.3 Detection of cleaved caspase-3

Using monoclonal anti-cleaved caspase-3 Alexa Fluor® 647 conjugated antibodies was a direct method to detect cleaved (active Caspase-3) by cytometry (see section Materials and Methods 3.10).

2.6 Assessment of cell cycle

Effect of VPA on cell cycle was assessed using DNA PREP Reagents kit *(Beckman Coulter Inc., Brea, CA, USA)* according to the manufacturer's instructions. Cells were collected by trypsinization, washed with PBS and centrifuged. A 100 µl of permeabilization reagent was applied on cells and mixed gently, followed by addition of 1000 µl of “DNA Prep Stain” containing PI solution with RNase. Cells were incubated in room temperature for 10 min and at least 30,000 cells were analyzed by flow cytometry LSR II *(BD, USA).* The proliferation index was calculated using the following formula: proliferation index = (G2M+ S)/ (G0G1 + S + G2M). All measurements were independently repeated at least three times. PI is a fluorescent DNA stain that can’t cross the intact plasma membrane. 4',6-diamidino-2-phenylindole (DAPI) stain is also a fluorescent DNA intercalating agent that we used in combination with CD133 antibodies to assess the cell cycle of CD133− and CD133+ populations, (see section Materials and Methods 3.10).

2.7 Isolation of histones

We used the methods described by Shechter *et al* (Shechter et al., 2007) that is based on acid extraction followed by precipitation of histones using TCA. The initial step to estimate the acetylation status of histones H3 and H4 was isolation of nuclear histones.

Mechanically harvested cell samples were washed with PBS, centrifuged and re-suspended in 1 ml of hypotonic lysis buffer supplemented with 1 mM DTT and *cOmplete™ Protease Inhibitor* Cocktail *(Roche, Basel, Switzerland*, 1 tablet for 50 mL of buffer). The suspension was incubated for 30 minutes on a rotator in the refrigerator (4°C). After centrifugation 10,000 g at 4°C for 10 minutes, the pellet containing the nuclear fraction was re-suspended in 400 µl of 0.2 M H_2SO_4 (acid extraction step). The mixture was incubated on a rotating stand in a refrigerator for 30 minutes and then centrifuged 16,000 g at 4°C for 10 minutes. The supernatant was transferred to a new tube and precipitated by the gradual dropwise addition of 132 µl of 100% TCA. Samples were incubated on ice for 30 minutes and then centrifuged 16,000 g at 4°C for 10 minutes. The histones stacked on the tube wall, were carefully rinsed twice with ice cold acetone. The acetone-washed histones were air dried at room temperature and subsequently dissolved in 40-70 µl of distilled water. The samples were stored at -80°C. The histone concentration was determined by the method mentioned in section 3.8.

2.8 Determination of protein concentration

Protein concentration was assessed as described by Lowry (Lowry et al., 1951). The DC Protein Assay kit from *BioRad (Hercules, CA, USA)* was used to determine the protein concentration according to the manufacturer's instructions.

Seven prepared standard dilutions of BSA (ranging from 0.125 to 2.8 mg/ml) and the blank well (consisting of DNA-free distilled water) were the references used to determine the protein concentration of the sample. Solution A' was

prepared by mixing 1000 µl of solution A with 20 µl of solution S and then 25 µl of solution A' were added to each 5 µl of standards and samples in the microplate. 200 µl of solution B was then added. After 15 minutes incubation at room temperature with gentle rotation, absorbance was measured on a VERSA max spectrometer *(Molecular Devices, Sunnyvale, CA, USA)* at a wavelength of 750 nm. The detected data were evaluated by the SoftMax Pro software, which is part of the spectrophotometer.

2.9 Western blot

2.9.1 Detection of CD133

Cells were collected mechanically, washed with PBS, centrifuged and lysed in RIPA buffer containing *cOmplete™ Protease Inhibitor* Cocktail *(Roche Diagnostics, Basel, Switzerland)*. Protein concentration was measured using above mentioned DC protein assay *(Bio-Rad Laboratories, Hercules, CA, USA).* Thirty micrograms of extracted proteins were separated by SDS-PAGE electrophoresis using 10% gel. Separated proteins were transferred to a nitrocellulose membrane and blocked with 3% non-fat milk/ 0.1% TWEEN for one hour at 4°C. The membrane was exposed to mouse anti-human CD133/1 clone W6B3C1 (1:100*; Miltenyi Biotec GmbH, Bergisch Gladbach, Germany*) as the primary antibody for one hour at room temperature. Membrane was washed and exposed to peroxidase conjugated anti-mouse IgG secondary antibody (1:2000; *Bio-Rad Laboratories*) for 10 minutes. Antigen-antibody complex was visualized using an enhanced Immun-Star HRP Substrate chemiluminescence detection system *(Bio-Rad Laboratories)* according to the manufacturer's instructions. Beta-actin antibody (1:2000; *Sigma-Aldrich*) was used as a loading control. Washing of the membranes by TBST was performed using SNAP i.d. 2.0 Protein Detection System (*Millipore*) 3 times for 5 minutes each. Detection of the fluorescent bands on X-ray films was done using *MEDIX XBU (Foma, Hradec Kralové, ČR)*. Stripping buffer was applied to the nitrocellulose membrane to

remove the previously used antibodies and thus the membrane can be reused for detecting other proteins on the same membrane.

2.9.2 Detection of Phosphorylated Akt (p-Akt)

We used rabbit monoclonal anti-p-Akt (Ser473) antibody (clone D9E) and rabbit polyclonal anti-Akt (total) antibody (both, 1:1000; *Cell Signaling Technology Inc., Beverly, MA, USA*) for detection of p-Akt expression on same membrane where CD133 was detected.

2.9.3 Detection of pluripotency transcriptional factors

Pluripotency transcription factors were examined according to the manufacturer's instructions using *StemLight*™ Pluripotency Transcription Factor Antibody Kit *(Cell Signaling Technology)* containing rabbit monoclonal anti Oct4 clone C30A3 (1:1000), Sox2 clone D609 (1:1000) and Nanog clone D73G4 (1:2000) antibodies. Peroxidase conjugated anti-rabbit IgG (1:2000; *Bio-Rad Laboratories*) was used as secondary antibody. Same membrane where CD133 was detected was used after stripping.

2.9.4 Detection of acetylated histones H3 and H4

Due to the low molecular weight of the histones, 5 μg of the isolated histones were electrophoretically separated using 4-20% TGX precast gels or 16% prepared gel. After migration, histones were transferred to a nitrocellulose membrane and incubated with 3% non-fat milk to block non-specific binding. The membranes were then exposed to specific rabbit polyclonal anti-acetyl-histone H3 (1:4,000) and anti-acetyl-histone H4 (1:1,000) antibodies (both from *Upstate Biotechnology Inc., Lake Placid, NY, USA*) overnight at 4˚C. Membranes were washed and exposed to peroxidase conjugated anti-rabbit IgG secondary antibodies (1:2000, *Bio-Rad Laboratories*) and the antigen-antibody complex was visualized by enhanced chemiluminescence detection system according to the manufacturer's instructions (Immun-Star HRP Substrate, *Bio-Rad*). Mouse anti-histone H3 antibody (1:10,000; *Millipore, Billirica, MA, USA*) was used as a loading control.

2.10 Immunofluorescence staining of CD133

Cells were harvested using accutase *(Sigma-Aldrich),* washed with PBS and blocked with 0.1% bovine serum albumin for 15 minutes. Cells were incubated with primary mouse anti-human CD133/2 PE conjugated antibodies (1:10, *Miltenyi Biotec*) for 30 minutes in dark at room temperature. Cells were fixed with a solution of 3.6% paraformaldehyde/PBS for 10 minutes. After a washing step, cells were incubated in Hoechst 33342/PBS solution *(Sigma-Aldrich)* in a final concentration of 5 µg/ml for 30 minutes at 4˚C. Slides were observed under the Olympus AX70 fluorescence microscope *(Olympus Optical Co., Ltd., Japan)* with a CCD camera *(Jenoptik, Jena, Germany)*. Cells stained with mouse IgG2b-PE (1:100, *Miltenyi Biotec*) isotype was used as control.

2.11 Confocal microscopy

UKF-NB-3 cells were fixed with 4% paraformaldehyde for 15 min at room temperature, washed three times with PBS and then blocked with a PBS-based solution containing 1% bovine serum albumin and 0.25% Triton X-100 *(Sigma-Aldrich).* Cells were incubated overnight at 4°C with mouse monoclonal anti-CD133 (1:30, clone W6B3C1, *Miltenyi Biotec*). After being washed three times with PBS, cells were co-incubated with goat anti-mouse DyLight 488 IgG (1:400; *Abcam*). Nuclei were counterstained with DAPI (1µg/mL; *Life Technologies*). Immunofluorescent images were collected using Leica TCS SP5 confocal microscope *(Leica Microsystems, Mannheim, Germany).*

2.12 Cytometric measurement of cell cycle and cleaved caspase-3 in CD133 populations

We combined CD133 measurement with cell cycle or with cleaved caspase-3 assessment for detection of apoptosis-sensitive cells in CD133− and CD133+ populations. UKF-NB-3 cells were cultured at a density of 2×10^5 cells/ml in 60-mm

dish and left for 24 hrs to adhere and then were treated with CDDP (1 μM) or VCR (0.20 nM) as well as in combination with 1mM VPA. After 72 hrs, the medium was removed and cells were rinsed twice with PBS. Attached cells were collected using *Accutase® (Sigma-Aldrich),* mixed gently in IMDM with 10% FBS and centrifuged. About one million cells were re-suspended in 100 μL PBS containing 0.5% BSA *(Sigma-Aldrich)* and then incubated with mouse anti-human CD133/2 PE-conjugated primary antibody clone 293C3 (1:10, *Miltenyi Biotec*) for 15 min in darkness at 4°C. Cells were washed and fixed with 3.6% paraformaldehyde/PBS for 10 min on ice. After washing, cells were permeabilized and nuclei stained with DAPI at a final concentration of 10 μg/ml *(Life Technologies, CA, USA)* in a 0.15% TritonX/PBS solution for 15 min on ice. Cells were washed and incubated with monoclonal anti-cleaved caspase-3 Alexa Fluor® 647 conjugated antibodies clone D3E9 (1:50; *Cell Signaling*) for 30 min on ice. Identically treated samples stained with Mouse IgG2b-PE antibodies (1:10; *Miltenyi Biotec*) were used as isotype controls. Labeled cells were measured immediately by LSR II Flow Cytometer *(BD Bioscience)* using 405 nm, 488 nm and 640 nm laser for excitation. The fluorescence emission was collected using 575/26 bandpass filters for PE, 660/20 for Alexa Fluor 647 and DAPI was detected with a 450/50 bandpass filter. FACS Diva version 5.0 software (*BD Biosciences, Heidelberg, Germany*) was used for data acquisition and data were analyzed using FlowJo X software *(Tree Star, Oregon, USA).* All measurements were independently repeated at least three times

2.13 Determination of histone H2AX phosphorylation status

$0.8x10^6$ cells were plated in 60-mm dishes and treated with individual drugs or their combinations. Control or treated cells were washed with cold PBS, trypsinized and collected by centrifugation. Cell pellets were washed with PBS, centrifuged and then fixed in 2% formaldehyde / PBS for 10 min. After washing step, the cells were re-suspended in ice-cold 90% methanol / PBS and incubated for 60 min at -20˚C. Cells were washed three times in blocking buffer and finally

incubated in 50 µl of blocking buffer containing 5 µl of pH2AX antibody [Alexa Fluor® 647 anti‑H2A.X-Phosphorylated (Ser139), *Biolegend, San Diego, CA, USA*] for 60 min at 4˚C. Cells were washed and measured using the LSR II *(BD, Franklin Lakes, CA, USA)* and analyzed with FlowLogic software.

2.14 CD133 promoter methylation profiling

2.14.1 Treatment with 5-aza-2'-deoxycytidine

Cells were cultured in a density of 4×10^5 cells/ml in 60 cm^2 dishes and left to adhere overnight. Cultured cells were treated with 5-aza-2'-deoxycytidine (AZA) *(Sigma-Aldrich)* for 6 days at a dose of 4 µM for IMR-32 and 8 µM for UKF-NB-4. VPA was added 48 hrs before collecting the cells. The medium was changed and replaced with new AZA containing medium every two day. Adherent cells were collected for western blot and DNA isolation.

2.14.2 Methylation-sensitive high resolution melting analysis

Bisulfite conversion: DNA was extracted using a Puregene Core KitA *(Qiagen, Hilden, Netherlands).* Whole genomic DNA was treated with sodium bisulfite using an Epitect Bisulfite Kit *(Qiagen)* to convert unmethylated cytosine to uracil, following the manufacturer´s protocol.

Methylation-sensitive high resolution melting (MS-HRM): Real-time PCR followed by HRM was carried out using a high-performance Eco Real-Time PCR system *(Illumina, San Diego CA, USA).* CD133 primers specific for bisulfite converted DNA of the promoter P1 and P3 (Shmelkov et al., 2004) were designed (Table 2) using Methyl Primer Express Software v1.0 *(Applied Biosystems, Carlsbad, CA, USA).* The reaction mixture consisted of 10 ng of template DNA, 1x EpiTect HRM Master Mix *(Qiagen)* and 300 nmol/l of each primer. PCR was initiated by incubation at 95°C for 5 min, followed by 50 cycles at 95°C for 10 sec, 56°C for 20 sec, and 72°C for 10 sec. The HRM thermal profile was set up according to the manufacturer's recommendations. For each assay, a standard

dilution series using EpiTect Control DNA *(Qiagen)* was run. Fluorescence data were converted into melting peaks using Eco Software v3.0.16.0 *(Illumina).*

Table 2: CD133 primers specific for bisulfite converted DNA of the promoter P1 and P3.

Primer name	Primer sequence	Tm [°C]	Ta [°C]	[bp]	Number of CpG
HRM-P1-F	5' TGGGATTAGGTAATAGAAGGGTT 3'	60.5	56	179	5
HRM-P1-R	5' CAACACCTAAACAACATCCATT 3'	60.2			
HRM-P3-F	5' TTATTGTATTGGGGGTGTATAGTGA 3'	61.9	58	135	8
HRM-P3-R	5' CAATTCCTCTAACCCCCAAC 3'	62.1			

[bp], base pairs of the PCR product;[Ta], annealing temperature of primers; [Tm], melting temperature of primers.

2.15 Colony assay

Cells pretreated with 1mM VPA for 72 hrs and the untreated control were rinsed with PBS, trypsinized and passed through a 40 µm size mesh filter to remove clumps. Trypan blue was used to perform a cell count which showed 96 to 98% viability using TC20 cell counter *(Bio-Rad Laboratories, Hercules, CA, USA).* Cells pretreated with 1mM VPA for 72 hrs and the untreated control were counted using TC20 cell counter *(Bio-Rad Laboratories, Hercules, CA, USA).* One hundred cells per well were seeded in 6-well plates and left to grow in IMDM with 10% FBS at 37°C and 5% CO_2 for 14 days. Formed colonies were fixed in acetic acid/methanol 1:7 solution for 5 min, then the fixative solution was withdrawn and colonies were left to dry. Dried colonies were stained with Giemsa stain overnight. Colonies greater than 50 cells were counted and plating efficiency was calculated as follows: plating efficiency= (number of colonies formed / number of cells seeded) × 100.

2.16 Neurosphere formation assay

Cells were seeded at a density of 100 cells per well in 6-well ultra-low attachment multiwall polystyrene plates *(Falcon, Becton Dickinson, Franklin Lakes, NJ, USA).* Cells were maintained in serum-free media (SFM) contained a 1:1 mixture of Ham´s F12 Nutrient Mixture and advanced DMEM *(Gibco Life Technologies),*

supplemented with 40 ng/ml EGF, 20 ng/ml bFGF (both from *Invitrogen, Fisher Scientific*),1% B27 supplement *(Gibco Life Technologies)*, 2 µg/ml heparin *(Sigma Aldrich)* and 100 units/ml penicillin/ streptomycin. Aliquots of EGF and bFGF were supplied every other day. On day 14, formed neurospheres were counted under microscope *(Olympus IX51; Olympus Corporation, Tokyo, Japan).*

2.17 RNA isolation and real-time RT-PCR

Total RNA was extracted from cells lines using TRIzol reagent *(Invitrogen, Carlsbad, CA, USA).* The quality of the isolated RNA was verified using horizontal agarose gel electrophoresis and RNA quantity was measured using Nanodrop 1000 *(Thermo Scientific, Waltham, MA, USA)*. The complementary DNA (cDNA) was obtained by reverse transcription of 1µg of RNA samples using *TaqMan*™ Reverse Transcription Reagents including random hexamers primers *(Applied Biosystems, Foster City, CA, USA)* according to the manufacturer's instructions. The following cycling conditions were used for the reverse transcription reaction: incubation at 25 ºC for 10 min followed by 37 ºC for 50 min then at 95 ºC for 5 min and finally incubation at 4 ºC. The prepared cDNA was used for real-time (RT) polymerase chain reaction (PCR) under the following cycling conditions: incubation at 50 ºC for 2 min and initial denaturation at 95 ºC for 10 min, then 40 cycles of denaturation at 95 ºC for 15 sec and annealing at 60 ºC for 1 min. The reaction mixture (20 µl) contained 2 µl cDNA, 10 µl Power SYBR Green PCR Master *Mix (Applied Biosystems, Foster City, CA, USA)* and 1 µl of forward and reverse CD133 primers ordered from *Generi Biotech (Hradec Kralove, Czech Republic)*. β-2-microglobulin (B2M) primers purchased from *Generi Biotech (Hradec Kralove, Czech Republic)* were used as the reference gene (Table 3). All samples were analyzed in triplicate. Negative controls had the same composition as samples but ultra-pure water was used instead of cDNA. RT-PCR samples were analyzed using 7500 Real-Time PCR System *(Applied Biosystems, Foster City, CA, USA)*. Data were evaluated by comparative cycle threshold (C_T) method for relative quantitation of gene expression using the relative expression software

tool (REST) (Pfaffl et al., 2002). Cycle thresholds, at which a significant increase in fluorescence signal was detected, were measured for each sample. Then ΔC_T was evaluated according to the following equations: $\Delta C_T = C_T$ (target) - C_T (internal standard).

Table 3: List of the CD133 and reference gene primers used for the RT-PCR

Primer name	Forward	Reverse
CD133	5' GCATTGGCATCTTCTATGGTT 3'	5' CGCCTTGTCCTTGGTAGTGT 3'
B2M	5' CTATCCAGCGTACTCCAAAG 3'	5' GAAAGACCAGTCCTTGCTGA 3'

2.18 Statistical analysis

Numerical data were expressed as mean ± standard deviation (SD). Paired Student's t-test (two tailed) was used for statistical analysis using SPSS.v16.0 for windows *(SPSS Inc., Chicago, IL, USA).* GraphPad Prism6 software *(GraphPad Software, La Jolla, CA, USA)* and Excel 2007 was used for graphical processing of data. *P* values less than 0.05 were considered statistically significant and indicated with (*), *P* values less than 0.01 represented high significance (**) and the highly significant difference (***) when p values were less than 0,001. Each experiment was performed independently at least three times.

Chapter 3

Results

Most of the results presented in this dissertation work were published in scientific journals with an impact factor. Individual publications are listed as attachments to the dissertation (Page 104)

3.1 Assessment of the cytotoxic effect of 1 mM VPA on NB cell lines.

The cytotoxic effect of 1 mM VPA at 72 hrs was evaluated by determination of its effect on inhibitory of the cell cycle, induction of apoptosis and the IC_{50}.

3.1.1 Effect of VPA on cell cycle

In this experiment, cytometric assessment of the cell cycle was performed using PI staining. Our results showed that proliferation of the NB cells was significantly reduced after treatment with 1 mM VPA with a significant increase in G_0/G_1 phases that was noticed almost in all examined NB cell lines. Interestingly, SH-SY5Y was the only tested NB cell line which did not show decrease in the proliferation index or increase in G_0/G_1 phases after exposure to VPA (Figure.8).

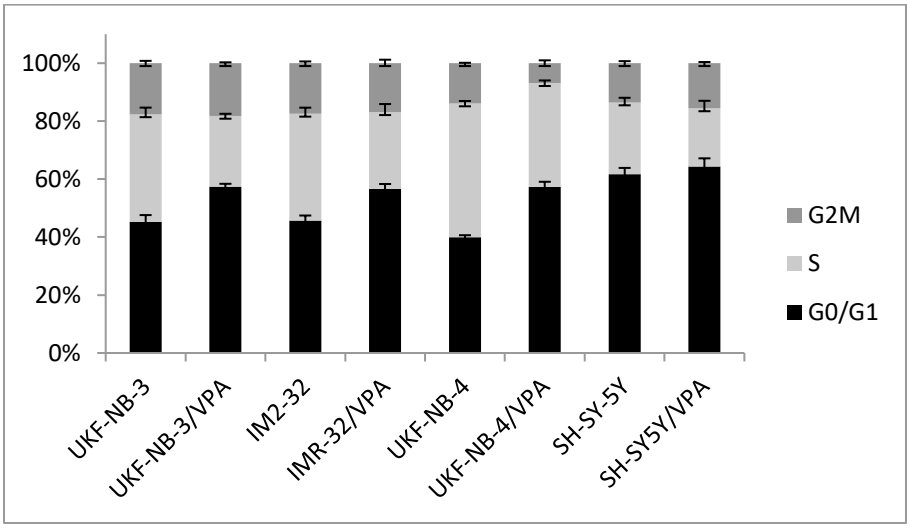

Figure 8: Effect of 1 mM VPA on cell cycle of NB cell lines. The graph shows the changes in different phases of cell cycle after treatment with 1 mM VPA which is manifested by increased G_0/G_1 phases with exclusion of this effect in SH-SY5Y cell line.

Additionally, we monitored the proliferation of UKF-NB-3 cells in different concentrations of VPA (1, 2 and 5 mM) using real-time monitoring system (xCELLigence). Surprisingly, we found that the dose of 1 mM VPA could effectively maintain UKF-NB-3 cells alive for 330 hrs without the need to supply the cell culture with new medium or any nutritional factor. The other used doses (2 and 5 mM) were toxic and inhibited the cell growth (Figure.9). Control cells were rapidly growing in the culture with greater consumption of nutrients in the medium which resulted in early death (168 hrs). Here, we would like to underscore that the VPA concentration we used in our experiments (1 mM) is similar as recommended serum concentration of patients in clinical trials (Wheler et al., 2014).

3.1.2 Effect of 1 mM VPA on induction of apoptosis

Apoptosis was measured by the Annexin V-FITC/PI double staining assay. This method allows differentiation of early apoptotic cells with intact membranes (Annexin V+/PI-) from late apoptotic/necrotic cells with leaky membranes (Annexin V+/PI+) while normal cells were not stained by any of the dyes (Annexin V-/PI-). Our results show that 1 mM VPA induced significant apoptosis at 72 hrs in all

tested cell lines but the percent of apoptosis did not exceed 5% at maximum (i.e. IMR-32) compared to the controls. In table 4, the sum values of early and late apoptosis are presented after treatment with VPA for 72 hrs.

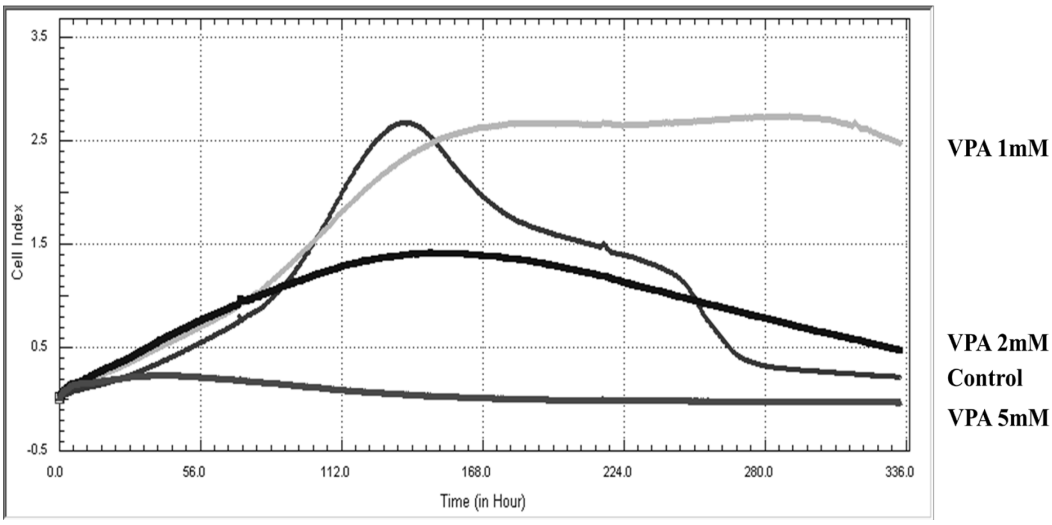

Figure 9: Real-time monitoring of UKF-NB-3 cells viability treated with 1, 2, and 5 mM VPA. Proliferation of cells was measured by the xCELLigence system and expressed as cell index. Representative data from one of three independent experiments are shown.

3.1.3 IC_{50} of 1 mM VPA in NB cell lines

The average IC_{50} for UKF-NB-3, IMR-32, UKF-NB-4, and SH-SY5Y were 1.27, 1.3, 2, and 9 mM respectively (Table 4). These low IC_{50} values (except for SH-SY5Y) were mainly due to the inhibitory effect of VPA on cell cycle rather than apoptosis which was significant but so few to result in such low IC_{50} (Table 4). In fact, VPA reduced the cell number due to shifting of cells toward G_0/G_1 phases of the cell cycle which consequently decreased the proliferation index and resulted in remarkable difference in cell number between control cells and cells treated with VPA leading to low IC_{50} as detected by MTT test (MTT test compares number of living cells in control and treated sample regardless the decrease of number in treated sample is due to apoptosis or cell cycle arrest) (Table 4). Taking in mind that cell cycle inhibition associated with 1 mM of VPA was markedly obvious in UKF-NB-3, IMR-32, and UKF-NB-4, while it was insignificant in SH-SY5Y during

the examined period. Thus, this explains the high IC_{50} value in SH-SY5Y as it represents mainly the apoptotic effect induced by 1 Mm VPA due to irrelevant effect on the cell cycle.

Table 4: IC_{50}, apoptosis, and proliferation index of NB cell lines after treatment with 1 mM VPA for 72 hrs.

Cell line	IC_{50}VPA mM	Apoptosis Annexin V / PI labeling		Proliferation index (G_2M + S) / (G_0G_1 + S + G_2M)	
		Control (%)	VPA (%)	Control	VPA
UKF-NB-3	1.27 ± 0.46	2.27 ± 0.49	4.86 ± 1.74**	0.50 ± 0.05	0.43 ± 0.02*
IMR-32	1.30 ± 0.69	2.08 ± 0.26	7.02 ± 0.88**	0.55 ± 0.01	0.43 ± 0.01**
UKF-NB-4	2.00 ± 0.60	0.61 ± 0.15	4.72 ± 0.48**	0.64 ± 0.02	0.58 ± 0.01**
SH-SY5Y	9.00 ± 1.44	3.84 ± 1.02	7.38 ± 0.78**	0.35 ± 0.04	0.34 ± 0.03^{Ns}

Ns, Non-significant
* $p < 0.05$
** $p < 0.01$
- paired t-test

3.2 Cytotoxic effect of 1 mM VPA in combination with DNA-damaging conventional chemotherapy

In this part of our work, we explored which type of cytostatics can be efficiently combined with VPA to enhance their cytotoxic effect as well the best drug regimen administration for this combination.

3.2.1 VPA synergizes cytotoxicity of cisplatin on UKF-NB-4 human neuroblastoma cells.

Treatment of UKF-NB-4 cells with 1 mM VPA for 48 hrs obviously did not induce significant apoptosis and the amount of Annexin V-/PI- cells were almost the same as in the control sample (Figure 10A and 10B). On the other hand, treatment with cisplatin alone or simultaneously with VPA significantly induced apoptosis in UKF-NB-4 cells (Figure 10C and 10D and figure 11). As shown in figure 10, treatment of UKF-NB-4 cells with 20 μM cisplatin for 48 hrs decreased the percentage of viable cells to 61.3% (shown in a lower-left panel in figure 10C) with a concomitant increase in percentage of early apoptotic cells to 15.5% (shown in a lower-right panel in figure 10C), and late apoptotic cells to 22.2% (shown in an

upper-right panel in figure 10C). These results confirm the high degree of cisplatin activity in triggering apoptosis in NB cells (Mastrangelo et al., 1995). However, UKF-NB-4 cells co-treated with cisplatin and 1 mM VPA displayed a further decrease in the percentage of viable cells rather than treatment with cisplatin alone, 61,3% and 43.8% respectively (Figure 10D). The decrease in viable cells was concomitant with an increase in amounts of early apoptotic cells to 20.7% and late apoptotic cells to 34.2% (Figure 10D). These data indicate that VPA elevates the potency of DNA-damaging agent cisplatin to induce apoptosis in UKF-NB-4 cells. Similarly, treatment with low dose of cisplatin (4 μM) also induced apoptosis in UKF-NB-4. Even though this dose showed low toxicity to the tested cells, it was augmented in combination with VPA (Figure 11).

Caspases, a family of cysteine-aspartic proteases, are known to be crucial mediators in the apoptotic signaling pathways (Earnshaw et al., 1999). Since caspase-3 is the major executioner caspase essential for activation of one of the primary apoptotic signaling pathways and its activation ultimately leads to cell death (Slee et al., 2001), thus it is suited as a read-out in an apoptosis assay. Therefore, we evaluated whether apoptosis induced by the above mentioned treatment regimens is associated with changes in caspase-3 activation. A similar result to that found using Annexin V for induction of apoptosis by the combined effect of VPA and cisplatin was detected by measuring the percentage of cells with activated caspase-3. Exposure of UKF-NB-4 cells to 1 mM VPA simultaneously with 4 or 20 μM cisplatin increased percentage of cells with active caspase-3, by up to 2-times as compared with cells treated with cisplatin alone (Figure 12). These results indicate that induction of apoptosis in UKF-NB-4 cell line caused by cisplatin was triggered by the activation of caspase-3 that is enhanced by co-treatment with VPA.

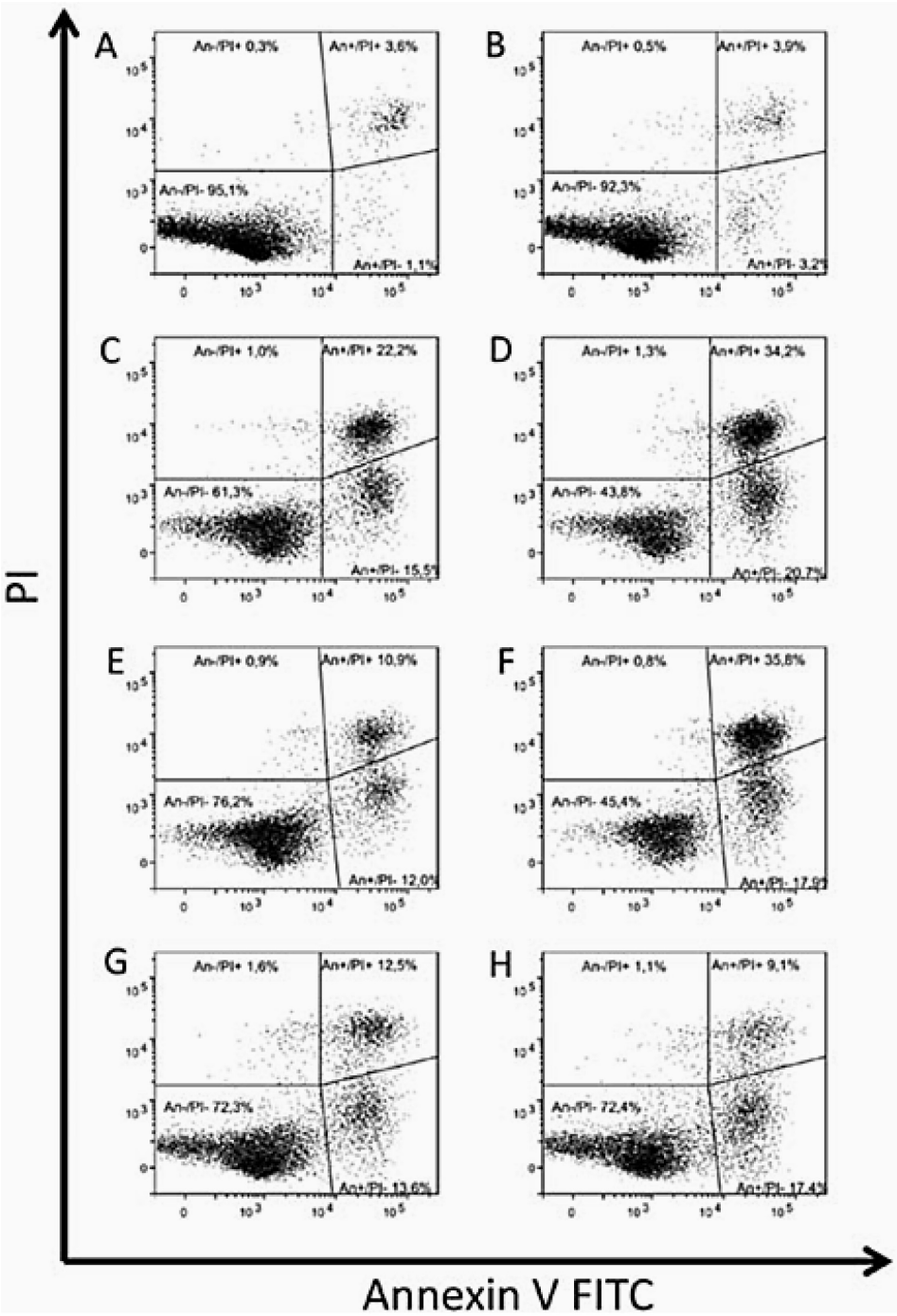

Figure 10: Apoptosis induction in UKF-NB-4 cells at 48 hrs by 1 mM VPA (B), 20 µM cisplatin (C), 8 µM etoposide (E), 20 nM vincristine (G) and their combination with 1 mM VPA [VPA + cisplatin (D), VPA + etoposide (F), VPA+ vincristine (H)]. (A) Control cells incubated in a medium without drugs. Apoptosis was measured using Annexin V-FITC/PI labeling. Figure shows representative data from one of three independent experiments.

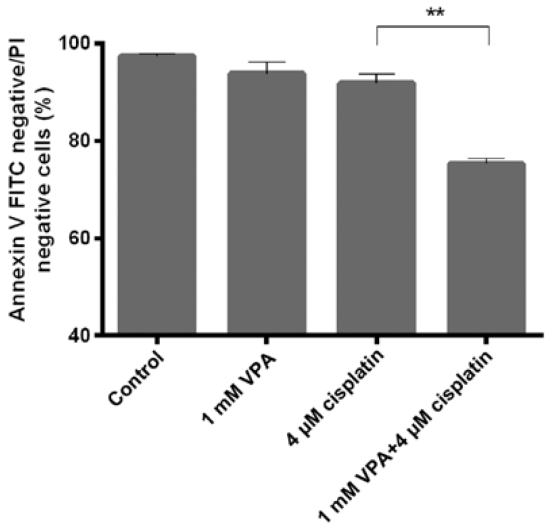

Figure 11: Apoptosis induction in UKF-NB-4 cells at 48 hrs by 1 mM VPA, 4 µM cisplatin and their combination. Apoptosis was measured using Annexin V-FITC/PI labeling. Mean and SD from three independent experiments is shown. **P <0.01, a significant difference between cells treated with cisplatin combined with VPA and cisplatin alone, (Student's t-test) (n=3).

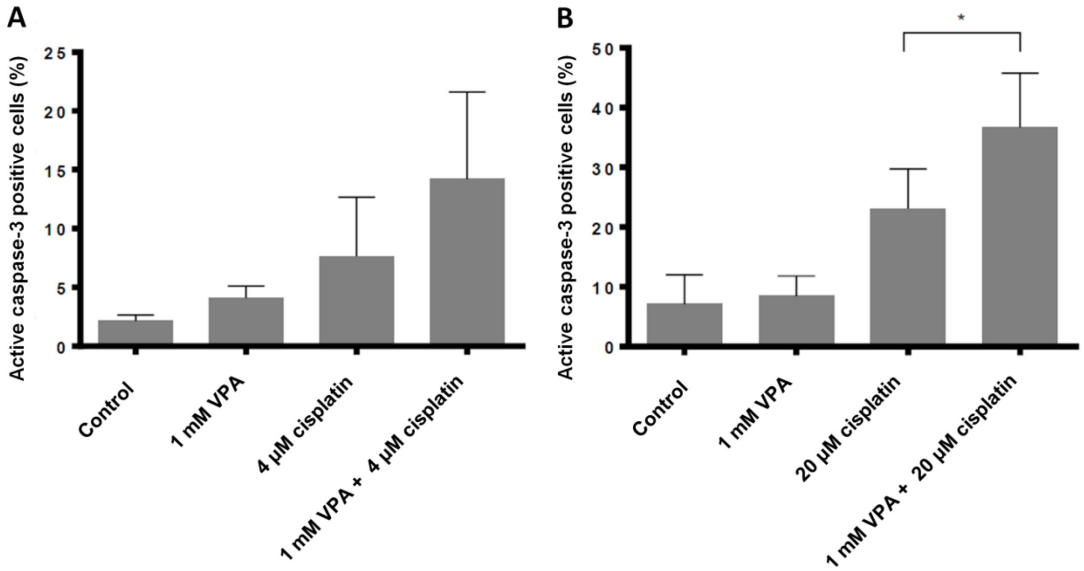

Figure 12: The percentage of active caspase-3 in UKF-NB-4 cells when treated with 1 mM VPA, 4 µM cisplatin (A), 20 µM cisplatin (B) and their combination for 48 h. Mean and SD from three independent experiments is shown. *P<0.05, a significant increase in percentage of cells with active caspase-3 treated with cisplatin combined with VPA, as compared to cells treated with cisplatin alone (Student's t-test).

An increase in the cytotoxic potency of 4 μM cisplatin by 1 mM VPA was also proved by analyzing cell growth with the xCELLigence system for real-time monitoring of cell viability using electrical impedance that represents the readout (Figure 13). As shown in figure 13, cells cultivated with VPA grew slowly up to ~ 90 hrs, while their cell index was not increasing after this time period. UKF-NB-4 cells treated with cisplatin grow exponentially till 50 hrs of cultivation, but after this time period, cisplatin caused a decrease in their viability. However, after >100 hrs of cultivation, cells incubated with 4 μM cisplatin started to grow again. Hence, treatment of cells with 4 μM cisplatin alone is not sufficient to inhibit cell growth totally. The most efficient cytotoxic effect on UKF-NB-4 cells was produced by their co-cultivation with VPA and cisplatin; when this combination was applied, the value of cell index decreased close to zero (Figure 13).

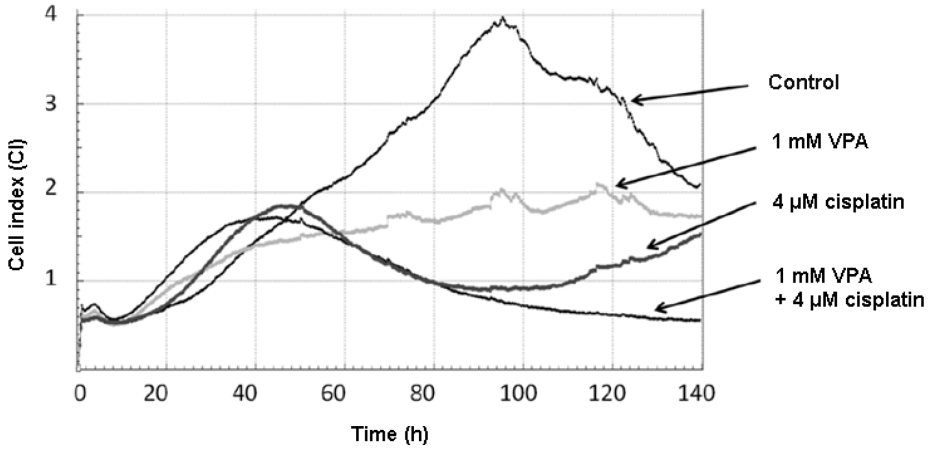

Figure 13: Viability of UKF-NB-4 cells treated with 1 mM VPA, 4 μM cisplatin and with both drugs. Viability was measured by the xCELLigence system and expressed as cell index. Representative data from one of three independent experiments are shown.

Computation analysis of cell survival calculated by Compusyn software (Chou and Talalay, 1984) was used to estimate whether activities of these two drugs are synergistic. Namely, we calculated the value of the combined effect of VPA and cisplatin and expressed it as combination index (CoI). When the values of CoI are <0.90, activities of two drugs are synergistic (the combination index ranging from 0.70 to 0.89 corresponds to a moderate synergism of drugs). However, the values

of ≥0.9 indicate that the activities of two drugs are not synergistic (Chou, 2006). The value of CoI for the simultaneous effect of 4 μM cisplatin and 1 mM VPA equals 0.70, which corresponds to a moderate synergism of this combination. In contrast to VPA, a non-toxic concentration of TSA (40 nM) (another HDAC inhibitor tested in our study) could not potentiate the cytotoxic effect of cisplatin on UKF-NB-4 cells that was found using Annexin V-FITC/PI double staining assay or active caspase-3 assay (data not shown).

3.2.2 Suggested regimen for combination of cisplatin with HDAC inhibitors

Because the effect of the combination of cytostatic drugs with HDAC inhibitors may vary according to the treatment regimens that would result in either an increase or decrease in cytotoxic effects (Das et al., 2010; Luchenko et al., 2011), we examined various treatment regimens for a combination of the tested chemotherapy with VPA.

The different combination regimens of VPA and cisplatin applied to the UKF-NB-4 cells are listed in (Table 5). The induction of apoptosis in cells cultivated under these treatment regimens is shown in figure 14. The most effective drugs combination resulted in a decrease in viability of UKF-NB-4 cells was exposure to cisplatin followed by VPA (the cells treated with 20 μM cisplatin for 24 h and then with 1 mM VPA for 48 h) (see a combination cisplatin/VPA in figure 14). On the contrary, the opposite sequence of drug application (VPA/cisplatin) led to essentially no changes in viability of cells as compared with cultivation of cells with cisplatin alone (see VPA/cisplatin versus 0/cisplatin regimens in figure 14). These results demonstrate that VPA can potentiate the toxic effects of cisplatin only if UKF-NB-4 cells are primarily exposed to DNA-damaging drugs.

Table 5: Combination regimens used for treatment of UKF-NB-4 cells with VPA and cisplatin.[a]

Designation	0-24 h	24-72 h
Control	Medium	Fresh medium
Cisplatin/cisplatin	20 μM cisplatin	20 μM cisplatin
0/cisplatin	medium	1 mM VPA
Cisplatin/0	20 μM cisplatin	Fresh medium
Cisplatin/VPA	20 μM cisplatin	1 mM VPA
VPA/0	1 mM VPA	Fresh medium
0/cisplatin	medium	20 μM cisplatin
VPA/cisplatin	1 mM VPA	20 μM cisplatin

[a] 0 indicates medium cultivation without any drug added.

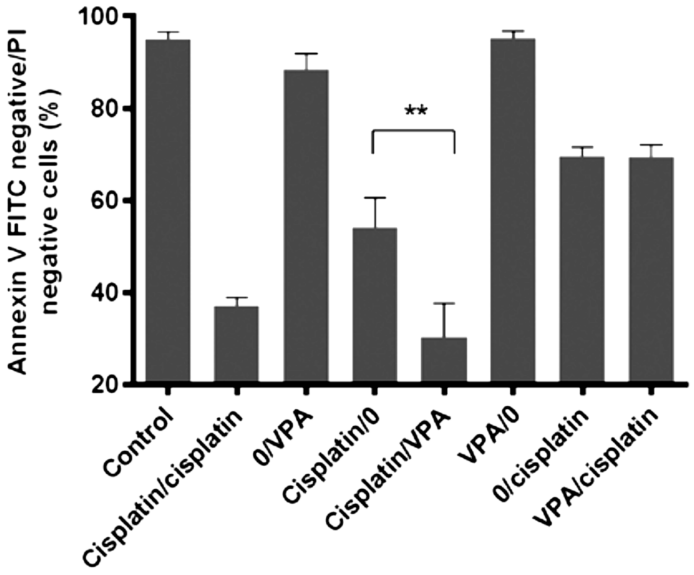

Figure 14: Apoptosis induction in UKF-NB-4 cells by 1 mM VPA, 4 μM cisplatin and their various combinations. Control, cells treated with a medium without any drug. Experimental conditions for combined treatment of cells are described in Table I. Mean and SD from three independent experiments is shown. **P<0.01, a significant decrease in viable cells caused by their pretreatment with cisplatin before incubation with VPA as compared to the cells incubated with cisplatin alone (Student's t-test) (n=3).

3.2.3 VPA synergizes cytotoxicity of etoposide on UKF-NB-4 human neuroblastoma cells.

The effect of combined treatment of UKF-NB-4 neuroblastoma cells with VPA and etoposide was also investigated. Treatment of these cells with 8 μM etoposide and in combination with 1 mM VPA resulted in induction of apoptosis (Figure 10E and 10F). Treatment of UKF-NB-4 cells with etoposide for 48 h induced a decrease in the percentage of viable cells to 76.2% (shown in a lower-left panel in figure 10E) with a concomitant increase in percentage of early apoptotic cells, to 12.0% (shown in a lower-right, panel in figure 10E) and late apoptotic cells, to 10.9% (shown in an upper-right panel in figure 10E). Analogously to exposure of the tested NB cells to cisplatin combined with VPA, a 1.7-fold decrease in cell viability (expressed as percentage of Annexin V-/PI- cells) was generated in these cells by their exposure to VPA combined with etoposide as compared to their exposure to etoposide alone (Figure 10E and 10F). This decrease in viability was parallel with an increase in amounts of early apoptotic cells, to 17.9%, and predominantly late apoptotic cells, to 35.8% (Figure 10F). These data indicate that VPA also potentiate the cytotoxic effect of the second tested DNA-damaging drug, etoposide, to induce apoptosis in UKF-NB-4 cells. In addition, exposure of UKF-NB-4 cells to VPA simultaneously with etoposide increased an amount of cells expressing active caspase-3, by ≤1.7-times (Figure 15). These results indicate that apoptosis induced in NB cells by the effect of the combination of these drugs is mediated by caspase-3 activation.

It should be emphasized that the most effective treatment leading to the highest decrease in viability of NB cells was the combined exposure of cells to etoposide followed by their treatment with VPA (cells treated with 8 μM etoposide for 24 h and then with 1 mM VPA for 48 h) (Groh et al., 2012). Hence, this regimen analogous is similar to that found to be most efficient in treatment of cells with cisplatin combined with VPA. These results demonstrate that VPA can exhibit the potentiating effect only if UKF-NB-4 NB cells are primarily influenced either by cisplatin or by etoposide. Computation analysis was again used to estimate

whether activities of VPA with etoposide are synergistic. The value of CoI for the simultaneous effect of 8 μM etoposide and 1 mM VPA equals 0.52 that corresponds to a synergism of these drugs. On the other hand, combination of etoposide with non-toxic concentration of TSA (40 nM) did not influence its cytotoxicity to UKF-NB-4 (data not shown).

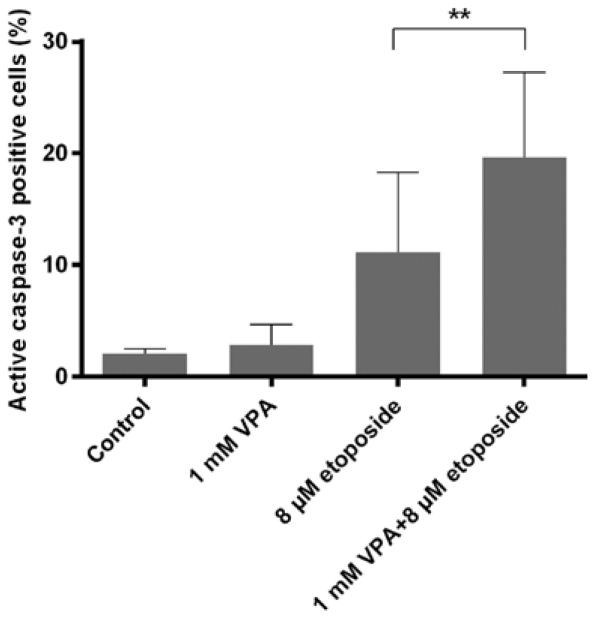

Figure 15: The percentage of UKF-NB-4 cells with active caspase-3 when treated with 1 mM VPA, 8 μM etoposide or their combination for 48 h. Mean and SD from three independent experiments is shown. **P<0.01, a significant increase in percentage of cells with active caspase-3 treated with etoposide combined with VPA, as compared to cells incubated with etoposide alone (Student's t-test)

3.3 VPA does not potentiate cytotoxicity of a mitotic inhibitor vincristine on UKF-NB-4 cells.

In further experiments, the influence of VPA and TSA on cytotoxicity of vincristine, the anticancer drug acting by a mechanism not based on DNA damage, was investigated. Vincristine is known to induce cell death in tumor cells including NB by inhibiting the assembly of microtubule structures and disrupting mitosis in the metaphase (Jordan and Wilson, 2004). As shown in figure 10, treatment

of UKF-NB-4 neuroblastoma cells with 20 nM vincristine led to induction of apoptosis in these cells. The Annexin V-FITC/PI double staining assay indicated that treatment of UKF-NB-4 cells with vincristine for 48 h induced a decrease in the percentage of viable cells to 72.3% (as shown in a lower-left panel in figure 10G), with a concomitant increase in percentage of early apoptotic cells to 13.6% (as shown in a lower-right panel in figure 10G), and late apoptotic cells to 12.5% (as shown in an upper-right panel in figure 10G). These results confirm that vincristine is an efficient drug that can induce apoptosis in UKF-NB-4 cells. However, neither VPA nor TSA (data not shown) potentiated the effect of vincristine on induction of apoptosis (Figure 10H). Likewise, in the case of measuring the activation of caspase-3 in the tested cells treated with vincristine simultaneously with VPA, no increase in caspase-3 activation was detected (Figure 16). These findings demonstrate that the sensitizing effect of VPA on the tested cells is produced only when they are affected by the DNA-damaging drugs (cisplatin and etoposide) before their treatment with this HDAC inhibitor.

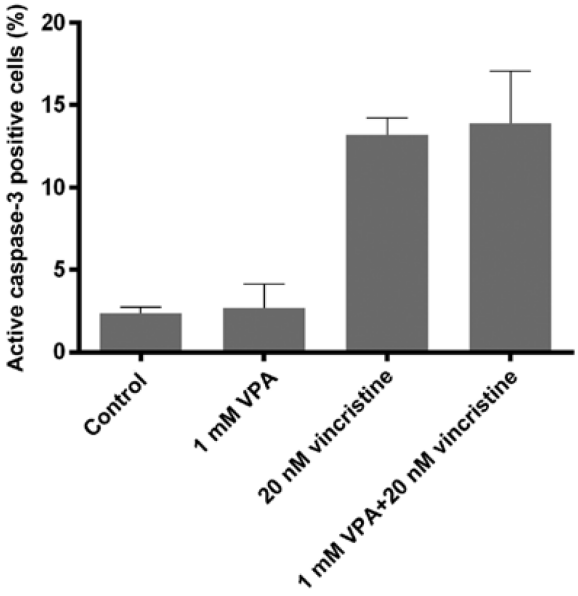

Figure 16: The percentage of UKF-NB-4 cells with active caspase-3 when treated with 1 mM VPA, 20 nM vincristine and their combination for 48 h. Mean and SD from three independent experiments are shown.

3.4 Effect of VPA in potentiating the potency of DNA-damaging drugs is related to its influence on acetylation of histones

Acetylation of histones is an important epigenetic phenomenon that is dictated by HDAC activities. Therefore, here we investigated the changes in acetylation of core histones H3 and H4 in UKF-NB-4 cells treated with VPA and TSA, as well as with VPM.

3.4.1 Treatment of UKF-NB-4 cells with valpromide has no effect on cisplatin cytotoxicity.

In additional experiments, we investigated cytotoxicity of valpromide (VPM) on UKF-NB-4 NB cells. VPM is a derivative of VPA which is also used as an antiepileptic drug, but does not exhibit HDAC inhibition activity (Phiel et al., 2001). We evaluated the effect of this drug on induction of apoptosis (measured by Annexin V/PI labeling) in these cells. Treatment of UKF-NB-4 cells with different concentrations of VPM (up to 4 mM) did not induce apoptosis in these cells and this non-toxic concentration of VPM did not potentiate apoptosis induced by 20 μM cisplatin (data not shown). When activation of caspase-3 in cells treated with VPM together with cisplatin was determined, no increase in the potency of cisplatin to activate caspase-3 by VPM was found (Figure 17). Exposure of UKF-NB-4 cells to 20 μM cisplatin combined with simultaneous treatment with 4 mM VPM does not increase amounts of cells with active caspase-3. These results indicate that the sensitizing effect of VPA on cisplatin toxicity in UKF-NB-4 NB cells is related to its HDAC inhibition activity.

3.4.2 Acetylation status of histones H3 and H4 in UKF-NB-4 cells treated with VPA, VPM, TSA, cisplatin, etoposide, and cytostatics combined with VPA

Cultivation of UKF-NB-4 cells with VPA and TSA at their non-toxic concentrations led to the different effects on acetylation of histones H3 and H4. Whereas 1 mM VPA increases acetylation of these histones in UKF-NB-4 cells, confirming its HDAC inhibitory efficiency, a negligible effect of 40 or 50 nM TSA on acetylation of these

histones was found (Figure 18). Therefore, TSA in such concentrations (40 or 50 nM) are insufficient to inhibit HDAC activities in UKF-NB-4 cells. However, when these cells were cultivated in a medium containing a higher (toxic) concentration of TSA (150 nM), a pronounced increase in acetylation of histones H3 and H4 was detected. In our experiments, we were not able to use this high concentration of TSA in combination with cytostatics due to its high cytotoxicity. In contrast to these results, no increase in acetylation of these histones was caused by VPM (Figure 18). This confirms the absence of HDAC inhibitory effects of this derivative of VPA.

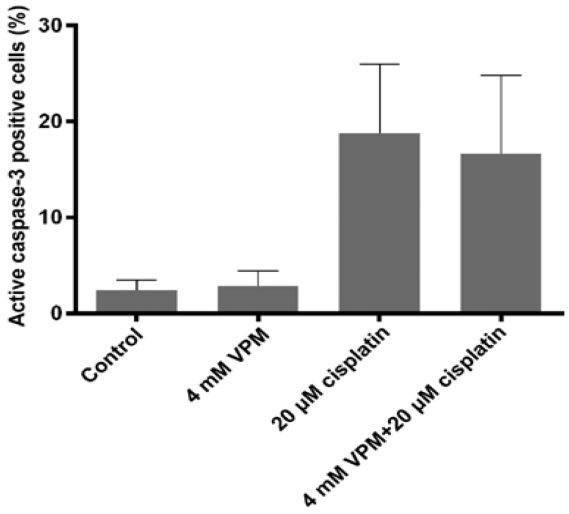

Figure 17: The percentage of UKF-NB-4 cells with active caspase-3 when treated with 4 mM VPM, 20 µM cisplatin and their combination for 48 hrs. Mean and SD from three independent experiments is shown.

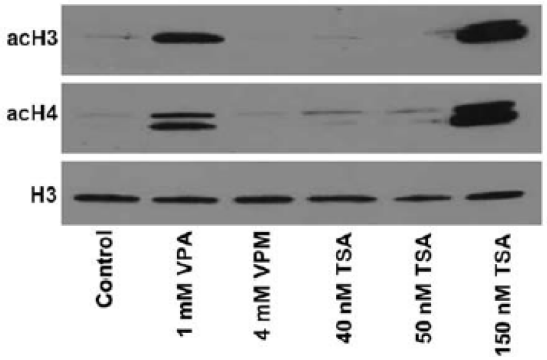

Figure 18: Western blot analysis of acetylated histones H3 and H4 in extracts from cells treated with 1 mM VPA, 4 mM VPM, 40, 50 and 150 nM TSA for 8 h. Histone H3 was used as loading control.

In addition, when UKF-NB-4 cells were treated with cisplatin or etoposide, a low decrease in acetylation of histone H3 and essentially no effect on acetylation of histone H4 were found (Figure 19).

In further experiments, two combination treatment regimens of the cells with VPA and cisplatin or VPA with etoposide were used to investigate the effects of combined treatment on the histones H3 and H4 acetylation status. Only the regimen, where UKF-NB-4 cells were pretreated with cisplatin or etoposide and then treated with VPA produced an increase in acetylation of histones H3 and H4 (Figure 19). This increase in histone acetylation paralleled the potentiation of toxic effects of cisplatin (Figure 14) or etoposide (Groh et al., 2012). Therefore, only if UKF-NB-4 cells were primarily affected by the tested DNA-damaging drugs prior to cultivation with VPA, a pronounced increase of histones acetylation can occur (Figure 19) and thus potentiated the cytotoxicity of both DNA-damaging drugs on UKF-NB-4 cells (Fig. 10).

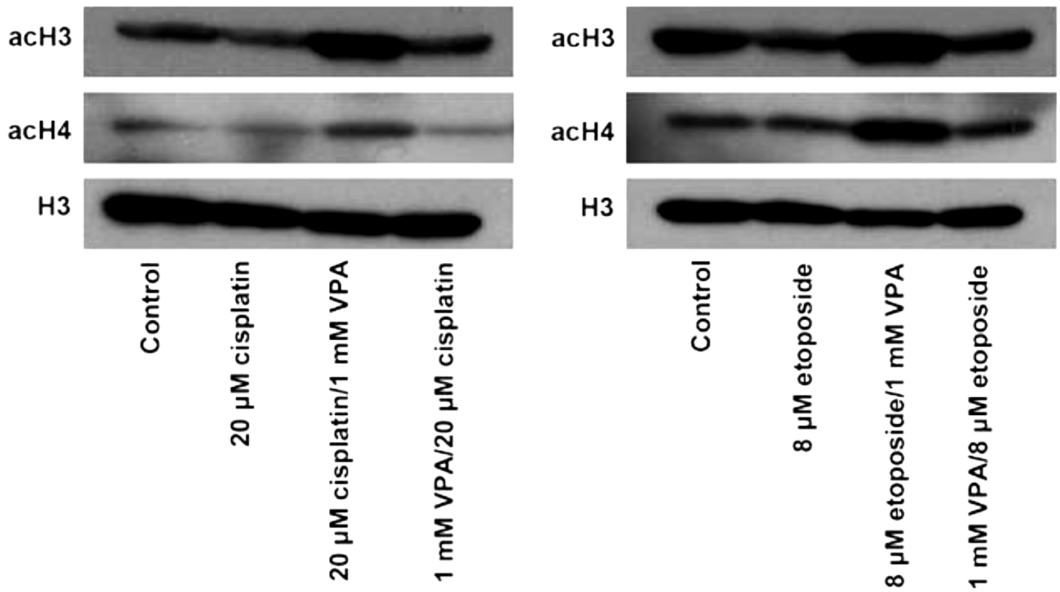

Figure 19. Levels of acetylated histones H3 and H4 in extracts from cells treated with 20 µM cisplatin and 8 µM etoposide, and these drugs combined with 1 mM VPA under different regimens, analyzed by western blotting. Histone H3 was used as loading control.

.

3.4.3 VPA does not influence etoposide-mediated phosphorylation of histone H2AX.

Etoposide is known to be the DNA-damaging drug acts as an inhibitor of topoisomerase-II activity, beside its intercalation into DNA, which enhance the formation of double-strand breaks in DNA (Baldwin and Osheroff, 2005; Hande, 1998; Wozniak and Ross, 1983). Phosphorylation of histone H2A on serine 139, termed γH2AX (pH2AX), by kinases sensing the double-strand DNA break is a sensitive marker of this type of DNA damage (Mah et al., 2010; Nakamura et al., 2010; Sokolov et al., 2007). Therefore, the levels of pH2AX were determined to determine whether treatment of cells with etoposide is influenced by VPA. After 48 h cultivation of cells in a medium containing 1 mM VPA, 4 μM etoposide and their combination, the levels of pH2AX were examined by flow cytometry. Representative histograms of pH2AX fluorescence found in these experiments are shown in figure 20. Whereas essentially no increase in pH2AX was induced by VPA (Figure 20B), a pronounced enhancement in pH2AX was caused by cell exposure to etoposide (Figure 20C). Co-cultivation of UKF-NB-4 cells with etoposide and VPA (Figure 20D) did not induce further enhancement of the percentage of pH2AX-positive cells as compared with cultivation of UKF-NB-4 cells with etoposide alone (Figure 20C and 20D).

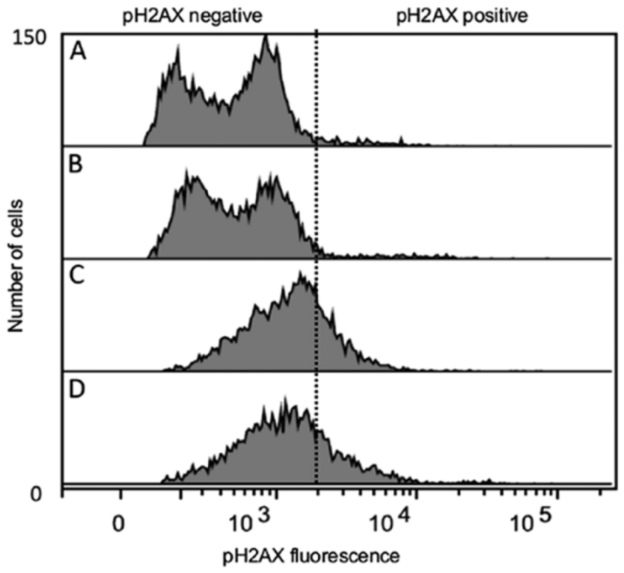

Figure 20: The effects of 1 mM VPA (B), 4 μM etoposide (C) or their combination (D) on generation of pH2AX in UKF-NB-4 cells treated with these drugs for 48 h. (A) Control cells that were incubated without any drug. Representative histogram of pH2AX fluorescence as a marker of double strand breaks is shown.

3.5 CD133 expression is influenced by epigenetic modifiers in neuroblastoma

In this part of our work, we investigated the relation of epigenetic changes (histone acetylation and promoter methylation) on the expression of the stem cell marker CD133 in the tested NB cell lines. VPA was the main drug we used to induce acetylation in the core histones and then we detected the subsequent changes in the CD133 expression. We also examined the methylation state of CD133 promoters in all tested cell lines and its relation to CD133 expression. We applied the demethylating agent AZA to cell lines with highly methylated CD133 promoters and detected its effect on CD133 re-expression.

3.5.1 Effect of VPA on the expression of CD133

VPA increased the expression of CD133 protein as detected by western blot (Figure 21) and the number of CD133+ cells detected by flow cytometry (Figure 22). The increase of CD133 expression was only seen in UKF-NB-3 and SH-SY5Y (Figure 21A and figure 22), while CD133 protein was not detected in UKF-NB-4 (Figure 21B) or in IMR-32 as revealed by western blot.

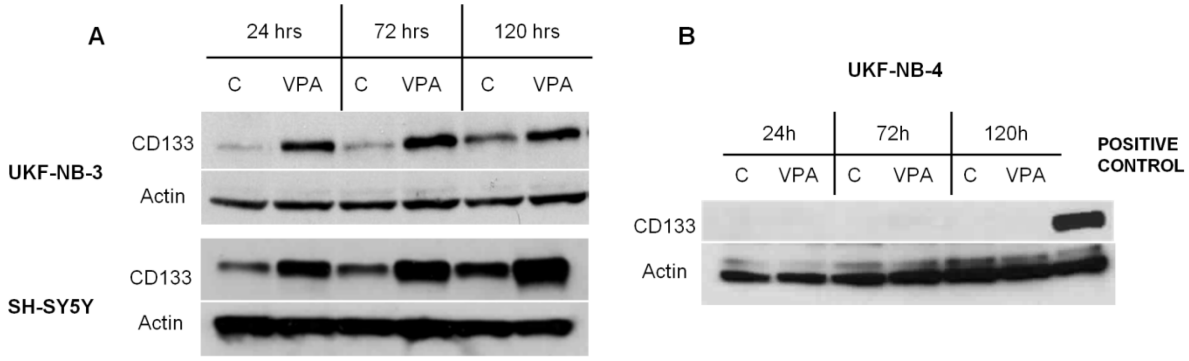

Figure 21: Changes of CD133 protein expression after cultivation with 1mM VPA in UKF-NB-3, SH-SY5Y and UKF-NB-4 by western blot. (A) VPA increased CD133 protein expression in UKF-NB-3 and SH-SY5Y in different time intervals. (B) CD133 protein was undetected in UKF-NB-4 cell line whether in the control or after cultivation with VPA in different periods of time. Positive control- UKF-NB-3 cells treated with VPA.

The induction of CD133 protein by VPA was obvious during the first 24 hrs of cultivation and was gradually increasing over time (Figure 21A). Noticeably, CD133 protein was consistently higher in VPA supplemented cultures than in control. Over-expression of CD133 protein following VPA treatment was accompanied by a parallel rise in the CD133 mRNA (Figure 23) as demonstrated in our article (Khalil et al., 2012). Note that the small amount of apoptosis induced by 1 mM VPA at 72 hrs (Table 4) excludes that CD133+ cells were increased as a relative result of the reduction of CD133− cells (as we suggest that CD133− cells are more liable for apoptosis than CD133+)

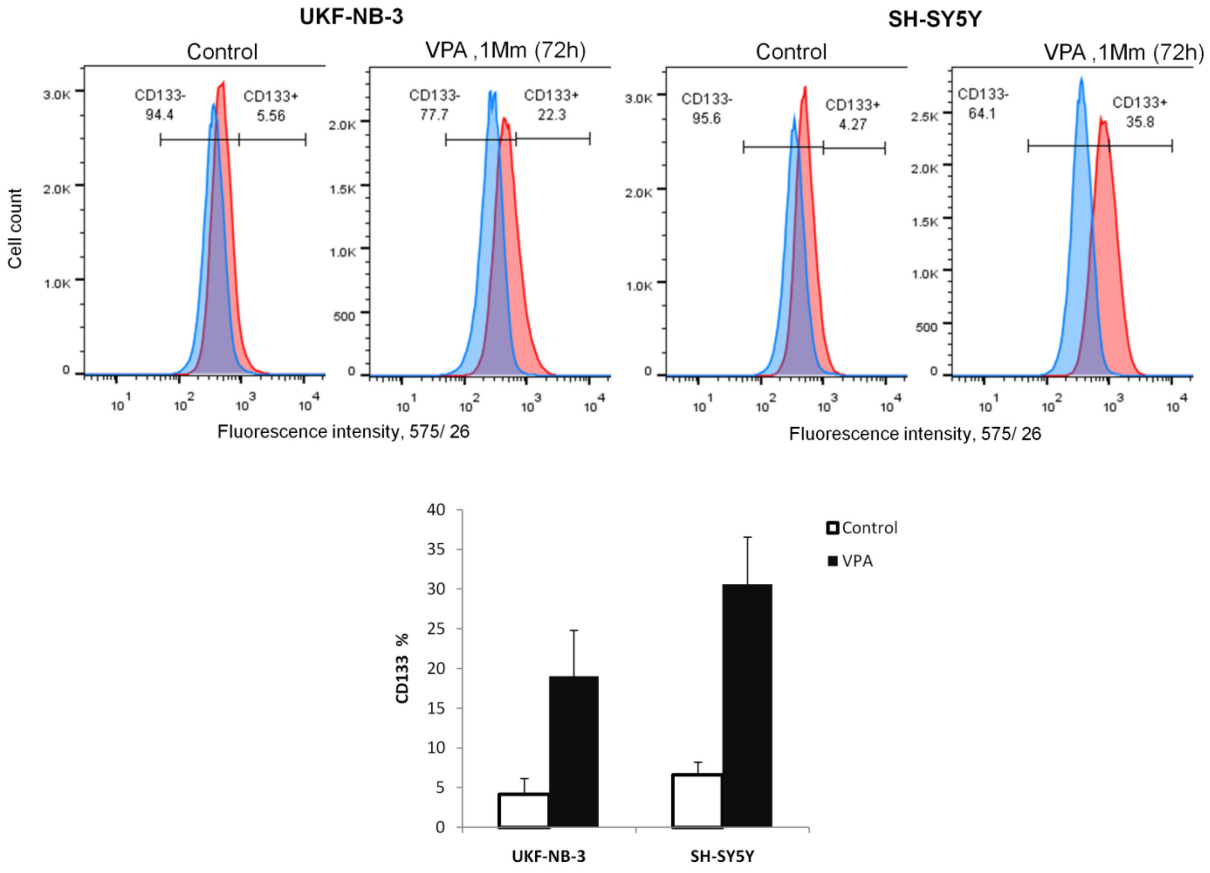

Figure 22: Cytometric measurements of CD133− and CD133+ in control cells and after cultivation with 1mM VPA for 72 hrs in UKF-NB-3 and SH-SY5Y. VPA increased the number of CD133+ cells in both cell lines. *Blue*—isotype control (IgG2b-PE); *red*—CD133 expression was detected using 293C3-PE (CD133/2) antibody.

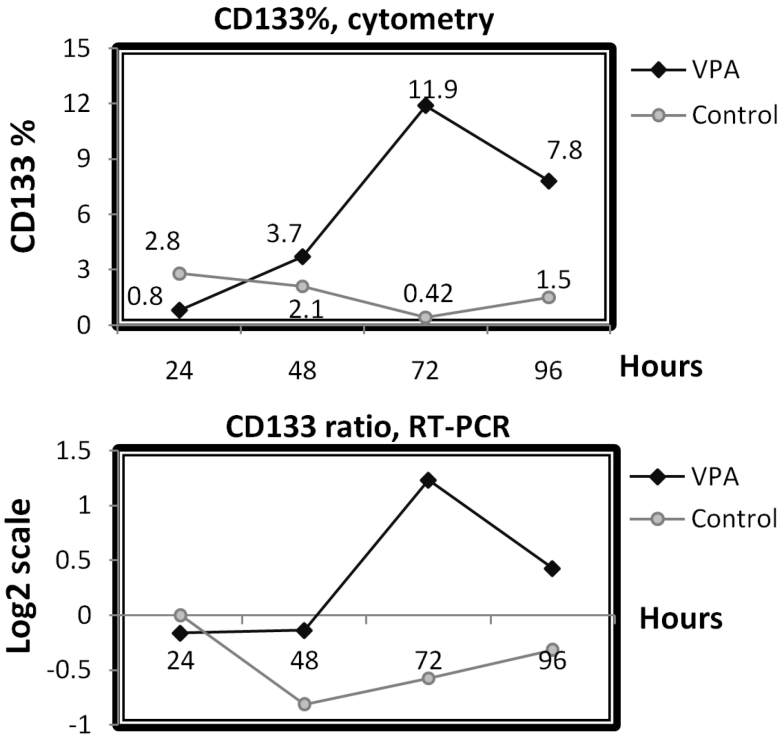

Figure 23: Cytometric measurements of CD133 surface antigen and its relation to mRNA expression in UKF-NB-3 cells after cultivation with 1 mM VPA. Upper graph represents CD133 measurements by flow cytometry (surface expression) – lower graph represents the mRNA values of CD133 detected by RT-PCR. mRNA was collected from the same cells as measured by flow cytometry in the upper graph. Black curve – incubation with VPA; grey curve – controls without VPA. Typical results of one of the four experiments.

3.5.2 Methylation status of CD133 promoter P1 and P3

Methylation level of CD133 promoters P1 and P3 was assessed using MS-HRM analysis (Figure 24). The methylation status of these promoters correlated with CD133 protein expression in all tested cell lines. For instance, cell lines with highly methylated promoters (UKF-NB-4 and IMR-32) did not express CD133 protein, while those with low methylation (UKF-NB-3 and SH-SY5Y) expressed CD133 as detected by western blot and flow cytometry (Figure 21 and figure 22).

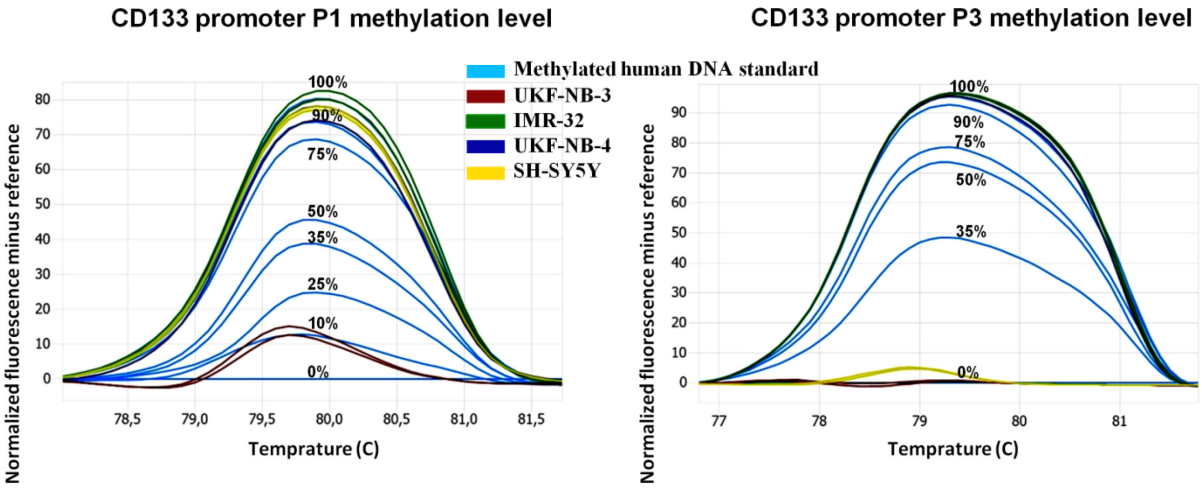

Figure 24: Normalized melt curves showing methylation status of promoters P1 and P3 in examined cell lines. In UKF-NB-3, methylation of both promoters were ranged from 0% to 10%, in SH-SY5Y (P1, > 90% and P3, 0%), in UKF-NB-4 (P1, 90% and P3, 100%) and in IMR-32 (P1, 100% and P3, 100%).

3.5.3 Effect of AZA and VPA on expression of CD133 in neuroblastoma cell lines

To assess whether CD133 expression was silenced by methylation, cell lines that showed no expression of CD133, even after incubation with VPA (UKF-NB-4 and IMR-32), were treated with the demethylating agent AZA. We found that CD133 protein was restored again in a small amount after AZA treatment and in a larger amount when AZA was combined with VPA (Figure 25). The re-expression of CD133 was associated with a drop in promoters P1 and P3 methylation levels (Figure 25). The increase of CD133 expression after VPA did not seem to coincide with changes in CD133 promoter methylation.

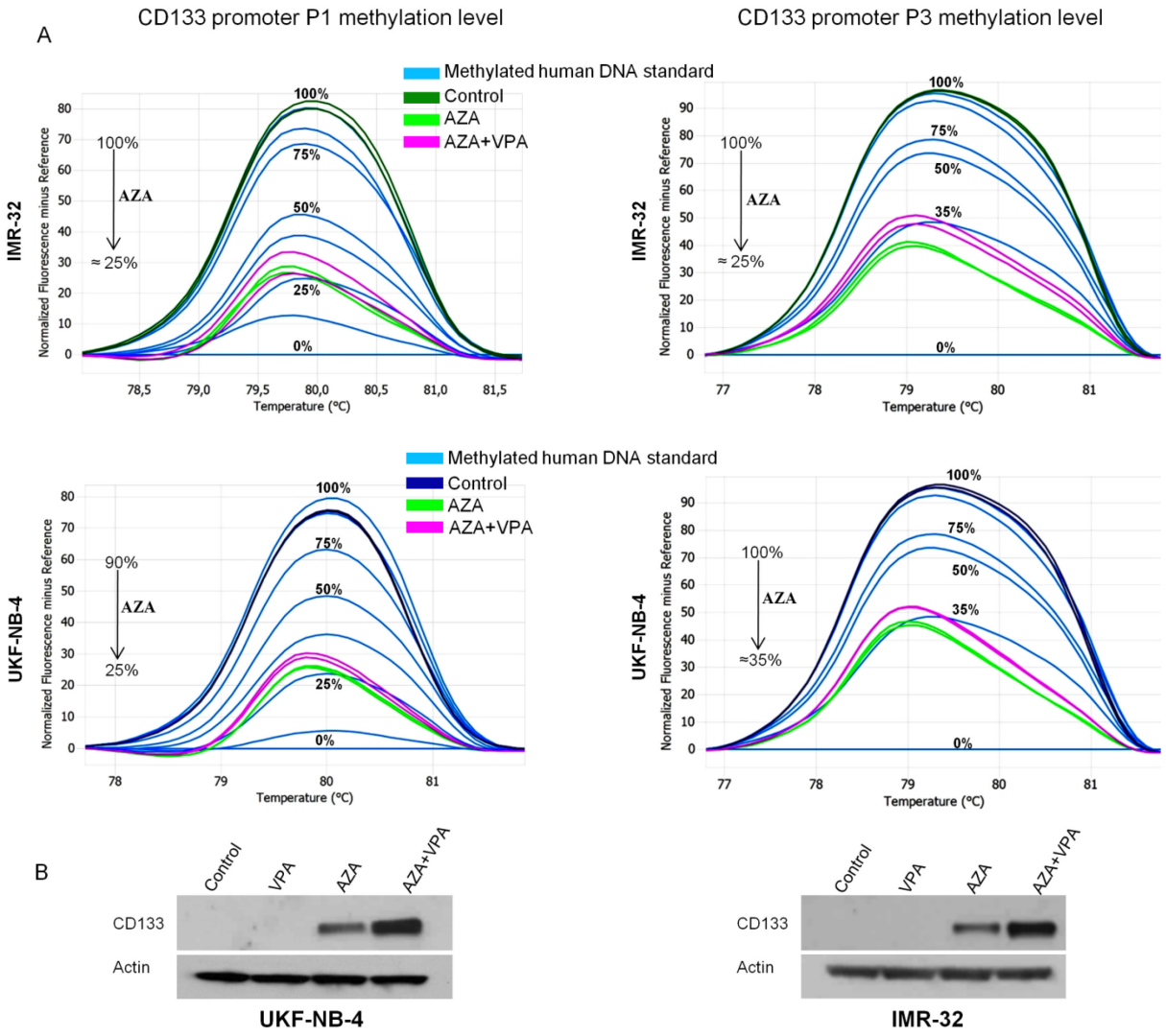

Figure 25: Normalized melt curves showing methylation status of promoters P1 and P3 in UKF-NB-4 and IMR-32 before and after using AZA and in combination with VPA. Western blot is showing the effect of 1mM VPA and AZA on CD133 expression in methylated cell lines. (A) Treatment with AZA decreased the methylation of both promoters P1 and P3 in UKF-NB-4 (P1 from 90% to 25% and P3 from 100%.to 35%) and IMR-32 (P1 from 100% to 25% and P3 from 100%.to < 35%) (B) CD133 was not detected in cell lines with methylated promoters (UKF-NB-4, IMR-32). Re-expression of CD133 was seen in a small amount after applying AZA and in high amount when AZA was combined with VPA. Treatment with VPA alone did not induce CD133 protein in UKF-NB-4 and IMR-32.

3.6 Relation of CD133 expression and acetylation of histones H3 and H4

We tested the cell line of unmethylated CD133 promoters (UKF-NB-3) in various conditions that variably affect the acetylation of histones H3 and H4 and we detected the changes in CD133 expression in each condition as follow

3.6.1 Effect of various histone deacetylase inhibitors on expression of CD133

We noticed that changes of CD133 protein expression were accompanied by parallel changes in histones H3 and H4 acetylation levels in all our experiments. We analyzed the expression of CD133 in UKF-NB-3 after 72 hrs incubation with different classes of HDAC inhibitors. Our results revealed that induction of CD133 by SAHA (0.5 μM), MS-275 (0.5 μM) and TSA (50 nM) or a lower dose of VPA (0.5 mM) correlated with the changes in H3 and H4 acetylation. For example, the maximum acetylation we noticed was induced by entinostat and was associated with highest expression of CD133. Similarly, the low dose of TSA that we tested did not seem to affect the acetylation of histones H3 and H4 and was not associated with increased expression of CD133 (Figure 26).

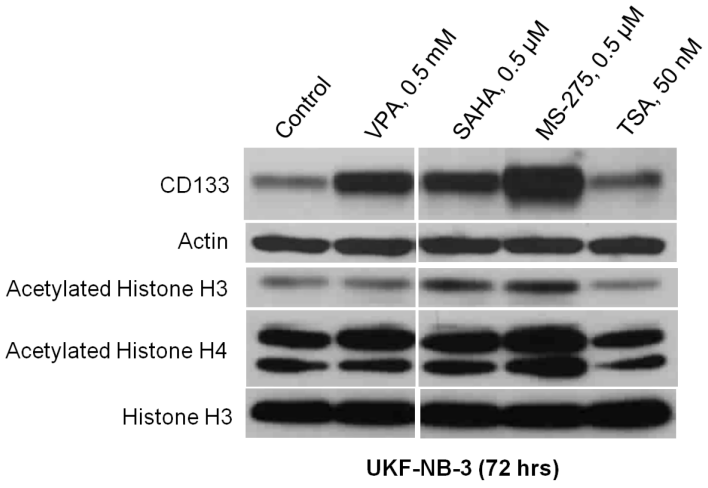

Figure 26: Changes of CD133 expression and histones H3 and H4 acetylation in UKF-NB-3 after cultivation with different classes of HDAC inhibitors. CD133 expression correlated with the changes of histones H3 and H4 acetylation when cultured with different HDAC inhibitors.

3.6.2 Effect of VPM on expression of CD133

Treatment of the UKF-NB-3 cells with different concentrations of VPM (1 mM, 2 mM and 3 mM) for 72 hrs showed no effect on the expression of CD133 as well as on the acetylation status of histones H3 and H4 at any of the tested concentrations (Figure 27). These concentrations were not cytotoxic and did not induce cell cycle arrest (data not shown). Of note, VPM is a carboxamide derivative of VPA which is used as antiepileptic drug but it does not inhibit HDAC (Phiel et al., 2001).

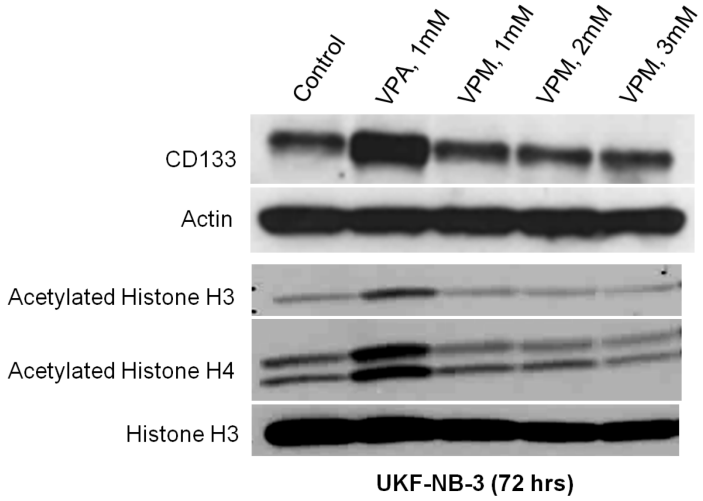

Figure 27: Changes of CD133 expression and histones H3 and H4 acetylation in UKF-NB-3 after cultivation with valpromide, VPM failed to influence CD133 expression and the histone acetylation after cultivation with non-toxic doses for 72 hrs.

3.6.3 Effect of high dose of cytostatics on CD133 expression

Furthermore, treatment for 24 hrs with high doses of CDDP (40 µM, IC_{50}/24 hrs = 11.12 µM ± 1.93) or VCR (200 nM, a dose that did not show cytotoxicity by MTT test within the first 24 hrs) was associated with low acetylation of histones H3 and H4 as well as a down-regulation of CD133 (Figure 28).

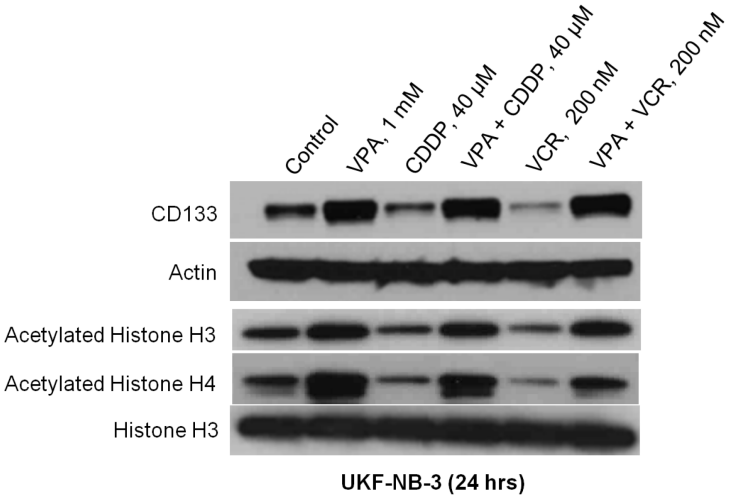

Figure 28: Changes of CD133 expression and histones H3 and H4 acetylation in UKF-NB-3 after cultivation with high doses of cytostatics. CD133 expression correlated with the changes of histones H3 and H4 acetylation when cultured with high doses of CDDP or VCR and in combination with VPA for 24 hrs.

3.7 Features of CD133+ neuroblastoma cells and cell lines treated with VPA

We determined the chemo-resistance of CD133+ and CD133− populations and their location along the cell cycle phases by co-staining cells with CD133 and cleaved caspase-3 or DAPI.

3.7.1 CD133+ cells are resistant to chemotherapeutic agents

We detected the cleaved caspase-3 in CD133+ and CD133− populations in UKF-NB-3 cell line after incubation with 1 µM CDDP (IC_{50} /72 hrs = 0.97 µM ± 0.10), 0.20 nM VCR (IC_{50} /72 hrs = 0.22 nM ± 0.03) and in combination with 1 mM VPA for 72 hrs. The percentage of cleaved caspase-3 was significantly higher in CD133− compared to CD133+ cells whether cells were cultured with cytostatics alone or in combination with VPA (Figure 29).

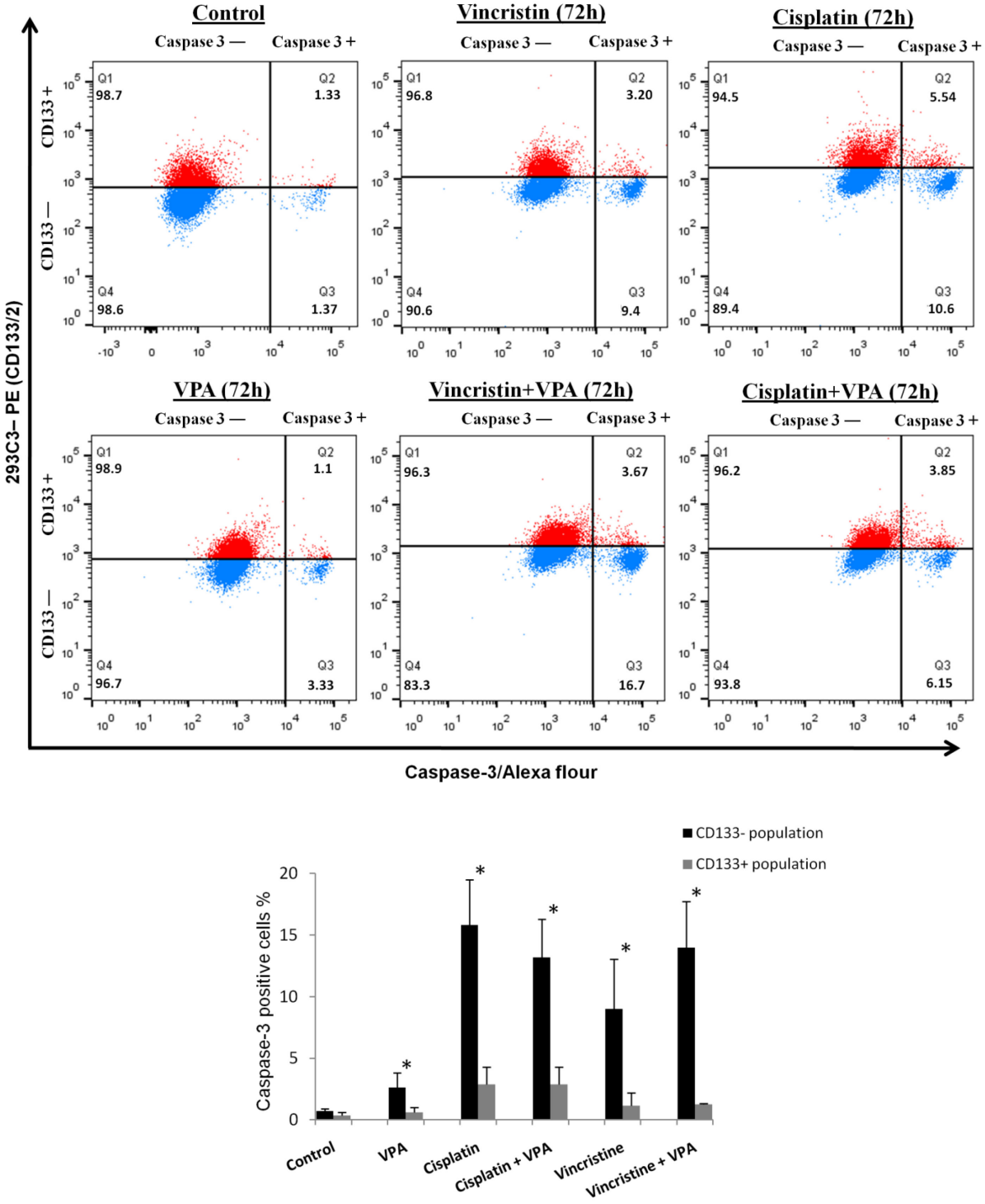

Figure 29: Activated caspase-3 in CD133– versus CD133+ populations after treatment with VPA combined therapy for 72 hrs. Activated caspase-3 was higher in CD133− cells compared to CD133+ cells; blue dots represent the CD133 negative cells and red dots represent CD133 positive cells. The lower graph shows that mean percentage of cells with cleaved caspase-3 was significantly higher in CD133− than in CD133+ cells in all tested samples.*$p < 0.05$— paired t-test.

3.7.1.1 Neuroblastoma cell lines rich in CD133 protein are expressing higher phosphorylated Akt

We compared the p-Akt (Ser 473) in two N-type NB cell lines, UKF-NB-3 which expressed high level of CD133 protein and IMR-32 which contained highly methylated CD133 promoters and did not express CD133 protein. The association of CD133 and Akt activation was tested through detection of p-Akt in different conditions that markedly influence the CD133 expression such as treatment with 1mM of VPA, with high dose of VCR (200mM) and their combination for 24 hrs. Our results clearly demonstrated a higher basal level of p-Akt in UKF-NB-3 than in IMR-32 where neither the CD133 nor the p-Akt was detected. The changes of p-Akt in UKF-NB-3 correlated with the changes of CD133 under all examined conditions (Figure 30).

Moreover, treatment with 1 mM VPA for 72 hrs enhanced the expression of p-Akt significantly in UKF-NB-3 while its expression was not detected in UKF-NB-4 or mildly increased in IMR-32 (both cell lines that did not express CD133). The level of p-Akt in SH-SY5Y was extremely high whether in control or in cells treated with VPA (see section 3.7.5).

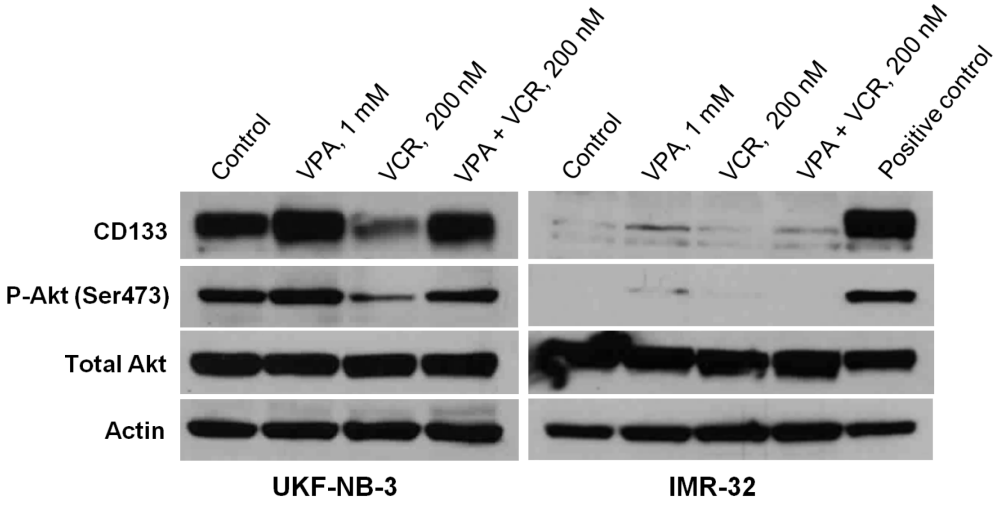

Figure 30: Expression of CD133 and p-Akt, in NB cell lines after treatment with1mM VPA. Changes of p-Akt in UKF-NB-3 correlated with the changes of CD133 under all examined conditions (1mM VPA or 200nM VCR for 24 hrs). Positive control- UKF-NB-3 cells treated with 1mM VPA for 24 hrs

3.7.2 CD133+ neuroblastoma cells are mainly located in the proliferative phases

Our results showed that CD133+ cells either in UKF-NB-3 or SH-SY5Y were mainly located in the S and G_2/M phases compared to CD133− cells which were predominantly seated in the G_0/G_1 phases whether in control or in samples incubated with 1mM VPA for 72 hrs (Figure 31). This indicates that CD133+ cells represent a proliferating fraction even under the cell cycle inhibitory effect of VPA. CD133+ cells were also induced by VPA combined therapy and were predominantly located in the S/G_2M phases during treatment with 1 µM CDDP or 0.20 nM VCR and in combination with 1mM VPA for 72 hrs (Figure 32).

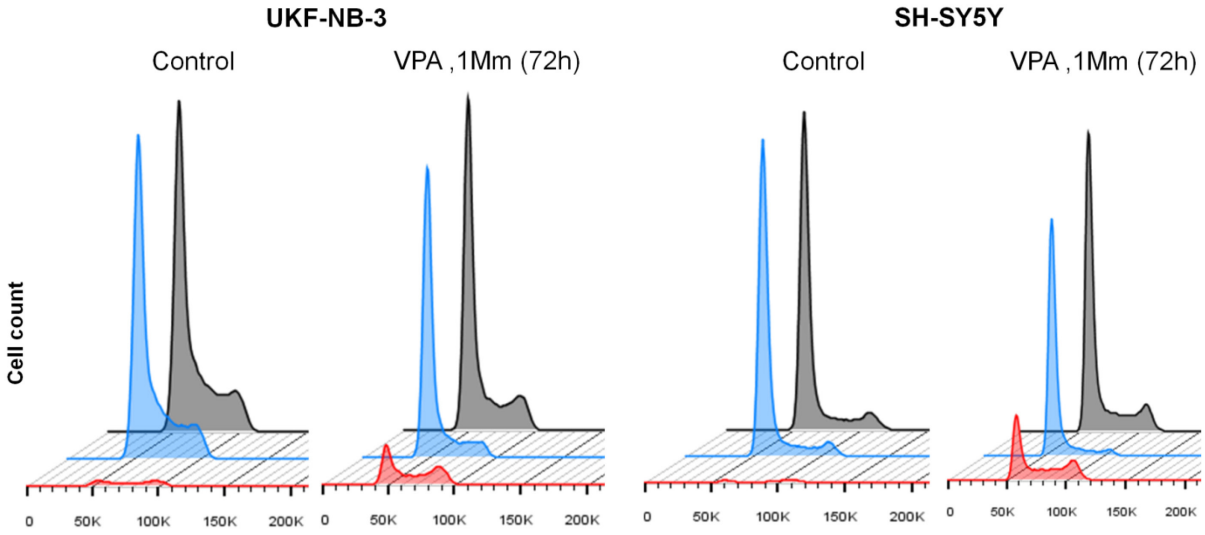

Control	G_0G_1	S/G_2M
CD133+	20.37 ± 1.59*	78.10 ± 2.82*
CD133-	62.64 ± 9.38*	35.25 ± 6.81*
ALL	51.43 ± 1.16	46.40 ± 3.26

VPA	G_0G_1	S/G_2M
CD133+	33.73 ± 9.54**	65.59 ± 10.87**
CD133-	77.73 ± 11.62**	19.84 ± 9.15**
ALL	58.23 ± 1.10	39.67 ± 2.6

Control	G_0G_1	S/G_2M
CD133+	22.17 ±1.72**	75.45 ±2.66**
CD133-	74.20 ±3.03**	24.73 ±3.68**
ALL	63.07 ±2.32	32.37 ±1.68

VPA	G_0G_1	S/G_2M
CD133+	35.40 ±1.85**	60.83 ±4.86**
CD133-	76.13 ±1.03**	21.97 ±1.4**
ALL	60.67 ±0.96	34.53 ±1.17

Figure 31: Cytometric assessment of CD133− and CD133+ cell cycles in control cells and after cultivation with 1 mM VPA for 72 hrs. CD133+ cells were mainly located in the S and G_2/M phases, while CD133− were mainly present in the G_0/G_1 phases in both cell lines UKF-NB-3 and SH-SY5Y. *Blue*— represents CD133 negative cells; *red*—represents CD133 positive cells; and grey represents both populations.

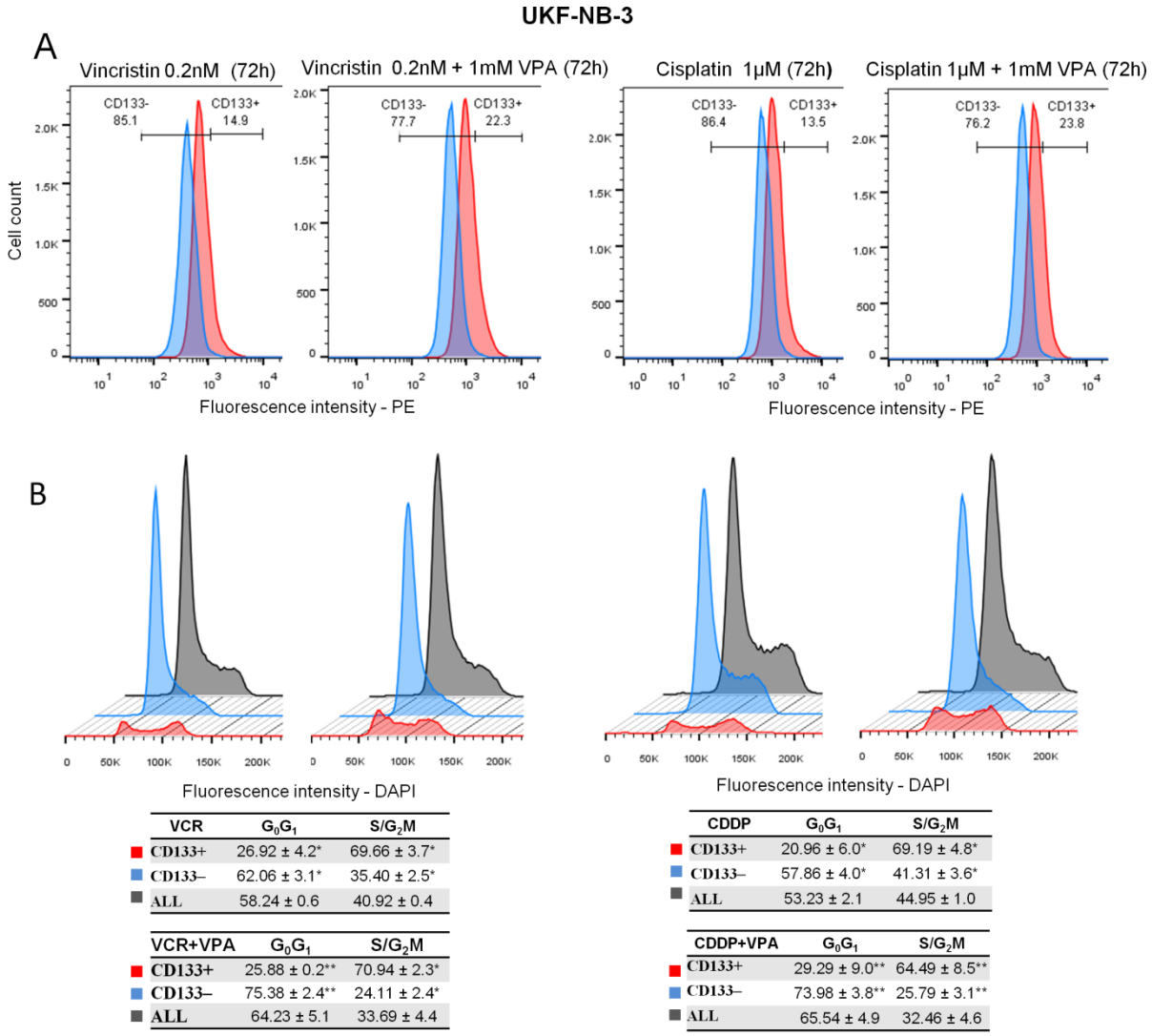

VCR	G_0G_1	S/G_2M
CD133+	26.92 ± 4.2*	69.66 ± 3.7*
CD133–	62.06 ± 3.1*	35.40 ± 2.5*
ALL	58.24 ± 0.6	40.92 ± 0.4

VCR+VPA	G_0G_1	S/G_2M
CD133+	25.88 ± 0.2**	70.94 ± 2.3*
CD133–	75.38 ± 2.4**	24.11 ± 2.4*
ALL	64.23 ± 5.1	33.69 ± 4.4

CDDP	G_0G_1	S/G_2M
CD133+	20.96 ± 6.0*	69.19 ± 4.8*
CD133–	57.86 ± 4.0*	41.31 ± 3.6*
ALL	53.23 ± 2.1	44.95 ± 1.0

CDDP+VPA	G_0G_1	S/G_2M
CD133+	29.29 ± 9.0**	64.49 ± 8.5**
CD133–	73.98 ± 3.8**	25.79 ± 3.1**
ALL	65.54 ± 4.9	32.46 ± 4.6

Figure 32: Changes of CD133 expression and cell cycle in VPA combined with different cytostatics at 72 hrs. (A) Increased CD133+ cells in VPA combined with vincristine and cisplatin. *Blue*—isotype control (IgG2b-PE); *red*—CD133 expression detected by 239C3 (CD133/2) antibodies. (B) CD133+ cells were mainly located in the S and G_2/M phases, while CD133− were mainly present in the G_0/G_1 phases during treatment with vincristine or cisplatin in combination with VPA.

3.7.3 VPA pretreated cells acquired higher colony formation capacity

UKF-NB-3 cells pretreated with VPA for 72 hrs showed significantly higher colony forming capacity compared to control, while the IMR-32 cell line which lacks for CD133 had fewer colonies than control (Figure 33). There was no significant

difference in the clonogenicity either in SH-SY5Y (Kovalevich and Langford, 2013) or UKF-NB-4 when pretreated with VPA.

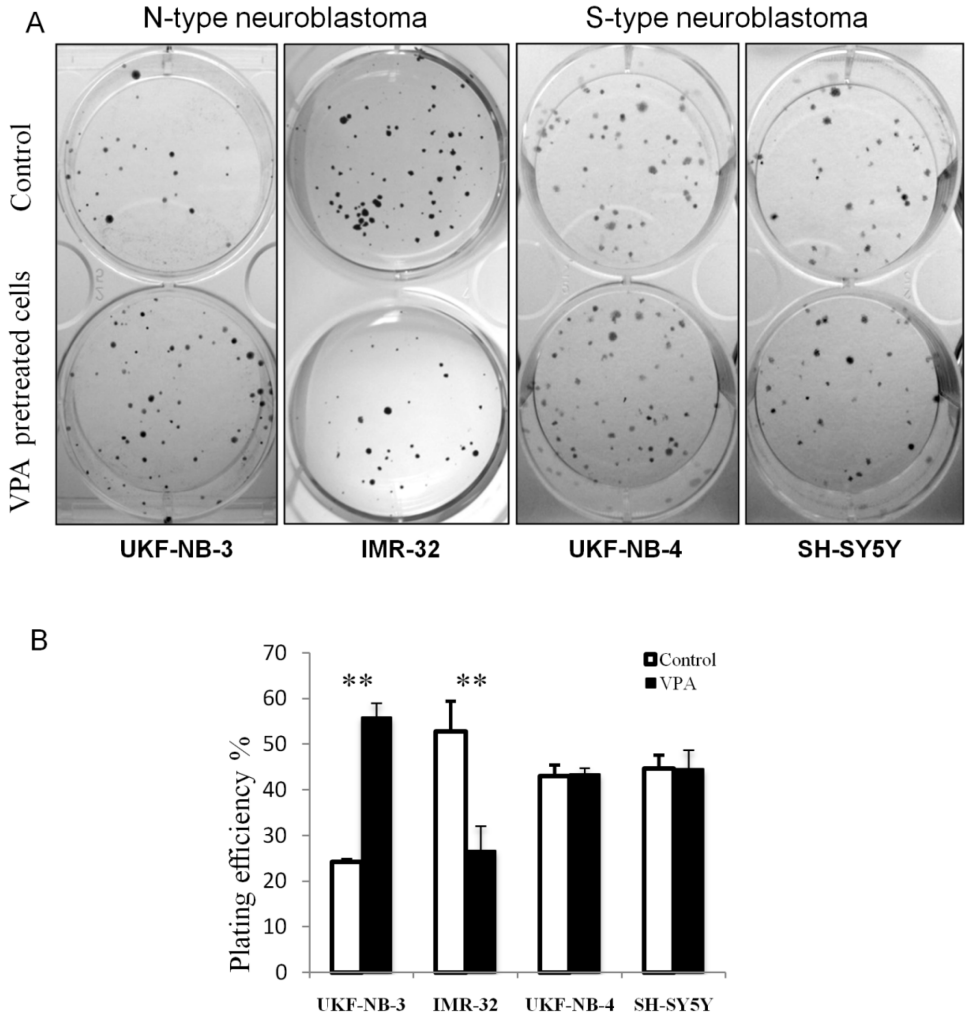

Figure 33: Effect of 1mM VPA on clonogenicity in NB cell lines. (A) Pretreatment with VPA significantly increased the clonogenicity in UKF-NB-3, while it decreased in IMR-32. In S-type NB (UKF-NB-4, SH-SY5Y) clonogenicity was not affected by pretreatment with VPA. VPA- cells pretreated with 1mM VPA for 72 hrs.

3.7.4 VPA pretreated cells acquired higher neurosphere formation capacity

Since sphere forming capacity is an indicator of the self-renewal activity of CSCs *in vitro*, we examined the effect of 72 hrs pretreatment with 1mM VPA on the frequency of neurospheres formation. UKF-NB-4 and SH-SY5Y cells maintained in

SFM were strictly adherent to the culture surface, forming monolayer, spreading without neurosphere formation. UKF-NB-3 and IMR-32 grown in SFM consistently formed organized neurospheres. UKF-NB-3 cells pretreated with VPA showed significantly higher capacity for neurospheres formation than control cells. IMR-32 pretreated with VPA showed slight increase in the neurospheres formation that was statistically insignificant (Figure 34).

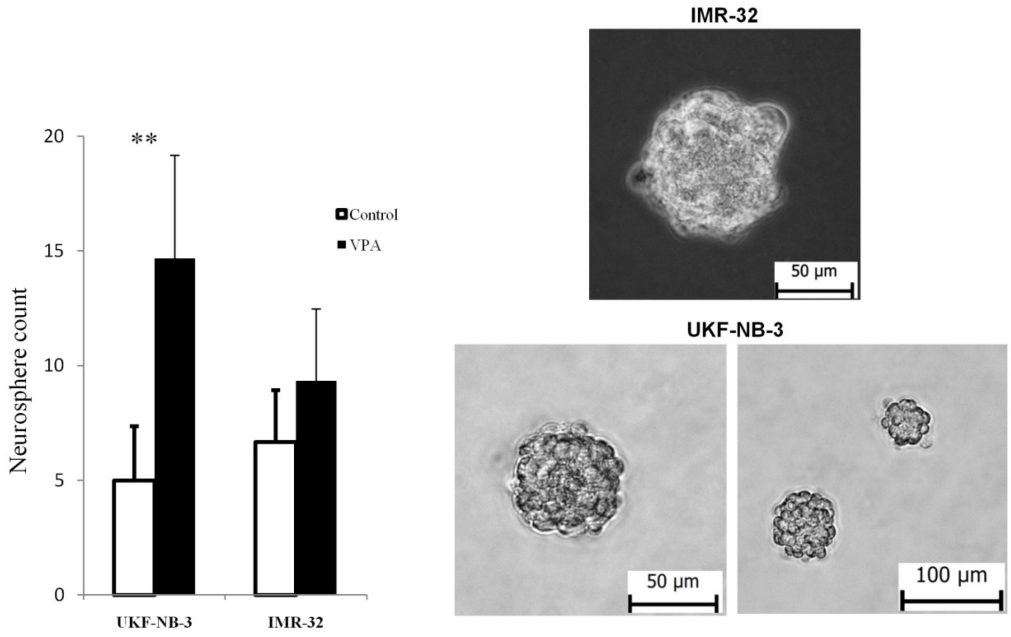

Figure 34: Effect of 1mM VPA on neurosphere formation in NB cell lines. Both UKF-NB-3 and IMR-32 were able to form neurospheres in SFM. Pretreatment with 1mM VPA increased the number of formed neurospheres with high statistical significance in UKF-NB-3.

3.7.5 VPA induced pluripotent transcriptional factors Oct4 and Sox2 in cell lines expressing CD133

We have examined the expression of stem cell transcription factors Oct4, Sox2 and Nanog in NB cell lines by western blot. We found that Oct4 is highly expressed in MYCN amplified cell lines UKF-NB-3, UKF-NB-4 (Poljaková et al., 2014) and IMR-32 (Veas-Perez de Tudela et al., 2010) and to a lesser extent in MYCN non-amplified cell line SH-SY5Y (Veas-Perez de Tudela et al., 2010). Treatment with VPA obviously enhanced the protein expression of Oct4 in

UKF-NB-3, IMR-32 and SH-SY5Y (Figure 35). On the other hand, Sox2 has been extensively expressed in SH-SY5Y and its low expression in UKF-NB-3 was enhanced by VPA treatment. Nanog was detected in low amount in UKF-NB-3, IMR-32 and SH-SY5Y that was enhanced by VPA treatment while it was overexpressed in UKF-NB-4 either in the control or VPA treated samples (Figure 35). Collectively, VPA enhanced the expression of stemness related markers (Oct4, Sox2 and Nanog) in variable amounts in NB cell lines particularly in those expressing CD133 (UKF-NB-3 and SH-SY5Y).

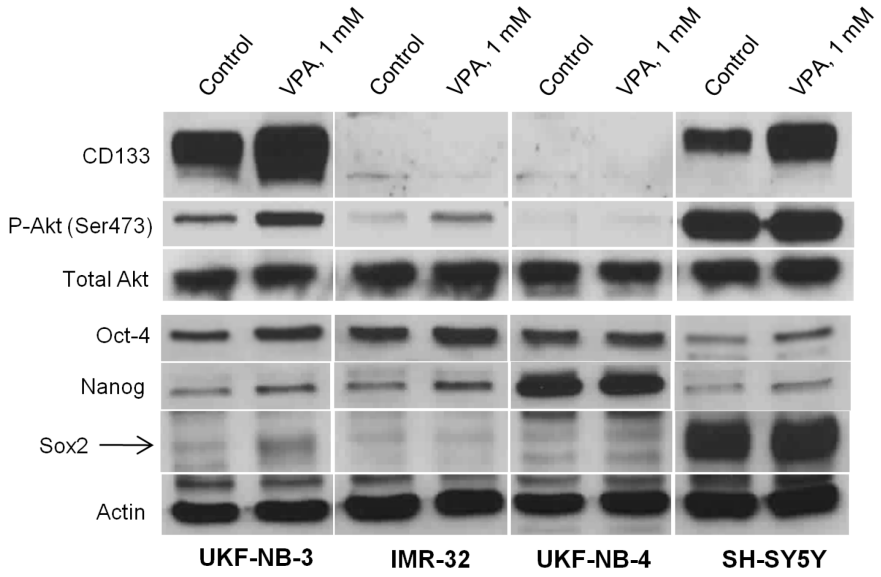

Figure 35: Expression of CD133, p-Akt, Oct4, Nanog and Sox2 in NB cell lines after treatment with 1 mM VPA. 72 hrs cultivation with VPA induced CD133 overexpression only in UKF-NB-3 and SH-SY5Y cell lines. p-Akt was highly expressed in CD133-expressing cell lines. Phophorylation of Akt was increased with VPA treatment in UKF-NB-3, whereas its expression was extremely high in SH-SY5Y whether in the control or in VPA treated sample. Oct4 was mainly expressed in MYCN amplified cell lines (UKF-NB-3, IMR-32 and UKF-NB-4) and was enhanced after treatment with VPA in UKF-NB-3, IMR-32 and SH-SY5Y. Nanog expression was detected in low amount that was enhanced by VPA in UKF-NB-3, IMR-32 and SH-SY5Y, while it was highly expressed in UKF-NB-4. Sox2 was slightly expressed in UKF-NB-3 and was induced by VPA while it was over expressed in SH-SY5Y independent of VPA effect.

3.8 Distribution of the CD133 in the cell

Notably, we found that the location of CD133 protein was not only restricted to the cell membrane but was also retained intracellularly as revealed by confocal microscope (Figure 36B) and by cytometric measurements of intracellular CD133 expression after permeabilization of cell membrane (Figure 37). The intracellular positivity was increased significantly after treatment with 1 mM VPA (Figure 36B and Figure 37). This implies that CD133− cells detected by flow cytometry might express CD133 intracellularly after incubation with VPA. During performing cytometric measurements, we ensured the selection of high positive CD133 cells which harbor the numerous surface CD133 molecules (we did not target the intracellular CD133) to run out the experiments concerning the chemoresistance and cell cycle of CD133+ population. The aid to achieve this selection was done by using the anti-Mouse IgG2b antibodies linked to phycoerythrin that was used as negative control to exclude the non-specific binding during the measurements. On the other hand, we followed a strict protocol concerning the flow cytometric experiments that based on double staining of cells with surface anti-CD133/2 antibody and the antibody that target the intracellular cleaved caspase-3 to only detect the surface CD133 and not the intracellular portion (Figure 29). In such experiments, we initially stained the cells with anti-CD133/2 antibody before permeabilization of cells, then fixing the cells with paraformaldehyde in a step that followed by wash then permeabilization of cells with gentle agent (diluted TritonX) prior to use anti cleaved caspase-3 antibody.

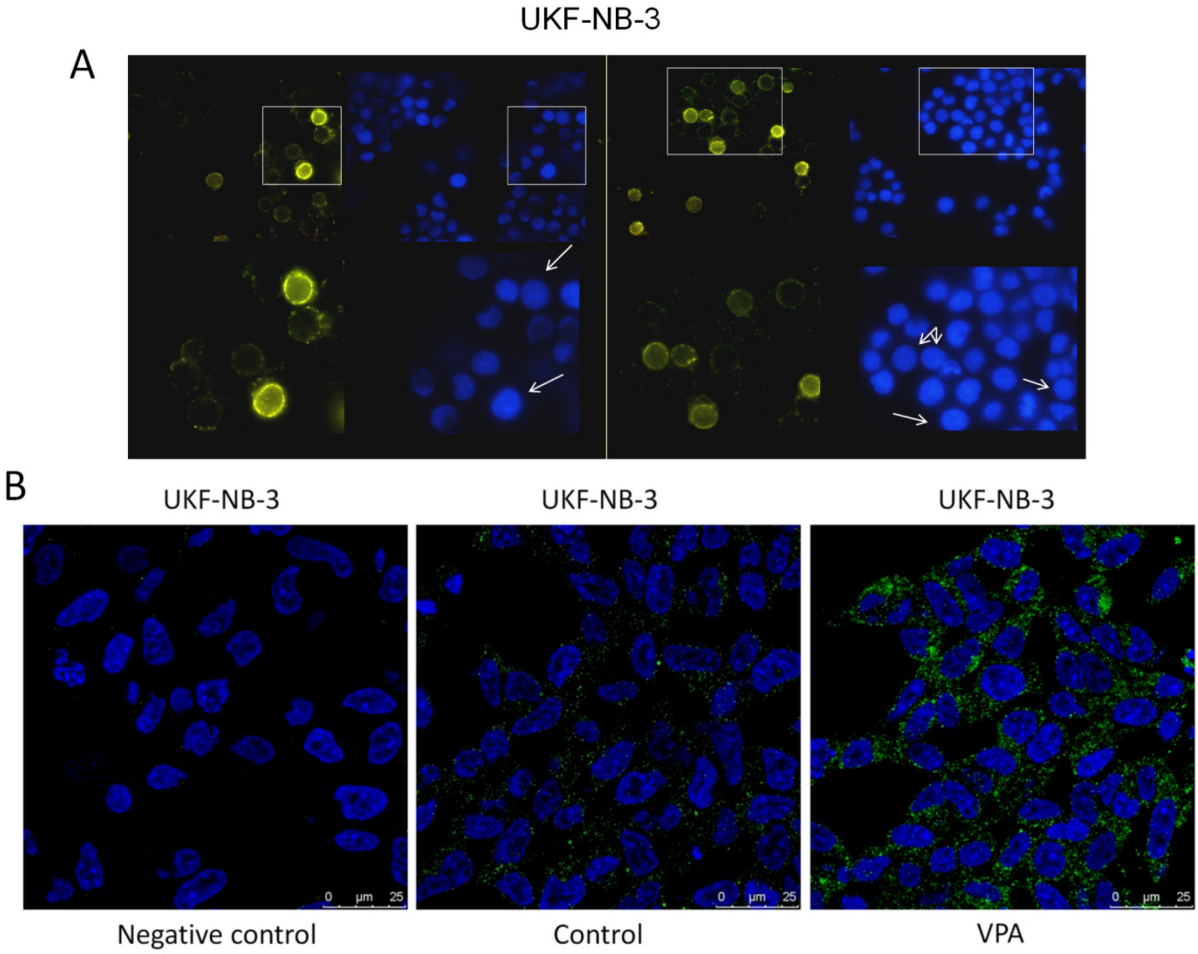

Figure 36: Surface and intracellular immunostaining of CD133 after treatment with 1 mM VPA for 72hrs. (A), Surface staining of CD133 in UKF-NB-3 using anti human CD133/2 PE conjugated antibodies and visualized under fluorescence microscope Olympus AX70. White arrows refer to corresponding nuclei of the CD133 positive cells that were counterstained with Hoechst 33342 dye. Left photo refers to control and the right photo refers to VPA treated sample **(B),** intracellular CD133 staining with primary monoclonal anti-CD133 clone W6B3C1 and secondary antibodies goat anti-mouse DyLight 488 IgG. permeabilization of cells in two steps using paraformaldehyde 3.6% followed by a 0.25% TritonX / PBS. Nuclei were counterstained with DAPI.

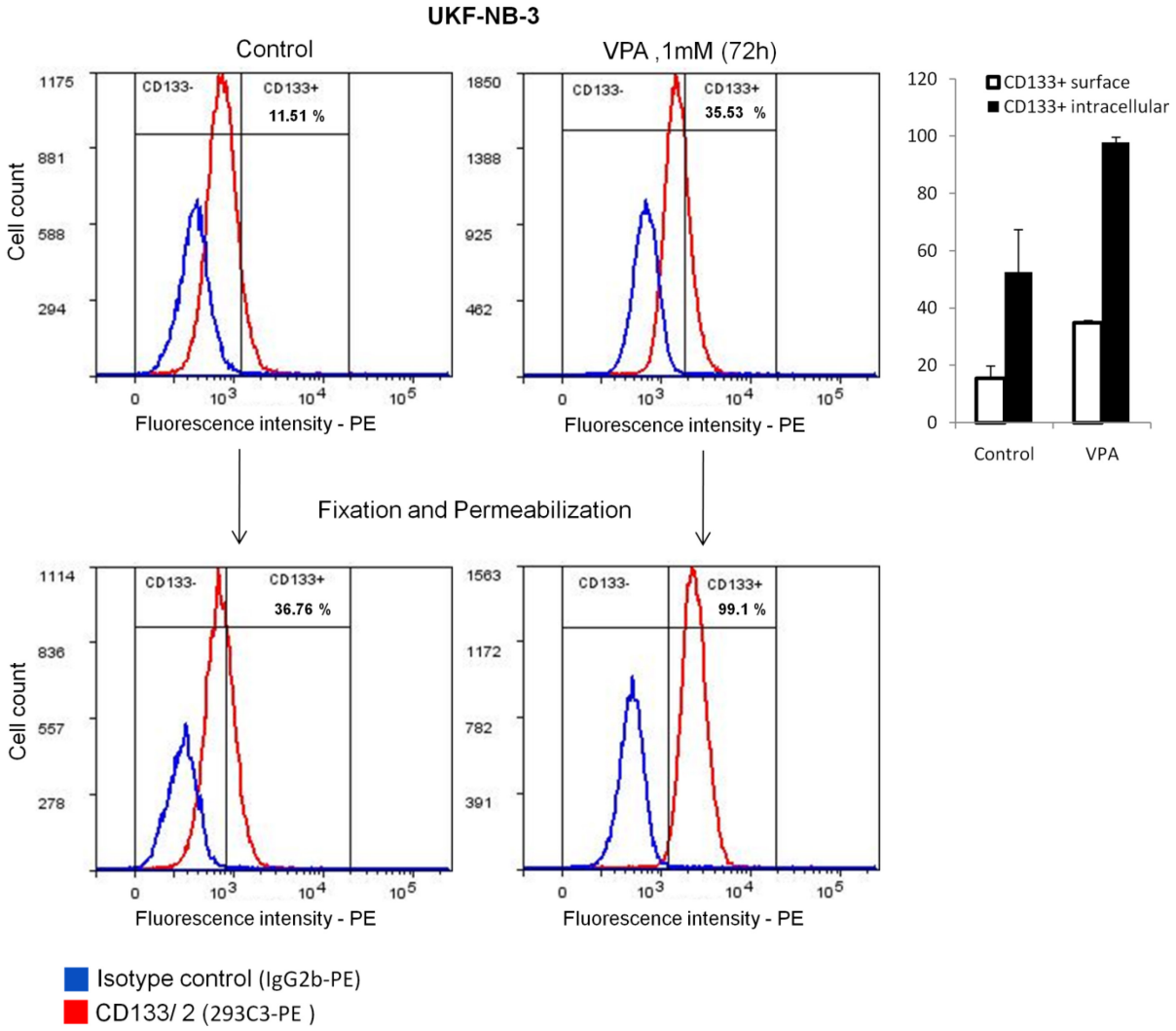

Figure 37: Comparison of the cytometric measurements of the surface and intracellular staining of CD133 in UKF-NB-3. CD133 was present on the surface as well as intracellularly either in the control or after treatment with VPA. VPA increased CD133 surface expression significantly and enriched almost all cells with CD133 molecule intracellularly. Intracellular staining was performed through fixation and permeabilization of cells in two steps using paraformaldehyde 3.6% followed by a 0.15% TritonX / PBS. Data were analyzed using Flowlogic software (Inivai Technologies, Mentone, Australia).

Chapter 4

Discussion

The poor response of high-risk NB to current treatment regimens suggests that novel therapeutic strategies should be developed. The inhibitors of HDACs, used in the combination with other drugs, were found to be promising anticancer regimens efficient against several cancer cells including NBs (Cipro et al., 2012; Das et al., 2010; Groh et al., 2012; Kim et al., 2003; Poljakova et al., 2011; Stiborova et al., 2012; Wang et al., 2013). In this work, we analyzed the cytotoxic effect of VPA in combination with other chemotherapeutics and we also highlighted the possible limitations of using VPA in some types of tumors due to its effect on expansion of CSCs. The results found in this study demonstrate that VPA used at the clinically relevant dose (1 mM) has potentiating effect on cytotoxicity and caspase-3-mediated induction of apoptosis caused by the tested DNA-damaging drugs cisplatin and etoposide. Analyzing the combination index of VPA combined with cisplatin or etoposide was revealed to act synergistically.

However, no sensitizing effect due to VPA was produced with the mitotic inhibitor vincristine. These results indicate that HDAC inhibitor-mediated capability of increasing cytotoxic efficiency of anticancer drugs is connected with the drugs that target cellular DNA. These findings correspond to the results found in the study of dos Santos *et al* (dos Santos et al., 2009) that also investigated the effect of a combination of etoposide or vincristine with the HDAC inhibitor sodium

butyrate (an HDAC inhibitor of the same group as VPA) on human lymphoblastic T-cells. The authors demonstrated that from these two drugs, only etoposide, but not vincristine, was sensitized by the used HDAC inhibitor. In their study, the sensitizing effect of the HDAC inhibitor on doxorubicin, another DNA-damaging drug, was also proved.

The mechanisms of the potentiating effects of HDAC inhibitors on the efficiency of DNA-damaging drugs have not yet been fully elucidated. It was suggested that HDAC inhibitors promote the lysine acetylation in nucleosomal histones that is thought to relax the chromatin, thereby allowing increased access of transcription factors and DNA-damaging agents to DNA (Kim et al., 2003; Stiborova et al., 2012). In our study, the increased toxicity of cisplatin and etoposide was indeed dependent on the acetylation status of core histones H3 and H4 dictated by the effect of HDAC inhibitors. VPA increased amounts of acetylated histones H3 and H4 and the elevated levels of these acetylated histones correlated with sensitization of UKF-NB-4 cells to cisplatin and etoposide. TSA (another HDAC inhibitor) at a concentration that essentially did not influence the acetylation of these histones (40 nM) was ineffective. Likewise, VPM (a structural analogue of VPA) that does not increase acetylation of histones H3 and H4 as well did not enhance cytotoxicity of the tested DNA-damaging drugs in our study. It should be, however, emphasized that the sequence of VPA application is the crucial feature for potentiating the cytotoxic effect of cisplatin and etoposide on NB cells. Namely, this HDAC inhibitor potentiated the cytotoxic effect of cisplatin or etoposide only when there were added simultaneously, or when cells were pre-incubated with cisplatin or etoposide before their cultivation with VPA. Only these regimens were efficient to increase acetylation of histones and thus suppress the viability of NB cells. In contrast, the reversed sequence (pretreatment of cells with VPA before treatment with cisplatin or etoposide) did not give any further increase in cytotoxicity of the DNA-damaging drugs or in the acetylation of histones. All these findings suggest that DNA damage is crucial for the additional effects of VPA, arguing against the hypothesis based on relaxed chromatin that increases accessibility of DNA-damaging drugs to DNA (Kim et al., 2003; Stiborova et al.,

2012). Similarly, the results found by Luchenko *et al* (Luchenko et al., 2011) indicated that DNA relaxation is not required for the synergy of two HDAC inhibitors they tested, belinostat and romidepsin, with cisplatin and etoposide. One can speculate that the changes in the structure of DNA caused by cisplatin and etoposide (i.e., formation of DNA adducts or DNA cross-links by cisplatin, intercalation of etoposide into DNA, and/or formation of reactive oxygen species by both drugs (Kurz et al., 2001; Luchenko et al., 2011; Yu et al., 2007)) increase accessibility of nucleosomal core histones to their acetylation, which additionally determines transcription of some genes involved in DNA repair or apoptosis. This suggestion needs, however, to be further investigated.

Despite the observed synergy of the combination where UKF-NB-4 cells were initially treated with etoposide before VPA in cell survival and apoptosis (Groh et al., 2012), we found no evidence for enhancement of etoposide-mediated H2AX phosphorylation when etoposide was combined with VPA. Double strand DNA breaks markedly increased in UKF-NB-4 cells treated with etoposide, but after simultaneous treatment of these cells with etoposide and VPA no further increase in the pH2AX foci formation was detected. This indicates that other mechanisms can be responsible for this synergistic effect of VPA on induction of cell death in UKF-NB-4 rather than enhancement of double-strand DNA breaks caused by etoposide (due to inhibition of topoisomerase-II activity)

One of the challenges in conducting a clinical trial when combining an inhibitor of HDACs VPA with DNA damaging agents will be to achieve optimal DNA damage in a given tumor tissue. The results found in the present study demonstrate that treatment of cells with VPA potentiates the cytotoxicity of DNA damaging agents, cisplatin and etoposide, on UKF-NB-4 cells without increasing their access to DNA. The data presented here show that treatment with cisplatin or etoposide prior to addition of VPA is superior to alternative schedules and supports the development of clinical trials using these combinations for NB cells. The clinical use of such combined treatment utilizing DNA damaging drugs with VPA can reduce frequent problems such as dose reductions, temporary discontinuation of treatment as a result of toxicity and thus can improve the

treatment itself and the patient's quality of life. Another option is to test the effect of the HDAC inhibitors in combination with two cytostatics, because in clinical practice, cytotoxic drugs are combined in virtually all cases.

In the second section of this thesis, we studied the effect of VPA on expression of the stem cell marker “CD133” in NB cell lines. CD133 gene is complex in its structure with seven splice variants and its protein expression pattern is still debated. Several authors have shown that sorted CD133+ cells from different solid tumors displayed greater tumorigenicity and resistance to chemotherapeutic agents compared to CD133– cells. However, other researchers demonstrated that CD133– cells can display similar capacities as CD133+ (Meng et al., 2009; Shmelkov et al., 2008). The reason for this contradiction can be explained by some factors which regulate and alter CD133 expression such as the glycosylation pattern (Kemper et al., 2010), the change in the bioenergetic status (hypoxia and mitochondrial dysfunction) (Griguer et al., 2008) and more importantly is the conclusion that CD133 protein expression is not synonymous to cell surface epitopes immunoreactivity (Barrantes-Freer et al., 2015; Kemper et al., 2010). In our study, we found that CD133 molecule can be located intracellularly as well as on the cell membrane. Treatment with VPA increased the intracellular expression of CD133, unlike CD133 surface expression that was increased as well but still limited to smaller cellular subpopulation. For this reason, we performed the cytometric staining of CD133 before permeabilization of cell membrane to ensure that the detected CD133+ cells are those expressing CD133 epitope on cell membrane and not intracellularly. This remark is of great value when working with CD133 to ensure the precise detection of CD133+ cells.

In our article, we examined the epigenetic effects of the HDAC inhibitor VPA on the expression of CD133+ in NB and we gave overview about the variability of CD133 protein expression in relation to the acetylation of histones and methylation status of CD133 promoters. We used two antibodies that can identify different epitopes of the CD133 protein, W6B3C1 (CD133/1) that we used for immunoblotting and 293C3 (CD133/2) for flow cytometric analysis. Even though 293C3 (CD133/2) antibody recognizes different epitope than AC133 (CD133/1)

(the conventional antibody used to detect and isolate CSCs), it has shown similar sensitivity in detecting CD133+ cells (Kemper et al., 2010). Our results offer evidence for induction and maintenance of CD133+ cells in NB cell lines through inhibition of HDAC by VPA. We relate this effect to its action on increasing the acetylation of histones which leads to chromatin accessibility and consequent transcription of many genes including CD133. In contrast, valpromide (carboxamide derivative of VPA that does not inhibit HDAC) did not alter the histone acetylation and was not accompanied by any change in the expression of CD133. We noticed a positive correlation between CD133 expression and the acetylation of histones H3 and H4 in all our experiments. A lower dose of VPA that was used in clinical trials (Wheler et al., 2014) as well as different classes of HDAC inhibitors increased the expression of CD133 in variable degrees that were in positive correlation with the amount of H3 and H4 acetylation. This suggests the concomitant relation between CD133 expression and acetylation of histones H3 and H4 induced by HDAC inhibitors. Interestingly, we noticed down-regulation of CD133 when treated with high doses of VCR or CDDP, which should not be interpreted to mean that CD133 permanently disappeared, because the same cells were able to significantly express CD133 when combined with VPA. This variability in CD133 expression is under control of the epigenetic modification which could explain why sorted CD133− cells can acquire the CD133 surface marker or CD133+ cells can lose it in some tumors as was described by Feng JM (Feng et al., 2012)

We also showed that CD133 could be controlled by methylation of its CpG promoters that can silence the expression of CD133 protein. In our study, CD133 was dramatically increased after using VPA in cell lines with unmethylated P1 and/or P3 promoters (UKF-NB-3 and SH-SY5Y). On the other hand, cell lines with methylated P1 and/or P3 promoters (UKF-NB-4 and IMR-32) failed to show any increase in CD133 after VPA treatment. CD133 expression in those lines was only restored by demethylating agent AZA and can be enhanced if the demethylation is followed by increasing histone acetylation by VPA. Thus, our work is in agreement

with Shmelkov et al., who stated that promoter methylation may play a key role in CD133 regulation (Shmelkov et al., 2004).

In our study, VPA induced both CD133 mRNA transcription and CD133 protein expression that was reflected on the increase of CD133+ cells as detected by flow cytometry (Khalil et al., 2012). The point to highlight here is that VPA had the potential to turn cells that were detected as CD133− using flow cytometry into CD133+. This led us to suggest two possibilities: first, VPA could maintain the CD133+ cells undifferentiated which explain the consistent expression of surface CD133 epitopes in VPA treated samples. Second, CD133− cells were able to synthesize CD133 protein and express it in accessible pattern on cell surface, thus acquire the characters of CD133+ cells.

This action of VPA can be related to the effect of HDAC inhibitors in cell reprogramming and induction of pluripotent cells (Kretsovali et al., 2012). In fact, we detected variable expression of pluripotent transcriptional factors Oct4, Sox2 and Nanog in CD133 expressing cell lines and they were obviously induced by VPA treatment. Although Oct4 and Nanog were also expressed in NBs lines with MYCN amplification such as IMR-32 and UKF-NB-4, these cell lines did not show evidence of Sox2 protein expression which was only detected in CD133 expressing cell lines. A previous reports have demonstrated that Oct4 and Sox2 orchestrate together to maintain the self-renewal and pluripotency of embryonic and neural stem cells (Rizzino, 2009). However, Oct4 alone is considered as a master pluripotency gene and is expressed in side-population cells of NB (Hämmerle et al., 2013). Knockdown of Oct4 inhibited the formation of spheres and the CD133 expression in MYCN-amplified human NBs cells (Kaneko et al., 2015). Additionally, high expression of Oct4 was correlated with poor prognosis especially in patients with MYCN-amplified NBs (Kaneko et al., 2015). Based on previous remarks, combined induction of these transcription factors together with CD133 expression after VPA treatment in MYCN amplified cell line (UKF-NB-3) might suggest induction of pluripotency. According to previously mentioned results, it was necessary to perform further experiments to assess the self-renewal and chemoresistance of VPA treated UKF-NB-3 cells.

Human NB cells occur in three different subtypes, S-type, N-type, and I-type, each with distinct morphology and behavior. S-type cells resemble glial precursor cells, which are highly substrate adherent, and are non-invasive. N-type cells have a neuronal morphology, and are less substrate adherent, but highly invasive (Ross et al., 2003). In our study, pretreatment with VPA significantly enhanced colony formation capacity in the N-type NB cell line UKF-NB-3 but not IMR-32, which lacks the CD133 protein. There was no difference in colony formation regarding the S-type NB cells. We suggest that pretreatment with a low dose of VPA can enhance colony formation capacity of susceptible tumors, which may be related to the increase in CD133+ cells. Additionally, it has been reported the role of CD133 in cell adhesion (Koyama-Nasu et al., 2013) which greatly can affect the colony formation in N-type with low attachment characters rather than the S-type with high attachment ability. Therefore, we examined the capacity of neurospheres formation which can be more reliable test for the self-renewal activity *in vitro*. We found that VPA significantly increased the number of formed neurospheres in UKF-NB-3 but not in IMR-32, whereas the S-type NBs consistently formed adherent colonies.

We used the cytometry to examine the cell cycle and apoptosis-sensitive cells within the pool of the cultured cells. We demonstrated that CD133+ cells are mainly present in the S/ G_2M phases, while CD133− cells largely reside in G_0/G_1 either in the control or in samples treated with VPA or cytostatics which agree with other published results (Barrantes-Freer et al., 2015). Regarding the cell cycle of stem cells, it is widely accepted that they are generally dormant *in vivo* and they tend to proliferate to regenerate tissue loss (Wakao et al., 2012). Similarly, cell lines growing in exponential phase seem to be a model of this regeneration (Tirino et al., 2008) . In particular, evidence suggests that CSCs may arise from normal stem cells, progenitor cells or more differentiated cells with dysregulated proliferation (Han et al., 2013). These remarks can explain high proliferation capacities of CD133+ cells which match with our findings and emphasis that CD133+ cells form a characteristic population in tumor. Previous results clarified that CD133 mRNA knockdown in highly expressing CD133 NB cells effectively

resulted in significant growth retardation in adherent cell cultures (Kamijo, 2012). Moreover, CD133 was considered as a marker for specific stages of the cell cycle (S, G_2 or M) in CSCs (Sun et al., 2009). Altogether, we suggest that CD133+ cells can represent a significant proliferative fraction in NB cell lines.

Caspase-3 is the effector caspase that cleaves some cellular proteins including caspase-activated DNAase, which causes DNA fragmentation that is characteristic for apoptosis (O'Donovan et al., 2003). Therefore, low level of cleaved caspase-3 detected in CD133+ compared to CD133− cells in UKF-NB-3 cell line when treated with VPA and cytostatics, indicates resistance to apoptosis. This is in agreement with published result showing lower sensitivity of sorted CD133+ NB cells to cisplatin, carboplatin, etoposide, and doxorubicin compared to CD133− cells (Vangipuram et al., 2010). Interestingly, we detected a high level of p-Akt (active form) in UKF-NB-3 and SH-SY5Y in contrast to IMR-32 which lacks for CD133 protein and showed low level of activated Akt. The level of activated Akt in UKF-NB-3 was enhanced by VPA therapy and repressed by high dose of VCR that goes along with the changes in the CD133 expression in both conditions. The level of p-Akt in SH-SY5Y was extremely high and did not show higher expression when treated with VPA. Our results is supported by previous studies reported the association between the expression of CD133 in different cancers and activation of Akt pathway (Ma etal., 2008; Wei et al., 2013). Wei et al., revealed that the phosphorylated Y828 residue in CD133 cytoplasmic tail binds to PI3K regulatory subunit p85 which results in the activation of PI3K/Akt pathway, subsequently promoting the self-renewal and tumor formation of glioma stem cells. They also explained that CD133 is phosphorylated on cytoplasmic Y828 by Src family kinases (nonreceptor tyrosine kinases that are activated rapidly on the engagement of multiple cell surface receptors) (Boivin et al., 2009). The activation of Akt is proposed to trigger pro-survival signaling via Akt mediated cell cycle arrest and anti-apoptotic mechanisms leading to chemotherapeutic resistance (Ellis et al., 2013). Altogether, we supposed that cancer cells expressing CD133 may get benefits from activation of Akt signaling during VPA therapy such as resisting apoptosis which manifested by low activated caspase-3 in our study.

Chapter 5

Conclusion

In conclusion, we found that addition of VPA to cancer chemotherapeutics could synergize the cytotoxicity of DNA-damaging chemotherapeutics effectively in UKF-NB4 cells. This synergism was related to increase the acetylation status of histones H3 and H4 and was significant either by simultaneous treatment with both drugs or by pretreatment of cells with DNA-damaging chemotherapeutics before their exposure to VPA.

On the other hand, we found that CD133 expression in NB can be regulated by histones acetylation and/or methylation of its CpG promoters. Thus, we showed that the HDAC inhibitors can increase CD133 expression significantly in neuroblastoma cell lines that show low methylated CpG promoters.

We also found that VPA treatment can increase the number of CD133+ cells that show higher resistance to cytostatics than CD133– cells. VPA treatment enhanced the ability of CD133 expressing cell line UKF-NB-3 to generate more colonies and neurospheres, induce Akt phosphorylation, induce expression of the pluripotency transcriptional factors which collectively may lead to induce chemoresistance and preserve tumor growth. Amplification of cancer stem like cells might be unwanted action of VPA during cancer treatment as it antagonizes the idea of cancer stem cell theory that gives attention to target the CSCs rather than the more differentiated tumor cells.

No doubt that addition of high doses of VPA to conventional chemotherapy has revealed a synergistic effect on cell cycle inhibition and apoptosis induction in tumor cells but we have to keep in mind that VPA dose is limited by its toxicity and has different anti-cancer effects depending on tumor cell biology. Therefore, it is of great value to determine the type of tumors that can be beneficial from VPA therapy.

Finally, further investigations are needed for evaluation of epigenetic therapy (HDAC inhibitors and demethylating agents) on induction of CSCs in tumors prior to their use in clinical medicine. In addition, Selective HDAC inhibitors should be designed to overcome the unwanted effects of pan HDAC inhibitors.

References

Burton,B. S. (1882). On the propyl derivatives and decomposition products of ethylacetoacetate. *Am. Chem. J.*, *3*:385–395.

Baba, T., Convery, P. A., Matsumura, N., Whitaker, R. S., Kondoh, E., Perry, T., Huang, Z., Bentley, R. C., Mori, S., Fujii, S., Marks, J. R., Berchuck, A., and Murphy, S. K. (2009). Epigenetic regulation of CD133 and tumorigenicity of CD133+ ovarian cancer cells. *Oncogene*, *28*(2):209–18.

Baldwin, E. L., and Osheroff, N. (2005). Etoposide, topoisomerase II and cancer. *Curr. Med. Chem. Anticancer Agents*, *5*(615):363–372.

Barrantes-Freer, A., Renovanz, M., Eich, M., Braukmann, A., Sprang, B., Spirin, P., Pardo, L. A., Giese, A., and Kim, E. L. (2015). CD133 Expression Is Not Synonymous to Immunoreactivity for AC133 and Fluctuates throughout the Cell Cycle in Glioma Stem-Like Cells. *PLoS ONE*, *10*(6): e0130519.

Bird, A. (2002). DNA methylation patterns and epigenetic memory. *Genes Dev*, *16*(1): 6–21.

Boivin, D., Labbé, D., Fontaine, N., Lamy, S., Beaulieu, E., Gingras, D., and Béliveau, R. (2009). The Stem Cell Marker CD133 (Prominin-1) is Phosphorylated on Cytoplasmic Tyrosine-828 and Tyrosine-852 by Src and Fyn Tyrosine Kinases. *Biochemistry*, *48*(18):3998–4007.

Bolden, J. E., Peart, M. J., and Johnstone, R. W. (2006). Anticancer activities of histone deacetylase inhibitors. Nat. Rev. Drug Discov., *5*(9):769–84.

Boudadi, E., Stower, H., Halsall, J. A., Rutledge, C. E., Leeb, M., Wutz, A., O'Neill, L. P., Nightingale, K. P., and Turner, B. M. (2013). The histone deacetylase inhibitor sodium valproate causes limited transcriptional change in mouse embryonic stem cells but selectively overrides Polycomb-mediated Hoxb silencing. *Epigenetics Chromatin*, *6*(1):11.

Brescia, P., Ortensi, B., Fornasari, L., Levi, D., Broggi, G., and Pelicci, G. (2013). CD133 is essential for glioblastoma stem cell maintenance. *Stem Cells*, *31*(5):857–869.

Brodeur, G. M., Minturn, J. E., Ho, R., Simpson, A. M., Iyer, R., Varela, C. R., Light, J. E., Kolla, V., and Evans, A. E. (2009). Trk receptor expression and inhibition in neuroblastomas. *Clin. Cancer Res*., 15(10):3244-50.

Brodeur, G. M., Pritchard, J., Berthold, F., Carlsen, N. L., Castel, V., Castleberry, R. P., De Bernardi, B., Evans, A. E., Favrot, M., Hedborg, F., and Voute, P. A. (1993). Revisions of the international criteria for neuroblastoma diagnosis, staging, and response to treatment. *J. Clin. Oncol.*, 11(8):1466–1477.

Burba, I., Colombo, G. I., Staszewsky, L. I., De Simone, M., Devanna, P., Nanni, S., Avitabile, D., Molla, F., Cosentino, S., Russo I., De Angelis, N., Soldo, A., Biondi, A., Gambini, E., Gaetano, C., Farsetti, A., Pompilio, G., Latini, R., Capogrossi, M. C., and Pesce, M. (2011). Histone deacetylase inhibition enhances self renewal and cardioprotection by human cord blood-derived CD34 cells. *PLoS ONE*, *6*(7):e22158.

Burkitt, K., and Ljungman, M. (2008). Phenylbutyrate interferes with the Fanconi anemia and BRCA pathway and sensitizes head and neck cancer cells to cisplatin. *Mol. Cancer*, *7*:24.

Camphausen, K., Cerna, D., Scott, T., Sproull, M., Burgan, W. E., Cerra, M. A., Fine, H., and Tofilon, P. J. (2005). Enhancement of in vitro and in vivo tumor cell radiosensitivity by valproic acid. *Int J Cancer*, *114*(3):380–386.

Camphausen, K., Scott, T., Sproull, M., and Tofilon, P. J. (2004). Enhancement of xenograft tumor radiosensitivity by the histone deacetylase inhibitor MS-275 and correlation with histone hyperacetylation. *Clin. Cancer Res.*, *10*(18 I):6066–6071.

Ceccacci, E., and Minucci, S. (2016). Inhibition of histone deacetylases in cancer therapy: lessons from leukaemia. *Br. J. Cancer*, *114*(6):605–611.

Chen, C. L., Sung, J., Cohen, M., Chowdhury, W. H., Sachs, M. D., Li, Y.,

Lakshmanan, Y., Yung, B. Y., Lupold, S. E., and Rodriguez, R. (2006). Valproic acid inhibits invasiveness in bladder cancer but not in prostate cancer cells. *J Pharmacol Exp Ther*, *319*(2):533–542.

Chen, C. S., Wang, Y. C., Yang, H. C., Huang, P. H., Kulp, S. K., Yang, C. C., Lu, Y. S., Matsuyama, S., Chen, C. Y., and Chen, C. S. (2007). Histone deacetylase inhibitors sensitize prostate cancer cells to agents that produce DNA double-strand breaks by targeting Ku70 acetylation. *Cancer Res.*, *67*(11):5318–5327.

Chou, T. C. (2006). Theoretical basis, experimental design, and computerized simulation of synergism and antagonism in drug combination studies. *Pharmacol. Rev.*, *58*(3):621–681.

Chou, T. C., and Talalay, P. (1984). Quantitative analysis of dose-effect relationships: the combined effects of multiple drugs or enzyme inhibitors. *Adv. Enzyme Regul.*, *22*:27–55.

Cinatl, J., Gussetis, E. S., Cinatl, J. J. R., Ebener, U., Mainke, M., Schwabe, D., Doerr, H. W., Kornhuber, B., and Gerein, V., (1990). Differentiation arrest in neuroblastoma cell culture. *J. Cancer Res. Clin. Oncol*, *116 Suppl*(1):9–14.

Cipro, Š., Hřebačková, J., Hraběta, J., Poljaková, J., and Eckschlager, T. (2012). Valproic acid overcomes hypoxia-induced resistance to apoptosis. *Oncol. Rep.*, *27*(4):1219–1226.

Clarke, M. F., Dick, J. E., Dirks, P. B., Eaves, C. J., Jamieson, C. H., Jones, D. L., Visvader, J., Weissman, I. L., and Wahl, G. M. (2006). Cancer stem cells - Perspectives on current status and future directions: AACR workshop on cancer stem cells. *Cancer Res.,* 66(19):9339–9344.

Colarossi, L., Memeo, L., Colarossi, C., Aiello, E., Iuppa, A., Espina, V., Liotta, L., and Mueller, C. (2014). Inhibition of histone deacetylase 4 increases cytotoxicity of docetaxel in gastric cancer cells. *Proteomics Clin. Appl.*, *8*(11–12):924–931.

Das, C. M., Zage, P. E., Taylor, P., Aguilera, D., Wolff, J. E. A., Lee, D., and Gopalakrishnan, V. (2010). Chromatin remodelling at the topoisomerase II-beta

promoter is associated with enhanced sensitivity to etoposide in human neuroblastoma cell lines. *Eur. J. Cancer*, *46*(15), 2771–2780.

Dawson, M. A., and Kouzarides, T. (2012). Cancer epigenetics: from mechanism to therapy. *Cell*, 150(1):12-27.

De Felice, L., Tatarelli, C., Mascolo, M. G., Gregorj, C., Agostini, F., Fiorini, R., Gelmetti, V., Pascale, S., Padula, F., Petrucci, M. T., Arcese, W., Nervi, C. (2005). Histone deacetylase inhibitor valproic acid enhances the cytokine-induced expansion of human hematopoietic stem cells. *Cancer Res*, 65(4):1505–1513.

Dokmanovic, M., Clarke, C., and Marks, P. A. (2007). Histone deacetylase inhibitors: overview and perspectives. *Mol. Cancer Res*, *5*(10):981–9.

dos Santos, M. P., Schwartsmann, G., Roesler, R., Brunetto, A. L., and Abujamra, A. L. (2009). Sodium butyrate enhances the cytotoxic effect of antineoplastic drugs in human lymphoblastic T-cells. *Leuk. Res.*, *33*(2):218–221.

Dragu, D. L., Necula, L. G., Bleotu, C., Diaconu, C. C., and Chivu-Economescu, M. (2015). Therapies targeting cancer stem cells: Current trends and future. *World J. Stem Cells*, *7*(9):1185–201.

Du, W., Hozumi, N., Sakamoto, M., Hata, J., and Yamada, T. (2008). Reconstitution of Schwannian stroma in neuroblastomas using human bone marrow stromal cells. *Am J Pathol*, *173*(4):1153–1164.

Earnshaw, W. C., Martins, L. M., and Kaufmann, S. H. (1999). Mammalian caspases: structure, activation, substrates, and functions during apoptosis. *Annu. Rev. Biochem.*, *68*:383–424.

Ecker, J., Oehme, I., Mazitschek, R., Korshunov, A., Kool, M., Hielscher, T., Kiss J, Selt, F., Konrad, C., Lodrini, M., Deubzer, H. E., von Deimling, A., Kulozik A. E., Pfister, S. M., Witt, O., and Milde, T. (2015). Targeting class I histone deacetylase 2 in MYC amplified group 3 medulloblastoma. *Acta Neuropathol. Commun.*, 3:22.

Ellis, L., Ku, S., Ramakrishnan, S., Lasorsa, E., Azabdaftari, G., Godoy, A., and

Pili, R. (2013). Combinatorial antitumor effect of HDACs and the PI3K-Akt-mTOR pathway inhibition in a Pten deficient model of prostate cancer. *Oncotarget*, *4*(12):2225–36.

Evans, A. E., D'Angio, G. J., Propert, K., Anderson, J., and Hann, H. W. (1987). Prognostic factor in neuroblastoma. *Cancer*, *59*(11):1853–9.

Feng, J., Cen, J., Li, J., Zhao, R., Zhu, C., Wang, Z., Xie, J., and Tang, W. (2015). Histone deacetylase inhibitor valproic acid (VPA) promotes the epithelial mesenchymal transition of colorectal cancer cells via up regulation of Snail. *Cell Adh Migr*, *9*(6):495–501.

Feng, J. M., Miao, Z. H., Jiang, Y., Chen, Y., Li, J. X., Tong, L. J., Zhang, J., Huang, Y.R., and Ding, J. (2012). Characterization of the conversion between CD133+ and CD133 - cells in colon cancer SW620 cell line. *Cancer Biol. Ther.*, *13*(14):1396–1406.

Fish, J. D., and Grupp, S. A. (2008). Stem cell transplantation for neuroblastoma. *Bone Marrow Transplant.*, *41*(2):159–65.

Folkvord, S., Ree, A. H., Furre, T., Halvorsen, T., and Flatmark, K. (2009). Radiosensitization by SAHA in experimental colorectal carcinoma models-In Vivo effects and relevance of histone acetylation status. *Int. J. Radiat. Oncol. Biol. Phys.*, *74*(2):546–552.

Forlenza, C. J., Boudreau, J. E., Zheng, J., Le-Luduec, J. B., Chamberlain, E., Heller, G., Cheung, N. K., and Hsu, K. C. (2016). KIR3DL1 allelic polymorphism and HLA-B epitopes modulate response to Anti-GD2 monoclonal antibody in patients with neuroblastoma. *J. Clin. Oncol.*, *34*(21):2443–2451.

Gatei, M., Scott, S. P., Filippovitch, I., Soronika, N., Lavin, M. F., Weber, B., and Khanna, K. K. (2000). Role for ATM in DNA damage-induced phosphorylation of BRCA1. *Cancer Res.*, 60(12):3299–3304.

Griguer, C. E., Oliva, C. R., Gobin, E., Marcorelles, P., Benos, D. J., Lancaster, J. R., and Gillespie, G. Y. (2008). CD133 is a marker of bioenergetic stress in human glioma. *PLoS ONE*, *3*(11):e3655.

Groh, T., Hrabeta, J., Khalil, M. A., Doktorova, H., Eckschlager, T., & Stiborova, M. (2015). The synergistic effects of DNA-damaging drugs cisplatin and etoposide with a histone deacetylase inhibitor valproate in high-risk neuroblastoma cells. *Int. J. Oncol.*, *47*(1):343–352.

Groh, T., Hrabeta, J., Poljakova, J., Eckschlager, T., and Stiborova, M. (2012). Impact of histone deacetylase inhibitor valproic acid on the anticancer effect of etoposide on neuroblastoma cells. *Neuro Endocrinol. Lett.*, 33(SUPPL. 3):16–24.

Hämmerle, B., Yañez, Y., Palanca, S., Cañete, A., Burks, D. J., Castel, V., and Font de Mora, J. (2013). Targeting neuroblastoma stem cells with retinoic acid and proteasome inhibitor. *PLoS ONE*, 8(10):e76761.

Han, L., Shi, S., Gong, T., Zhang, Z., and Sun, X. (2013). Cancer stem cells: therapeutic implications and perspectives in cancer therapy. *Acta Pharm. Sin. B*, *3*(2), 65–75.

Hanahan, D., and Weinberg, R. A. (2011). Hallmarks of cancer: The next generation. *Cell*, 144(5):646-74

Hande, K. R. (1998). Etoposide: Four decades of development of a topoisomerase II inhibitor. *Eur. J. Cancer*, 34(10):1514-21

Hansford, L. M., Thomas, W. D., Keating, J. M., Burkhart, C. a, Peaston, A. E., Norris, M. D., Haber, M, Armati, P. J., Weiss, W. A., and Marshall, G. M. (2004). Mechanisms of embryonal tumor initiation: distinct roles for MycN expression and MYCN amplification. *Proc. Natl Acad Sci U S A*, *101*(34), 12664–12669.

Harms, K. L., and Chen, X. (2007). Histone deacetylase 2 modulates p53 transcriptional activities through regulation of p53-DNA binding activity. *Cancer Res.*, 67(7):3145–3152.

Higuchi, A., Ling, Q.-D., Kumar, S. S., Munusamy, M. A, Alarfaj, A. A, Chang, Y., Kao, S. H., Lin, K. C., Wang, H. C., and Umezawa, A. (2015). Generation of pluripotent stem cells without the use of genetic material. *Lab Invest*, *95*(300):26–42.

Hochedlinger, K., and Plath, K. (2009). Epigenetic reprogramming and induced pluripotency. *Development*, *136*(4):509–23.

Holohan, C., Van Schaeybroeck, S., Longley, D. B., and Johnston, P. G. (2013). Cancer drug resistance: an evolving paradigm. *Nat. Rev. Cancer*, 13(10):714–726.

Horst, D., Scheel, S. K., Liebmann, S., Neumann, J., Maatz, S., Kirchner, T., and Jung, A. (2009). The cancer stem cell marker CD133 has high prognostic impact but unknown functional relevance for the metastasis of human colon cancer. *J Pathol*, *219*(4):427–434.

Howlader, N., Noone, A. M., Krapcho, M., Miller, D., Bishop, K., Kosary, C. L., Yu, M., Ruhl, J., Tatalovich, Z., Mariotto, A., Lewis, D. R., Chen, H. S., Feuer, E. J., Cronin, K., A., (eds). (2016). SEER Cancer Statistics Review, 1975-2014, National Cancer Institute. Bethesda, MD, https://seer.cancer.gov/csr/1975_2014.

Hrebackova, J., Hrabeta, J., and Eckschlager, T. (2010). Valproic acid in the complex therapy of malignant tumors. *Curr Drug Targets*, *11*:361–379.

Huangfu, D., Maehr, R., Guo, W., Eijkelenboom, A., Snitow, M., Chen, A. E., and Melton, D. A. (2008). Induction of pluripotent stem cells by defined factors is greatly improved by small-molecule compounds. *Nat. Biotechnol.*, *26*(7): 795–7.

Huber, K. (2006). The sympathoadrenal cell lineage: Specification, diversification, and new perspectives. *Dev. Biol.*, 298(2):335-343

Insinga, A., Monestiroli, S., Ronzoni, S., Carbone, R., Pearson, M., Pruneri, G., Viale, G., Appella, E., Pelicci, P., and Minucci, S. (2004). Impairment of p53 acetylation, stability and function by an oncogenic transcription factor. *The EMBO J.*, *23*(5):1144–54.

Irollo, E., and Pirozzi, G. (2013). CD133 : to be or not to be , is this the real question ? *Am J Transl Res*, *5*(6):563–581.

Jones, P. A., and Taylor, S. M. (1980). Cellular differentiation, cytidine analogs and DNA methylation. *Cell*, *20*(1):85–93.

Jordan, M. A., and Wilson, L. (2004). Microtubules as a target for anticancer drugs. *Nat. Rev. Cancer*, *4(*4), 253–265.

Juan, L. J., Shia, W. J., Chen, M. H., Yang, W. M., Seto, E., Lin, Y. S., and Wu, C. W. (2000). Histone deacetylases specifically down-regulate p53-dependent gene activation. *J. Biol. Chem.*, *275*(27):20436–20443.

Jung, K. H., Noh, J. H., Kim, J. K., Eun, J. W., Bae, H. J., Xie, H. J., Chang, Y. G., Kim, M. G., Park, H., Lee, J. Y., and Nam, S. W. (2012). HDAC2 overexpression confers oncogenic potential to human lung cancer cells by deregulating expression of apoptosis and cell cycle proteins. *J. Cell. Biochem.*, *113*(6):2167–2177.

Kachhap, S. K., Rosmus, N., Collis, S. J., Kortenhorst, M. S. Q., Wissing, M. D., Hedayati, M., Shabbeer, S., Mendonca, J., Deangelis, J., Marchionni, L., Lin, J., Höti, N., Nortier,J. W. R., DeWeese, T. L., Hammers, H., and Carducci, M. A. (2010). Downregulation of homologous recombination DNA repair genes by HDAC inhibition in prostate cancer is mediated through the E2F1 transcription factor. *PLoS ONE*, *5*(6):e11208

Kamijo, T. (2012). Role of stemness-related molecules in neuroblastoma. *Pediatr. Res.*, *71*(4 Pt 2): 511–5.

Kaneko, Y., Suenaga, Y., Islam, S. M. R., Matsumoto, D., Nakamura, Y., Ohira, M., Yokoi, S., and Nakagawara, A. (2015). Functional interplay between MYCN, NCYM, and OCT4 promotes aggressiveness of human neuroblastomas. *Cancer Sci.*, *106*(7):840–847.

Kao, G. D., McKenna, W. G., Guenther, M. G., Muschel, R. J., Lazar, M. A., and Yen, T. J. (2003). Histone deacetylase 4 interacts with 53BP1 to mediate the DNA damage response. *J. Cell Biol.*, *160*(7):1017–1027.

Karantzali, E., Schulz, H., Hummel, O., Hubner, N., Hatzopoulos, A., and Kretsovali, A. (2008). Histone deacetylase inhibition accelerates the early events of stem cell differentiation: transcriptomic and epigenetic analysis. *Genome Biol.*, *9*(4):R65.

Ke, N., Wang, X., Xu, X., and Abassi, Y. A. (2011). The xCELLigence system for real-time and label-free monitoring of cell viability. *Methods Mol. Biol., 740*:33–43.

Kemper, K., Sprick, M. R., de Bree, M., Scopelliti, A., Vermeulen, L., Hoek, M., Zeilstra, J., Pals, S. T., Mehmet, H., Stassi, G., and Medema, J. P. (2010). The AC133 epitope, but not the CD133 protein, is lost upon cancer stem cell differentiation. *Cancer Res*, *70*(2):719–29.

Khalil, M. A., Hrabeta, J., Cipro, S., Stiborova, M., Vicha, A., and Eckschlager, T. (2012). Neuroblastoma stem cells - Mechanisms of chemoresistance and histonedeacetylase inhibitors. *Neoplasma*, 59(6):737-46

Khalil, M. A., Hraběta, J., Groh, T., Procházka, P., Doktorová, H., and Eckschlager, T. (2016). Valproic Acid Increases CD133 Positive Cells that Show Low Sensitivity to Cytostatics in Neuroblastoma. *PloS One*, *11*(9):e0162916.

Kim, I. A., Kim, I. H., Kim, H. J., Chie, E. K., and Kim, J. S. (2010). HDAC Inhibitor-Mediated Radiosensitization in Human Carcinoma Cells: A General Phenomenon?. *J. Radiat. Res*, *51(3):*257–263.

Kim, M. S., Blake, M., Baek, J. H., Kohlhagen, G., Pommier, Y., and Carrier, F. (2003). Inhibition of histone deacetylase increases cytotoxicity to anticancer drugs targeting DNA. *Cancer Res*, *63*(21):7291–7300.

Kong, D., Ahmad, A., Bao, B., Li, Y., Banerjee, S., and Sarkar, F. H. (2012). Histone Deacetylase Inhibitors Induce Epithelial-to-Mesenchymal Transition in Prostate Cancer Cells. *PLoS ONE*, *7*(9):e4504

Kovalevich, J., and Langford, D. (2013). Considerations for the Use of SH-SY5Y Neuroblastoma Cells in Neurobiology. *Methods Mol Biol*, *1078*:9–21.

Koyama-Nasu, R., Takahashi, R., Yanagida, S., Nasu-Nishimura, Y., Oyama, M., Kozuka-Hata, H., Haruta, R., Manabe, E., Hoshino-Okubo, A., Omi, H., Yanaihara, N., Okamoto, A., Tanaka, T., and Akiyama, T. (2013). The Cancer Stem Cell Marker CD133 Interacts with Plakoglobin and Controls Desmoglein-2

Protein Levels. *PLoS ONE*, *8*(1), e53710.

Kretsovali, A., Hadjimichael, C., and Charmpilas, N. (2012). Histone deacetylase inhibitors in cell pluripotency, differentiation, and reprogramming. *Stem Cells Int*, *2012*: Article ID 184154.

Kurz, E. U., Wilson, S. E., Leader, K. B., Sampey, B. P., Allan, W. P., Yalowich, J. C., and Kroll, D. J. (2001). The histone deacetylase inhibitor sodium butyrate induces DNA topoisomerase II alpha expression and confers hypersensitivity to etoposide in human leukemic cell lines. *Mol Cancer Ther*, *1*(2):121–131.

Lathia, J. D., Hitomi, M., Gallagher, J., Gadani, S. P., Adkins, J., Vasanji, A., Liu, L., Eyler, C. E., Heddleston, J. M., Wu, Q., Minhas, S., Soeda, A., Hoeppner, D. J., Ravin, R., McKay, R. D., McLendon, R. E., Corbeil, D., Chenn, A., Hjelmeland, A. B., Park, D. M., and Rich, J. N. (2011). Distribution of CD133 reveals glioma stem cells self-renew through symmetric and asymmetric cell divisions. *Cell Death Dis*, *2*: e200.

Lee, A., Kessler, J. D., Read, T. A., Kaiser, C., Corbeil, D., Huttner, W. B., Johnson, J. E., and Wechsler-Reya, R. J. (2005). Isolation of neural stem cells from the postnatal cerebellum. *Nat Neurosci*, *8*:723–729.

Lee, H.-Z., Kwitkowski, V. E., Del Valle, P. L., Ricci, M. S., Saber, H., Habtemariam, B. A., Bullock, J., Bloomquist, E., Li Shen, Y., Chen, X. H., Brown, j., Mehrotra, N., Dorff, S., Charlab, R., Kane, R. C., Kaminskas E., Justice, R., Farrell, A. T., and Pazdur, R. (2015). FDA Approval: Belinostat for the Treatment of Patients with Relapsed or Refractory Peripheral T-cell Lymphoma. *Clin Cancer Res*, *21*:2666–2670.

Li, Y., and Seto, E. (2016). HDACs and HDAC inhibitors in cancer development and therapy. *Cold Spring Harb. Perspect. Med.*, *6*(10):pii.a026831

Li, Y., Zhang, Q., Yin, X., Yang, W., Du, Y., Hou, P., Ge, J., Liu, C., Zhang, W., Zhang, X., Wu, Y., Li, H., Liu, K.,Wu, C. ,Song, Z., Zhao, Y., Shi, Y., and Deng, H. (2011). Generation of iPSCs from mouse fibroblasts with a single gene, Oct4, and small molecules. *Cell Res.*, *21*(1):196–204.

Li, Z., and Zhu, W. G. (2014). Targeting Histone Deacetylases for Cancer Therapy: From Molecular Mechanisms to Clinical Implications. *Int. J. Biol. Sci.*, *10*(7):757–770.

Liu, G., Yuan, X., Zeng, Z., Tunici, P., Ng, H., Abdulkadir, I. R., Lu, L, Irvin, D., Black, K. L., and Yu, J. S. (2006). Analysis of gene expression and chemoresistance of CD133+ cancer stem cells in glioblastoma. *Mol Cancer*, *5*(1):67.

London, W. B., Castleberry, R. P., Matthay, K. K., Look, A. T., Seeger, R. C., Shimada, H., Thorner P, Brodeur, G., Maris, J. M., Reynolds, C. P., and Cohn, S. L. (2005). Evidence for an age cutoff greater than 365 days for neuroblastoma risk group stratification in the Children's Oncology Group. *J. Clin. Oncol.*, *23*(27):6459–6465.

Lowry, O. H., Rosebrough, N. J., Farr, A. L., and Randall, R. J. (1951). Protein measurement with the Folin-Phenol Reagent. *J. Biol. Cem.*, *193*(1):265–275.

Morrison, R., Schleicher, S. M., Sun, Y., Niermann, K. J., Kim, S., Spratt, D. E., Chung, C. H. and Lu, B. (2011). Targeting the mechanisms of resistance to chemotherapy and radiotherapy with the cancer stem cell hypothesis. *J. Oncol.*, *2011*:941876

Luchenko, V. L., Salcido, C. D., Zhang, Y., Agama, K., Komlodi-Pasztor, E., Murphy, R. F., Giaccone, G., Pommier, Y., Bates, S. E., Varticovski, L. (2011). Schedule-dependent synergy of histone deacetylase inhibitors with DNA damaging agents in small cell lung cancer. *Cell Cycle*, *10*(18):3119–3128.

Lucke, A., Mayer, T., Altrup, U., Lehmenkuhler, A., Dusing, R., and Speckmann, E. J. (1994). Simultaneous and continuous measurement of free concentration of valproate in blood and extracellular-space of rat cerebral-cortex. *Epilepsia*, *35*(5):922–926.

Ma, S., Lee, T. K., Zheng, B.-J., Chan, K. W., and Guan, X. Y. (2008). CD133+ HCC cancer stem cells confer chemoresistance by preferential expression of the Akt/PKB survival pathway. *Oncogene*, *27*(12):1749–1758.

Ma, X., Ezzeldin, H. H., and Diasio, R. B. (2009). Histone deacetylase inhibitors: Current status and overview of recent clinical trials. *Drugs*, 69(14):1911-34

Maguire, L. H., Thomas, A. R., and Goldstein, A. M. (2015). Tumors of the neural crest: Common themes in development and cancer. *Dev. Dyn.,* 244(3):311-22.

Mah, L. J., El-Osta, A., and Karagiannis, T. C. (2010). gamma H2AX: a sensitive molecular marker of DNA damage and repair. *Leukemia*, *24*(4):679–686.

Maris, J. M. (2010). Recent Advances in Neuroblastoma. *N. Engl. J. Med.*, *362*(23):2202–2211.

Marshall, G. M., Carter, D. R., Cheung, B. B., Liu, T., Mateos, M. K., Meyerowitz, J. G., and Weiss, W. A. (2014). The prenatal origins of cancer. *Nat. Rev. Cancer*, *14*(4):277–289.

Mastrangelo, R., Tornesello, A., Riccardi, R., Lasorella, A., Mastrangelo, S., Mancini, A., Rufini, V., and Troncone, L. (1995). A new approach in the treatment of stage IV neuroblastoma using a combination of [131I] meta-iodobenzylguanidine (MIBG) and cisplatin. *Eur. J. Cancer*, *31*(4):606–611.

Matthay, K. K., Yanik, G., Messina, J., Quach, A., Huberty, J., Cheng, S. C., Veatch, J., Goldsby, R., Brophy, P., Kersun, L. S., Hawkins, R. A., and Maris, J. M. (2007). Phase II study on the effect of disease sites, age, and prior therapy on response to iodine-131-metaiodobenzylguanidine therapy in refractory neuroblastoma. *J. Clin. Oncol*, *25*(9): 1054–1060.

McCool, K. W., Xu, X., Singer, D. B., Murdoch, F. E., and Fritsch, M. K. (2007). The role of histone acetylation in regulating early gene expression patterns during early embryonic stem cell differentiation. *J. Biol. Chem*, *282*(9):6696–6706.

Meng, X., Li, M., Wang, X., Wang, Y., and Ma, D. (2009). Both CD133+ and CD133- subpopulations of A549 and H446 cells contain cancer-initiating cells. *Cancer Sci*, *100*(6):1040–6.

Mesdjian, E., Ciesielski, L., Valli, M., Bruguerolle, B., Jadot, G., Bouyard, P., and Mandel, P. (1982). Sodium valproate: Kinetic profile and effects on GABA levels

in various brain areas of the rat. *Prog. Neuropsychopharmacol. Biol Psychiatry*, *6*(3):223–233.

Milde, T., Oehme, I., Korshunov, A., Kopp-Schneider, A., Remke, M., Northcott, P., Deubzer, H. E., Lodrini, M., Taylor, M. D., von Deimling, A., Pfister, S., and Witt, O. (2010). HDAC5 and HDAC9 in medulloblastoma: novel markers for risk stratification and role in tumor cell growth. *Clin. Cancer Res.*, *16*(12):3240–3252.

Miller, K. M., Tjeertes, J. V, Coates, J., Legube, G., Polo, S. E., Britton, S., and Jackson, S. P. (2010). Human HDAC1 and HDAC2 function in the DNA-damage response to promote DNA nonhomologous end-joining. *Nat. Struct. Mol. Biol.*, *17*(9):1144–1151.

Mora, J., Cheung, N. K. V, Juan, G., Illei, P., Cheung, I., Akram, M., Chi, S., Ladanyi, M., Cordon-Cardo, C., and Gerald, W. L. (2001). Neuroblastic and Schwannian stromal cells of neuroblastoma are derived from a tumoral progenitor cell. *Cancer Res.*, *61*(18):6892–6898.

Mossé, Y. P., Laudenslager, M., Longo, L., Cole, K. A., Wood, A., Attiyeh, E. F., Laquaglia, M. J., Sennett, R., Lynch, J. E., Perri, P., Laureys, G., Speleman, F., Kim, C., Hou, C., Hakonarson, H., Torkamani, A., Schork, N. J., Brodeur, G. M., Tonini, G. P., Rappaport, E., Devoto, M., and Maris, J. M. (2008). Identification of ALK as a major familial neuroblastoma predisposition gene. *Nature*, *455*(7215):930–935.

Mottamal, M., Zheng, S., Huang, T. L., and Wang, G. (2015). Histone deacetylase inhibitors in clinical studies as templates for new anticancer agents. *Molecules*, 20(3):3898-94

Mueller, S., and Matthay, K. K. (2009). Neuroblastoma: Biology and staging. *Current Oncol. Rep.,* 11(6):431-8

Müller, B. M., Jana, L., Kasajima, A., Lehmann, A., Prinzler, J., Budczies, J., Winzer, K. J., Dietel, M.,Weichert, W., Denkert, C. (2013). Differential expression of histone deacetylases HDAC1, 2 and 3 in human breast cancer-

overexpression of HDAC2 and HDAC3 is associated with clinicopathological indicators of disease progression. *BMC Cancer*, *13*:215.

Munshi, A., Kurland, J. F., Nishikawa, T., Tanaka, T., Hobbs, M. L., Tucker, S. L., Ismail, S., Stevens, C., and Meyn, R. E. (2005). Histone deacetylase inhibitors radiosensitize human melanoma cells by suppressing DNA repair activity. *Clin. Cancer Res.*, *11*(13):4912–4922.

Nakamura, A. J., Rao, V. A., Pommier, Y., and Bonner, W. M. (2010). The complexity of phosphorylated H2AX foci formation and DNA repair assembly at DNA double-strand breaks. *Cell Cycle*, *9*(2):389–397.

Nome, R. V, Bratland, A., Harman, G., Fodstad, O., Andersson, Y., and Ree, A. H. (2005). Cell cycle checkpoint signaling involved in histone deacetylase inhibition and radiation-induced cell death. *Mol. Cancer Ther.*, *4*(8):1231–1238.

O'Brien, C. A., Pollett, A., Gallinger, S., and Dick, J. E. (2007). A human colon cancer cell capable of initiating tumour growth in immunodeficient mice. *Nature*, *445*(7123):106–110.

O'Donovan, N., Crown, J., and Stunell, H. (2003). Caspase 3 in breast cancer. *Clin. Cancer Res.*, *9*(2), 738–742.

Oehme, I., Linke, J.-P., Böck, B. C., Milde, T., Lodrini, M., Hartenstein, B., Wiegand, I., Eckert, C., Roth, W., Kool, M., Kaden, S., Gröne, H. J., Schulte, J. H. , Lindner, S., Hamacher-Brady, A., Brady, N. R., Deubzer, H. E., and Witt, O. (2013). Histone deacetylase 10 promotes autophagy-mediated cell survival. *Proc. Natl. Acad. Sci U S A*, *110*(28):E2592-601.

Opel, D., Poremba, C., Simon, T., Debatin, K.-M., and Fulda, S. (2007). Activation of Akt predicts poor outcome in neuroblastoma. *Cancer Res*, *67*(2):735–45.

Pezzolo, A., Parodi, F., Marimpietri, D., Raffaghello, L., Cocco, C., Pistorio, A., Mosconi, M., Gambini, C., Cilli, M., Deaglio, S., Malavasi, F., and Pistoia, V. (2011). Oct-4+/Tenascin C+ neuroblastoma cells serve as progenitors of tumor-derived endothelial cells. *Cell Res.*, *21*(10):1470–86.

Pfaffl, M. W., Horgan, G. W., and Dempfle, L. (2002). Relative expression software

tool (REST) for group-wise comparison and statistical analysis of relative expression results in real-time PCR. *Nucleic Acids Res.*, *30*(9):e36.

Phiel, C. J., Zhang, F., Huang, E. Y., Guenther, M. G., Lazar, M. A., and Klein, P. S. (2001). Histone deacetylase is a direct target of valproic acid, a potent anticonvulsant, mood stabilizer, and teratogen. *J. Biol. Chem.*, *276*(39):36734–41.

Pinto, N. R., Applebaum, M. A., Volchenboum, S. L., Matthay, K. K., London, W. B., Ambros, P. F., Nakagawara, A., Berthold, F., Schleiermacher, G., Park, J. R., Valteau-Couanet, D., Pearson, A. D. J., and Cohn, S. L. (2015). Advances in risk classification and treatment strategies for neuroblastoma. *J. Clin. Oncol.,* 33(27):3008–3017.

Poljaková, J., Groh, T., Gudino, Z. O., Hraběta, J., Bořek-Dohalská, L., Kizek, R., Doktorová, H., Eckschlager, T.,and Stiborová, M. (2014). Hypoxia-mediated histone acetylation and expression of N-myc transcription factor dictate aggressiveness of neuroblastoma cells. *Oncol Rep*, *31*(4):1928–34.

Poljakova, J., Hrebackova, J., Dvorakova, M., Moserova, M., Eckschlager, T., Hrabeta, J., Göttlicherova, M., Kopejtkova, B., Frei, E., Kizek, R., and Stiborova, M. (2011). Anticancer agent ellipticine combined with histone deacetylase inhibitors, valproic acid and trichostatin A, is an effective DNA damage strategy in human neuroblastoma. *Neuro. endocrinol. Lett*, *32*(SUPPL. 1):101–116.

Raabe, E. H., Laudenslager, M., Winter, C., Wasserman, N., Cole, K., LaQuaglia, M., Maris, D. J., Mosse, Y. P., and Maris, J. M. (2008). Prevalence and functional consequence of PHOX2B mutations in neuroblastoma. *Oncogene*, *27*(4):469–76.

Rettig, I., Koeneke, E., Trippel, F., Mueller, W. C., Burhenne, J., Kopp-Schneider, A., Fabian, J., Schober, A., Fernekorn, U., von Deimling, A., Deubzer, H. E., Milde, T., Witt, O., and Oehme, I. (2015). Selective inhibition of HDAC8 decreases neuroblastoma growth in vitro and in vivo and enhances retinoic acid-mediated differentiation. *Cell Death Dis.*, *6*(2):e1657.

Reya, T., Morrison, S. J., Clarke, M. F., and Weissman, I. L. (2001). Stem cells, cancer, and cancer stem cells. *Nature*, *414*(6859):105–11.

Reynolds, C. P., Matthay, K. K., Villablanca, J. G., and Maurer, B. J. (2003). Retinoid therapy of high-risk neuroblastoma. *Cancer Lett.,* 197(1-2):185-92

Rizzino, A. (2009). Sox2 and Oct-3/4: a versatile pair of master regulators that orchestrate the self-renewal and pluripotency of embryonic stem cells. *Wiley Interdiscip Rev Syst Biol Med*, *1*(2):228–36.

Ross, R. A., Biedler, J. L., and Spengler, B. A. (2003). A role for distinct cell types in determining malignancy in human neuroblastoma cell lines and tumors. *Cancer Lett*, *197*(1–2):35–39.

Rudà, R., Pellerino, A., and Soffietti, R. (2016). Does valproic acid affect tumor growth and improve survival in glioblastomas? *CNS Oncol.*, *5*(2): 51–53.

Sartelet, H., Imbriglio, T., Nyalendo, C., Haddad, E., Annabi, B., Duval, M., Victor, K., Alexendrov, L., Sinnett, D., Fabre, M., and Vassal, G. (2012). CD133 expression is associated with poor outcome in neuroblastoma via chemoresistance mediated by the AKT pathway. *Histopathology*, *60(7)*:1144–1155.

Schrump, D. S. (2009). Cytotoxicity mediated by histone deacetylase inhibitors in cancer cells: Mechanisms and potential clinical implications. *Clin. Cancer Res*., 15(12):3947-57

Shahbazian, M. D., and Grunstein, M. (2007). Functions of site-specific histone acetylation and deacetylation. *Annu. Rev. Biochem.*, *76*:75–100.

Shechter, D., Dormann, H. L., Allis, C. D., and Hake, S. B. (2007). Extraction, purification and analysis of histones. *Nat Protoc*, *2*(6):1445–1457.

Shi, G., Gao, F., and Jin, Y. (2011). The regulatory role of histone deacetylase inhibitors in Fgf4 expression is dependent on the differentiation state of pluripotent stem cells. *J Cell Physiol*, *226*(12):3190–3196.

Shin, J. H., Lee, Y. S., Hong, Y. K., and Kang, C. S. (2013). Correlation between

the prognostic value and the expression of the stem cell marker CD133 and isocitrate dehydrogenase1 in glioblastomas. *J Neurooncol*, *115*(3):333–41.

Shmelkov, S. V., Butler, J. M., Hooper, A. T., Hormigo, A., Kushner, J., Milde, T., St Clair, R., Baljevic, M., White, I., Jin, D. K., Chadburn, A., Murphy, A. J., Valenzuela, D. M., Gale, N. W., Thurston, G., Yancopoulos, G. D., D'Angelica, M., Kemeny, N., Lyden, D., and Rafii, S. (2008). CD133 expression is not restricted to stem cells, and both CD133 + and CD133- metastatic colon cancer cells initiate tumors. *J Clin Invest*, *118(6)*:2111–2120.

Shmelkov, S. V, Jun, L., St Clair, R., McGarrigle, D., Derderian, C. A., Usenko, J. K., Costa, C., Zhang, F., Guo, X., and Rafii, S. (2004). Alternative promoters regulate transcription of the gene that encodes stem cell surface protein AC133. *Blood*, *103*(6):2055–61.

Shmelkov, S. V, St Clair, R., Lyden, D., and Rafii, S. (2005). AC133/CD133/Prominin-1. *Int J Biochem Cell Biol*, *37*(4):715–9.

Singh, S. K., Hawkins, C., Clarke, I. D., Squire, J. A., Bayani, J., Hide, T., Henkelman, R. M., Cusimano, M. D., and Dirks, P. B. (2004). Identification of human brain tumour initiating cells. *Nature*, *432*(7015):396–401.

Slee, E. A., Adrain, C., and Martin, S. J. (2001). Executioner Caspase-3, -6, and -7 Perform Distinct, Non-redundant Roles during the Demolition Phase of Apoptosis. *J. Biol. Chem. 276*(10), 7320–7326.

Sokolov, M. V., Dickey, J. S., Bonner, W. M., and Sedelnikova, O. A. (2007). γ-H2AX in bystander cells: Not just a radiation-triggered event, a cellular response to stress mediated by intercellular communication. *Cell Cycle*, 6(18):2210-2

Stiborova, M., Eckschlager, T., Poljakova, J., Hrabeta, J., Adam, V., Kizek, R., and Frei, E. (2012). The synergistic effects of DNA-targeted chemotherapeutics and histone deacetylase inhibitors as therapeutic strategies for cancer treatment. *Curr Med Chem*, *19*(25):4218–4238.

Stockhausen, M. T., Sjölund, J., Manetopoulos, C., and Axelson, H. (2005).

Effects of the histone deacetylase inhibitor valproic acid on Notch signalling in human neuroblastoma cells. *Br J Cancer*, *92*(4):751–9.

Sun, Y., Kong, W., Falk, A., Hu, J., Zhou, L., Pollard, S., and Smith, A. (2009). CD133 (Prominin) negative human neural stem cells are clonogenic and tripotent. *PLoS ONE*, *4*(5):e5498.

Tabu, K., Sasai, K., Kimura, T., Wang, L., Aoyanagi, E., Kohsaka, S., Tanino, M., Nishihara, H., and Tanaka, S. (2008). Promoter hypomethylation regulates CD133 expression in human gliomas. *Cell Res*, *18*(10):1037–46.

Takahashi, K., Tanabe, K., Ohnuki, M., Narita, M., Ichisaka, T., Tomoda, K., and Yamanaka, S. (2007). Induction of Pluripotent Stem Cells from Adult Human Fibroblasts by Defined Factors. *Cell*, *107*(5):861–872.

Takahashi, K., and Yamanaka, S. (2006). Induction of pluripotent stem cells from mouse embryonic and adult fibroblast cultures by defined factors. *Cell*:*126*(4):663–676.

Thurn, K. T., Thomas, S., Raha, P., Qureshi, I., and Munster, P. N. (2013). Histone deacetylase regulation of ATM-mediated DNA damage signaling. *Mol Cancer Ther*, *12*(10):2078–87.

Tirino, V., Desiderio, V., D'Aquino, R., De Francesco, F., Pirozzi, G., Galderisi, U., Cavaliere, C., De Rosa, A., and Papaccio, G. (2008). Detection and characterization of CD133+ cancer stem cells in human solid tumours. *PLoS ONE*, *3*(10):e3469.

Todaro, M., Alea, M. P., Di Stefano, A. B., Cammareri, P., Vermeulen, L., Iovino, F., Tripodo, C., Russo, A., Gulotta, G., Medema, J. P. and Stassi, G. (2007). Colon cancer stem cells dictate tumor growth and resist cell death by production of Interleukin-4. *Cell Stem Cell*, *1*(4):389–402.

Tong, Q. S., Zheng, L. D., Tang, S. T., Ruan, Q. L., Liu, Y., Li, S. W., Jiang, G.S., and Cai, J. B. (2008). Expression and clinical significance of stem cell marker CD133 in human neuroblastoma. *World J. Pediatr*, *4*(1):58–62.

VanDongen, A. M. J., VanErp, M. G., and Voskuyl, R. A. (1986). Valproate

Reduces Excitability by Blockage of Sodium and Potassium Conductance. *Epilepsia*, *27*(3):177–182.

Vangipuram, S. D., Wang, Z. J., and Lyman, W. D. (2010). Resistance of stem-like cells from neuroblastoma cell lines to commonly used chemotherapeutic agents. *Pediatr Blood Cancer*, *54*(3):361–368.

Veas-Perez de Tudela, M., Delgado-Esteban, M., Cuende, J., Bolaños, J. P., and Almeida, A. (2010). Human neuroblastoma cells with MYCN amplification are selectively resistant to oxidative stress by transcriptionally up-regulating glutamate cysteine ligase. *J Neurochem*, *113*(4):819–25.

Wakao, S., Kuroda, Y., Ogura, F., Shigemoto, T., and Dezawa, M. (2012). Regenerative Effects of Mesenchymal Stem Cells: Contribution of Muse Cells, a Novel Pluripotent Stem Cell Type that Resides in Mesenchymal Cells. *Cells*, *1*(4):1045–60.

Walton, J. D., Kattan, D. R., Thomas, S. K., Spengler, B. A., Guo, H.-F., Biedler, J. L., Cheung, N. K., and Ross, R. A. (2004). Characteristics of stem cells from human neuroblastoma cell lines and in tumors. *Neoplasia*, *6*(6), 838–45.

Wang, G., Edwards, H., Caldwell, J. T., Buck, S. A., Qing, W. Y., Taub, J. W., Ge, Y., and Wang, Z. (2013). Panobinostat Synergistically Enhances the Cytotoxic Effects of Cisplatin, Doxorubicin or Etoposide on High-Risk Neuroblastoma Cells. *PLoS ONE*, *8*(9): e7666

Wang, Y., Wang, L., Guan, S., Cao, W., Wang, H., Chen, Z., Zhao, Y., Yu, Y., Zhang, H., Pang, J. C., Huang, S. L., Akiyama, Y., Yang, Y., Sun, W., Xu, X., Shi, Y., Zhang, H., Kim, E. S., Muscal, J. A., Lu, F., and Yang, J. (2016). Novel ALK inhibitor AZD3463 inhibits neuroblastoma growth by overcoming crizotinib resistance and inducing apoptosis. *Sci. Rep.*, *6*:19423.

Ward, E., Desantis, C., Robbins, A., Kohler, B., and Jemal, A. (2014). Childhood and Adolescent Cancer Statistics, 2014. *CA. Cancer J. Clin.*, *64*(2):83–103.

Wei, Y., Jiang, Y., Zou, F., Liu, Y., Wang, S., Xu, N., Xu, W., Cui, C., Xing, Y., Liu, Y., Cao, B., Liu, C., Wu, G., Ao, H., Zhang, X., and Jiang, J. (2013). Activation

of PI3K/Akt pathway by CD133-p85 interaction promotes tumorigenic capacity of glioma stem cells. *Proc Natl Acad Sci U S A*, *110*(17), 6829–34.

Weichert, W., Roske, A., Niesporek, S., Noske, A., Buckendahl, A. C., Dietel, M., Gekeler, V., Boehm, M., Beckers, T., and Denkert, C. (2008). Class I histone deacetylase expression has independent prognostic impact in human colorectal cancer: specific role of class I histone deacetylases in vitro and in vivo. *Clin Cancer Res*, *14*(6):1669–1677.

Weichert, W., Röske, A., Gekeler, V., Beckers, T., Stephan, C., Jung, K., Fritzsche, F. R., Niesporek, S., Denkert, C., Dietel, M., and Kristiansen, G., (2008). Histone deacetylases 1, 2 and 3 are highly expressed in prostate cancer and HDAC2 expression is associated with shorter PSA relapse time after radical prostatectomy. *Br. J. Cancer*, *98*(3), 604–10.

Wheler, J. J., Janku, F., Falchook, G. S., Jackson, T. L., Fu, S., Naing, A., Tsimberidou, A. M., Moulder, S. L., Hong, D. S., Yang, H., Piha-Paul S. A., Atkins, J. T., Garcia-Manero, G., and Kurzrock, R. (2014). Phase I study of anti-VEGF monoclonal antibody bevacizumab and histone deacetylase inhibitor valproic acid in patients with advanced cancers. *Cancer Chemother. Pharmacol.*, *73*(3):495–501.

Wozniak, A. J., and Ross, W. E. (1983). DNA damage as a basis for 4'-demethylepipodophyllotoxin-9-(4,6-O-ethylidene-beta-D-glucopyranoside) (etoposide) cytotoxicity. *Cancer Res.*, *43*(1):120–124.

Wu, C. P., Xie, M., Zhou, L., Tao, L., Zhang, M., and Tian, J. (2013). Cooperation of side population cells with CD133 to enrich cancer stem cells in a laryngeal cancer cell line. *Head Neck*, *36*(9):1279–1287.

Wu, S., Luo, Z., Yu, P.-J., Xie, H., and He, Y.-W. (2016). Suberoylanilide hydroxamic acid (SAHA) promotes the epithelial mesenchymal transition of triple negative breast cancer cells via HDAC8/FOXA1 signals. *Biol. Chem.*, *397*(1):75–83.

Yi, J. M., Tsai, H.-C., Glöckner, S. C., Lin, S., Ohm, J. E., Easwaran, H., James, C.

D., Costello, J. F., Riggins, G., Eberhart, C. G., Laterra, J., Vescovi, A. L., Ahuja, N., Herman, J. G., Schuebel, K. E., and Baylin, S. B. (2008). Abnormal DNA methylation of CD133 in colorectal and glioblastoma tumors. *Cancer Res*, *68*(19):8094–103.

Yin, S., Li, J., Hu, C., Chen, X., Yao, M., Yan, M., Jiang, G., Ge, C. , Xie, H., Wan, D., Yang, S., Zheng, S., and Gu, J. (2007). CD133 positive hepatocellular carcinoma cells possess high capacity for tumorigenicity. *Int J Cancer*, *120*, 1444–1450.

Yu, C., Friday, B. B., Lai, J. P., McCollum, A., Atadja, P., Roberts, L. R., and Adjei, A. A. (2007). Abrogation of MAPK and Akt signaling by AEE788 synergistically potentiates histone deacetylase inhibitor-induced apoptosis through reactive oxygen species generation. *Clin. Cancer Res.*, *13*(4):1140–1148.

Yu, J. Y., Vodyanik, M. a, Smuga-Otto, K., Antosiewicz-Bourget, J., Frane, J. L., Tian, S., Nie, J., Jonsdottir, G. A., Ruotti, V., Stewart, R., Slukvin, I. I., and Thomson, J. A. (2007). Induced pluripotent stem cell lines derived from human somatic cells. *Science*, *318*(5858):1917–1920.

Zhang, Y., Carr, T., Dimtchev, A., Zaer, N., Dritschilo, A., and Jung, M. (2007). Attenuated DNA damage repair by trichostatin A through BRCA1 suppression. *Radiat. Res.*, *168*(1):115–24.

List of publications

Publications related to thesis:

- Khalil MA, Hrabeta J, Cipro S, Stiborova M, Vicha A, Eckschlager T. Neuroblastoma stem cells - mechanisms of chemoresistance and histone deacetylase inhibitors. *Neoplasma.* 2012; 59(6):737-46. *IF_{2011}= 1.44*

- Groh T, Hrabeta J, Khalil MA, Doktorova H, Eckschlager T, Stiborova M. The synergistic effects of DNA-damaging drugs cisplatin and etoposide with a histone deacetylase inhibitor valproate in high-risk neuroblastoma cells. *International journal of oncology.* 2015 Jul; 47(1):343-52. *IF_{2014}= 2.773*

- Khalil MA, Hraběta J, Groh T, Procházka P, Doktorová H, Eckschlager T. Valproic Acid Increases CD133 Positive Cells that Show Low Sensitivity to Cytostatics in Neuroblastoma. *PLoS One*. 2016 Sep 14; 11(9):e0162916. *IF_{2014}= 3.2*

Publications not related to thesis:

- Doktorova H, Hrabeta J, Khalil MA, Eckschlager T. Hypoxia-induced chemoresistance in cancer cells: The role of not only HIF-1. *Biomed Pap Med Fac Univ Palacky Olomouc Czech Repub*. 2015 Jun; 159(2):166-77. IF_{2014}= 1.15

- Hrabeta J, Groh T, Khalil MA, Poljakova J, Adam V, Kizek R, Uhlik J, Doktorova H, Cerna T, Frei E, Stiborova M, Eckschlager T. Vacuolar-ATPase-mediated intracellular sequestration of ellipticine contributes to drug resistance in neuroblastoma cells. *International journal of oncology*. 2015 Sep; 47(3):971-80. IF_{2014}= 2,773